

Targeted sampling from massive block model graphs with personalized PageRank*

Fan Chen¹, Yini Zhang², and Karl Rohe¹

¹Department of Statistics

²School of Journalism and Mass Communication

University of Wisconsin, Madison, WI 53706, USA

Abstract

This paper provides statistical theory and intuition for Personalized PageRank (PPR), a popular technique that samples a small community from a massive network. We study a setting where the entire network is expensive to thoroughly obtain or maintain, but we can start from a seed node of interest and “crawl” the network to find other nodes through their connections. By crawling the graph in a designed way, the PPR vector can be approximated without querying the entire massive graph, making it an alternative to snowball sampling. Using the degree-corrected stochastic block model, we study whether the PPR vector can select nodes that belong to the same block as the seed node. We provide a simple and interpretable form for the PPR vector, highlighting its biases towards high degree nodes outside of the target block. We examine a simple adjustment based on node degrees and establish consistency results for PPR clustering that allows for directed graphs. These results are enabled by recent technical advances showing the element-wise convergence of eigenvectors. We illustrate the method with the massive Twitter friendship graph, which we crawl using the Twitter API. We find that (i) the adjusted and unadjusted PPR techniques are complementary approaches, where the adjustment makes the results particularly localized around the seed node and (ii) the bias adjustment greatly benefits from degree regularization.

Keywords Community detection; Degree-corrected stochastic block model; Local clustering; Network sampling; Personalized PageRank

1 Introduction

Much of the literature on graph sampling has treated the entire graph, or all of the people in it, as the target population. However, in many settings, the target population is a small community in the massive graph. For example, a key difficulty in studying social media is to gather data that is sufficiently relevant for the scientific objective. A motivating example for this paper is to sample the Twitter friendship graph for accounts that report and discuss current political events.¹ This corresponds to sampling and identifying multiple different communities, each a potentially small part of the massive network. In such an application, the graph is useful for two primary reasons. First, via link tracing, we can find potential members of the

*This research is supported in part by NSF Grants DMS-1612456 and DMS-1916378 and ARO Grant W911NF-15-1-0423.

¹See our website <http://murmuration.wisc.edu> which does this.

target population. Second, the graph connections are informative for identifying community membership. Throughout, we presume that the sampling is initiated around a “seed node” that belongs to the target community of interest.

Personalized PageRank (PPR) can be thought of as an alternative to snowball sampling, a popular technique for gathering individuals close to the seed node. For some $d \geq 0$, snowball sampling gathers all individuals who are d friends away from the seed. This process has two competing flaws for our application which are addressed by PPR. First, snowball sampling fails to account for the density of common friendships. For example, perhaps i and j are both one friend removed from the seed, but i has 10 friends in common with the seed, while j only has 1 friend in common. It seems natural to suppose that i is closer than j to the seed. Hence, the metric for snowball sampling can be misleading. Second, the snowball sample size grows very quickly with d . For example, under the “six degrees of separation” phenomenon [Watts and Strogatz, 1998, Newman et al., 2006], snowballing gathers the entire graph if $d \geq 6$.

PPR gives a sample that is more localized around the seed node. The PPR vector is defined as the stationary distribution of what we call a *personalized random walk* [Page et al., 1998]. At each step of the personalized random walk, the random walker returns to the seed node with probability α , called the teleportation constant, and with probability $1 - \alpha$, the random walker goes to an adjacent node that is chosen uniformly at random. Consider the stationary distribution of this process as giving the inclusion probability for a sample of size 1. This is the PPR vector. PPR naturally leads to a clustering algorithm, where the cluster is made up of the nodes with a large inclusion probability. To quickly approximate the PPR vector, Berkhin [2006] proposed an algorithm that only examines nodes with large inclusion probabilities (i.e. nodes near the seed). As such, PPR is particularly useful for its computational efficiency – the running time and the amount of data it requires is nearly linear in the size of the output cluster, which is typically much smaller than that of the entire graph. Due to the local nature of the algorithm, it can be used to study large graphs such as Twitter where the entire graph is not available, but where one can query to find the connections to any small set of nodes.

One way to conduct local clustering is by exploring and ranking the nearby nodes of a seed node. [Andersen and Lang, 2006, Andersen and Peres, 2009, Alamgir and von Luxburg, 2010, Gharan and Trevisan, 2012]. Spielman and Teng [2004] pioneered local clustering by defining nearness as the landing probability of a random walk starting from the seed node. Their algorithm’s guarantee was improved in follow-up work by Andersen et al. [2006] which proposed using an approximate PPR vector. Local algorithms can be applied recursively to solving more complicated problems such as graph partitions (k-way partitions) [Spielman and Teng, 1996, Karypis and Kumar, 1998], and has many fruitful applications [Jeh and Widom, 2003, Macropol et al., 2009, Liao et al., 2009, Gupta et al., 2013, Gleich, 2015], particularly when it comes to sampling and studying massive graphs.

Along with the widespread use of PPR, there has been recent work to study its statistical estimation properties under a statistical model with latent community structure. Beyond the scope of local clustering, Kloumann et al. [2017] showed that the PPR vector is asymptotically equivalent to optimal linear discriminant analysis under the stochastic block model (SBM) [Holland et al., 1983], assuming a symmetry condition on the block structure. We add to this statistical understanding of PPR by providing a simple and more general representation for PPR vectors that allows for different block sizes, more than two blocks, degree heterogeneity, and directed edges. In order to understand the effects of heterogeneous node degrees, this paper uses the degree-corrected stochastic block model (DC-SBM) [Karrer and Newman, 2011] and examines when the PPR clustering recovers nodes within the same block as the seed node (local cluster). Breaking the

Table 1: Top 15 handles by PPR clustering. Column names represent seed nodes, and the sampled nodes are ranked by PPR values, with teleportation constant $\alpha = 0.15$ uniformly.

	@CNN	@BreitbartNews	@dailykos
1	CNN Breaking News	Alex Marlow	Hillary Clinton
2	CNN International	AndrewBreitbart	Stephen Colbert
3	Wolf Blitzer	Big Hollywood	Rachel Maddow MSNBC
4	Anderson Cooper	Big Government	Jake Tapper
5	Christiane Amanpour	James O’Keefe	Joy Reid
6	Pope Francis	Sean Hannity	Chris Hayes
7	Dr. Sanjay Gupta	Raheem	Emma Gonzlez
8	CNNMoney	Joel B. Pollak	Markos Moulitsas
9	Jake Tapper	Ann Coulter	Maggie Haberman
10	Brian Stelter	Allum Bokhari	Sarah Silverman
11	CNN Newsroom	Ben Kew	Lin-Manuel Miranda
12	Dana Bash	Brandon Darby	Elizabeth Warren
13	CNN Politics	Noah Dulis	Jon Favreau
14	BBC Breaking News	Michelle Malkin	Michelle Obama
15	Brooke Baldwin	Nate Church	Bill Clinton

Through the PPR vector, the top 15 handles returned to each of the three seed nodes fit well with the characteristics of the seed nodes. They are popular/high-status handles either directly related to the seed nodes or align with their political leanings. This shows the effectiveness of clustering via the PPR vector. It also shows the PPR vector’s preference for highly connected nodes.

symmetry that is imposed by Kloumann et al. [2017] reveals additional insight. In particular, given a seed node in the first block, we show that PPR is likely to contain high degree nodes outside of that block. We study an adjustment that was previously proposed in Andersen et al. [2006]. We show how this adjustment can correct for the bias. We illustrate these ideas with examples from the Twitter friendship graph.

1.1 An illustrative example in social media

Local clustering using PPR is particularly well suited to studying current political events on Twitter because (i) the accounts that discuss politics or current events are a small part of the entire Twitter graph, (ii) it is reasonable to believe that the accounts in our target population are well connected to one another in the Twitter friendship graph, and (iii) while the entire Twitter graph is not publicly available, the way that PPR (Algorithm 1 and 3) queries the graph matches the Twitter API protocol which is the primary mode of access for researchers.

While we do not suppose that the Twitter friendship graph is sampled from a DC-SBM, Twitter does have all of the heterogeneities that our results identify as important. The Twitter friendship graph is composed of users who can freely follow others but will not necessarily be followed back, or friended. Such asymmetry between following and friending forms a directed graph where follower count indicates status – some popular/high-status nodes command millions of followers while the majority of nodes are followed by far fewer.

The theoretical results in this paper suggest that such degree heterogeneities will make the PPR vector biased for detecting block memberships (Theorem 1). We propose a way to adjust for this bias (Algorithm 2) and show that it is a consistent estimator (Corollary 1). Not surprisingly, this section demonstrates that PPR with and without the bias adjustment give fundamentally different results on the Twitter graph. However, depending on the application, the biases in the PPR vector might be advantageous. In this way, PPR with and without the bias adjustment are complementary, not competing, approaches.

To illustrate, Table 1 displays the top 15 handles ranked by the PPR vector (without adjustment) for

Table 2: Top 15 handles by adjusted PPR (with regularization) sampling. Column names represent seed nodes, and the sampled nodes are ranked by adjusted PPR values, with teleportation constant $\alpha = 0.15$ uniformly.

	@CNN	@BreitbartNews	@dailykos
1	PowerZ	Robert	Two Thanks
2	Elissa Weldon	Lee Peace	Catherine Daligga
3	Tess Eastment	Wynn Marlow	exmearden
4	Chris_Dawson	Logan Churchwell	Faith Gardner
5	carol kinstle	Peter Schweizer	Andrew Thornton
6	erinmclaughlin	Breitbart Sports	UnreasonableFridays
7	Taylor Ward	Jon Fleischman	DKos Top Comments
8	Jennifer Z. Deaton	Nate Church	2016 relitigator
9	Pam Benson	Daniel Nussbaum	Daily Kos
10	amy entelis	Noah Dulis	Walter Einkenel
11	Grace Bohnhoff	Jon David Kahn	Candelaria Vargas
12	kate lazarus	Breitbart California	Mara Schechter
13	Newstron	Ken Klukowski	Emi Feldman
14	Becky Brittain	pam key	The Soulful Negress
15	CNN Ballot Bowl	Auntie Hollywood	Kim Soffen

After adjustment, PPR returns a more localized cluster. Instead of the highly visible public faces of the three seed organizations, the individuals in this table serve a central role to the internal organization (e.g. editors and writers). Depending on the application, one might prefer the results in Table 1 or Table 2.

three different seed nodes: @CNN, @BreitbartNews, and @dailykos, the Twitter accounts of three different types of media outlets that exhibit distinct political leanings (legacy broadcast news, online right-wing and online left-wing). For @CNN, all top 15 handles ranked by the PPR vector are its subsidiary accounts and its celebrity reporters and anchors (like Wolf Blitzer and Anderson Cooper), except for one account, Pope Francis, who enjoys an extremely larger following. The top 15 handles for @BreitbartNews are a mixed bag of influential conservatives (like Sean Hannity and Ann Coulter) and Breitbart’s editors/writers. However, the top 15 handles returned to @dailykos by the PPR vector are all famous liberal personalities not directly affiliated with Daily Kos, but one, its founder Markos Moulitsas. Those people range from democratic politicians to liberal media personalities and journalists, such as Hillary Clinton, Stephen Colbert, and Rachel Maddow. All the handles align with the characteristics of their respective media outlets, attesting to the clustering effectiveness. However, it is worth noting that the top handles ranked by the PPR vector tend to be popular handles with millions of followers. This shows that the PPR vector’s preference for high in-degree nodes.

In contrast, for each of the three seeds, adjusted PPR finds accounts that are more central to the internal functioning of these organizations. Table 2 lists those accounts. The bias adjustment also greatly benefits from a degree regularization [Qin and Rohe, 2013]. For @CNN, those handles include primarily its own staff/producers/journalists (like Elissa Weldon, Chris_Dawson, and Grace Bohnhoff), a freelance journalist (Tess Eastment). The pattern is similar for @BreitbartNews and @dailykos, their top 15 handles including their own journalists, editors as well as related writers/campaigners/activists. The general pattern is that the adjustment returns editors, journalists and staff working within each media outlet. As such, the adjustment is useful for identifying a more localized cluster.

1.2 Main contributions

The main contributions of the paper are (a) a simple and interpretable form for the PPR vector and (b) a statistical guarantee for clustering with the adjusted PPR vector.

- (a) This paper reveals a simple two-stage form of the PPR vector under the population (expectation) DC-SBM. Consider the v -th element of the PPR vector as the probability of sampling node v in a sample of size 1 from the stationary distribution of the personalized random walk. This inclusion probability is akin to stratified sampling:

The inclusion probability for node v is the product of two separate probabilities. First, the probability that the personalized random walk samples any node in v 's block. Second, the probability that the personalized random walk selects node v , conditional on sampling that block.

Both of these probabilities have simple expressions. If there are K blocks in the graph, then the block-wise probability comes from the PPR vector of a graph with K vertices, with edge weights specified by the “block connection matrix” in the DC-SBM. The second probability is proportional to the degree of node v . In addition to the population results, Theorem 2 demonstrates that when the graph is random, the PPR vector concentrates around its population (expectation) under certain conditions.

- (b) This paper identifies two sources of bias of using a PPR vector for local clustering under the DC-SBM – the ancillary effects of heterogeneous node degrees and block degrees. With this finding, the paper examines a simple bias adjustment that remedies the two biases simultaneously and suggests conditions when the adjusted PPR can be used to return the correct local cluster. In other words,

PPR clustering with the adjustment achieves the precise identification of the local cluster, provided the graph is sufficiently dense.

These results establish statistical performance (consistency) of PPR clustering under the DC-SBM, in the sparse regime where the minimum expected degree grows logarithmically with the number of nodes in the network. Our results provide an element-wise perturbation bound for PPR vectors, that allows the number of clusters to grow with the size of graphs, and generalize to a directed graph setting as PageRank does.

The rest of the paper proceeds as follows. Section 2 formally introduces the PPR method and some of the known results. Section 2 also introduces the degree-corrected stochastic block model. Section 3 gives a population analysis of the PPR clustering under directed block model graphs. Section 4 provides concentration results for the PPR vector when the graph is random and provides a statistical guarantee on the PPR local clustering method. Section 5 presents several numerical results showing the effectiveness of the PPR clustering. Section 6 illustrates the PPR clustering through the massive Twitter friendship graph and demonstrates the benefits of a smoothing step in the PPR adjustment.

2 Preliminaries

Throughout this paper, let $G = (V, E)$ denotes an unweighted and connected graph, where E is the edge set and V is the set of vertices indexed by $1, \dots, N$. When G is an undirected and unweighted graph, encode

E into a binary *adjacency* matrix $A \in \{0, 1\}^{N \times N}$ with $A_{uv} = A_{vu} = 1$ if and only if edge (u, v) appears in E . Define a diagonal matrix $D = \text{diag}(d_1, \dots, d_N)$ and the *graph transition* matrix P as follows:

$$d_u = \sum_{v \in V} A_{uv} \quad \text{and} \quad P = D^{-1}A.$$

When G is a directed graph, the adjacency matrix $A \in \{0, 1\}^{N \times N}$ accordingly becomes asymmetric with $A_{uv} = 1$ if and only if edge $(u, v) \in E$, and the graph transition matrix is defined as

$$P = [D^{\text{out}}]^{-1}A,$$

where $D^{\text{out}} = \text{diag}(d_1^{\text{out}}, \dots, d_N^{\text{out}})$ and $d_u^{\text{out}} = \sum_{v \in V} A_{uv}$ is the number of edges leaving from node u . In addition, define $D^{\text{in}} = \text{diag}(d_1^{\text{in}}, \dots, d_N^{\text{in}})$ where $d_v^{\text{in}} = \sum_{u \in V} A_{uv}$ is the number of edges pointing to node v .

2.1 Personalized PageRank and the local clustering algorithm

The personalized PageRank (PPR) is an extension of Google’s PageRank [Brin and Page, 1998, Haveliwala, 2003]. To illustrate, consider a personalized random walk (or originally called “surfing”) on the graph $G = (V, E)$ with a *seed node* $v_0 \in V$. At each step, the random walker either restarts from the seed node v_0 with probability α (called the *teleportation constant*) or continues the random walk from the current node to a neighbor uniformly at random. The *personalized PageRank vector* $p \in [0, 1]^N$ is the stationary distribution of this process, thus the solution to the equation

$$p^\top = \alpha \pi^\top + (1 - \alpha)p^\top P, \tag{1}$$

where P is the graph transition matrix, and π is the elementary unit vector in the direction of seed node v_0 . Here p is a column vector normalized by a positive scalar such that its elements sum to 1, and without loss of generality, we set $v_0 = 1$ and thus $\pi = (1, 0, \dots, 0)^\top$.

In general, the *preference vector* π does not have to be an elementary unit vector, but any probability distribution on V . For example, when $\pi = (1/N, \dots, 1/N)^\top$, PPR is equivalent to ordinary PageRank. Moreover, the PPR vector is a linear function of the preference vector. That is, let $p(\pi_1)$ and $p(\pi_2)$ be two PPR vectors corresponding to two preference vectors π_1 and π_2 respectively. Then, for a new preference vector that is a convex combination of π_i , the resulting PPR vector is constructive of $p(\pi_i)$,

$$p(w_1\pi_1 + w_2\pi_2) = w_1p(\pi_1) + w_2p(\pi_2),$$

where $w_i \geq 0$ and $w_1 + w_2 = 1$. Define Π to be an $N \times N$ matrix with repeating rows π^\top , and let $Q = \alpha\Pi + (1 - \alpha)P$, then Q is the Markov transition matrix for the stochastic process and Equation (1) becomes $p^\top = p^\top Q$. Below are some useful properties of the PageRank vector (also see Haveliwala [2003], Jeh and Widom [2003] and Appendix A).

Proposition 1. *For any fixed $\alpha \in (0, 1]$, the PPR vector p is*

- (a) *the left leading eigenvector of Q , associated with the simple eigenvalue 1; and*

(b) the infinite sum of landing probability $\{(P^s)^\top \pi\}_{s=0}^\infty$ with weights $\phi = \{\alpha(1-\alpha)^s\}_{s=0}^\infty$,

$$p^\top = \alpha \sum_{s=0}^{\infty} (1-\alpha)^s \pi^\top P^s. \quad (2)$$

Berkhin [2006] gives an iterative algorithm based on Proposition 1 to approximate the PPR vector (that scales to large graphs); each update requires only neighborhood information of one visited vertex. A few lines of linear algebra show that the PPR vector is equivalent to the solution to the linear system

$$p^\top = \alpha' \pi^\top + (1-\alpha') p^\top W,$$

where $W = (I + P)/2$ is the lazy graph transition matrix and $\alpha' = \alpha/(2-\alpha)$. Using this fact, Algorithm 1 approximates the PPR vector in running time of order $\mathcal{O}(\frac{1}{\epsilon\alpha})$, by reaching at most $\frac{2}{\epsilon(1-\alpha)}$ vertices. The following proposition gives a guarantee on the approximation error for this algorithm in terms of the *tolerance* parameter and the degrees of visited nodes.

Proposition 2 (Entrywise approximation error [Andersen et al., 2006]). *Let p be a PPR vector, and let $p^\epsilon \in [0, 1]^N$ be an approximate PPR vector computed by Algorithm 1 with a tolerance $\epsilon > 0$. For any vertex u that is sampled in Algorithm 1,*

$$|p_u - p_u^\epsilon| \leq \epsilon d_u.$$

Proposition 2 ensures that for any fixed graph, the approximate PPR vector is arbitrarily close to the exact PPR vector, as long as the tolerance $\epsilon > 0$ is sufficiently small. Appendix A contains a proof of this proposition for completeness. Given a seed node in the graph, Algorithm 2 uses the approximate PPR vector from Algorithm 1 and returns a set of nodes with the largest corresponding values in the *adjusted personalized PageRank* (aPPR) vector, which is defined as

$$p_v^* = \frac{p_v}{d_v}, \text{ for } v = 1, 2, \dots, N.$$

The aPPR vector was previously proposed in Andersen et al. [2006]. Algorithm 1 and 2 operate on undirected graphs. We will generalize them to directed graphs in Section 3 thanks to a simplified and interpretable form for the PPR vector.

Algorithm 1 Approximate PPR Vector (undirected) [Andersen et al., 2006]

Require: Undirected graph G , preference vector π , teleportation constant α , and tolerance ϵ .

Initialize $p \leftarrow 0$, $r \leftarrow \pi$, $\alpha' \leftarrow \alpha/(2-\alpha)$.

while $\exists u \in V$ such that $r_u \geq \epsilon d_u$ **do**

Uniformly sample a vertex u satisfying $r_u \geq \epsilon d_u$.

$p_u \leftarrow p_u + \alpha' r_u$.

for $v : (u, v) \in E$ **do**

$r_v \leftarrow r_v + (1-\alpha') r_u / (2d_u)$.

end for

$r_u \leftarrow (1-\alpha') r_u / 2$.

end while

Return: ϵ -approximate PPR vector p .

Algorithm 2 PPR Clustering (undirected)

Require: Undirected graph G , seed node v_0 , and the desired size of local cluster n .

- 1: Calculate the approximate PPR vector p (Algorithm 1).
- 2: Adjust the PPR vector p by node degrees, $p_v^* \leftarrow p_v/d_v$.
- 3: Rank all vertices according to the adjusted PPR vector p^* .

Return: local cluster – n top-ranking nodes.

2.2 Stochastic block model

In the stochastic block model (SBM), each node belongs to one of K blocks. The presence of each edge corresponds to an independent Bernoulli random variable, where the probability of an edge between any two nodes depends only on the block memberships of two nodes [Holland et al., 1983]. The formal definition is as follows.

Definition 1. For a vertex set $V = \{1, 2, \dots, N\}$, let $z : \{1, 2, \dots, N\} \rightarrow \{1, 2, \dots, K\}$ partition the N nodes into K blocks, so $z(v)$ is the block membership of vertex v . Let \mathbf{B} be a $K \times K$ matrix with all entries range in $[0, 1]$. Under the SBM, the probability of an edge between u and v is $\mathbf{B}_{z(u)z(v)}$. That is, $A_{uv} \mid z(u), z(v) \stackrel{\text{ind.}}{\sim} \text{Bernoulli}(\mathbf{B}_{z(u)z(v)})$, for any $u, v \in \{1, 2, \dots, N\}$.

Under the ordinary SBM, nodes in the same block have the same expected degree. One extension is the degree-corrected stochastic block model (DC-SBM), which adds a series of parameters ($\theta_v > 0$ for every vertex v) to create more heterogeneous node degrees [Karrer and Newman, 2011]. Let \mathbf{B} be a $K \times K$ matrix with $\mathbf{B}_{ij} > 0$ for any i and j . Then the probability of an edge between u and v is $\theta_u \theta_v \mathbf{B}_{z(u)z(v)}$. That is,

$$A_{uv} \mid z(u), z(v) \stackrel{\text{ind.}}{\sim} \text{Bernoulli}(\theta_u \theta_v \mathbf{B}_{z(u)z(v)}),$$

for $u, v \in \{1, 2, \dots, N\}$. Since θ_v 's are arbitrary to a multiplicative constant which can be absorbed into \mathbf{B} , Karrer and Newman [2011] suggest imposing the constraint that the θ_v 's sum to 1 within each block. That is, $\sum_{v:z(v)=i} \theta_v = 1$ for all $i = 1, 2, \dots, K$. With this constraint, \mathbf{B}_{ij} represents the expected number of edges between block i and j if $i \neq j$, and twice of that if $i = j$. Throughout this paper, we presume \mathbf{B} is positive definite ² and all blocks are connected (we ignore any blocks that are isolated from the seed). The DC-SBM can be generalized to directed graphs by giving each node two parameters, θ_v^{in} and θ_v^{out} , controlling its in-degree and out-degree respectively [Zhu et al., 2013]. Then, the presence of a directed edge from u to v , given the block memberships, corresponds to an independent Bernoulli random variable,

$$A_{uv} \mid z(u), z(v) \stackrel{\text{ind.}}{\sim} \text{Bernoulli}(\theta_u^{\text{out}} \theta_v^{\text{in}} \mathbf{B}_{z(u)z(v)}).$$

In order to make the model identifiable, we need to impose a structural constraint on θ^{in} 's and θ^{out} 's, that both of them sum up to 1 within each block,

$$\sum_{v:z(v)=i} \theta_v^{\text{in}} = \sum_{v:z(v)=i} \theta_v^{\text{out}} = 1, \text{ for any } i = 1, 2, \dots, K.$$

Because the off-diagonal elements of \mathbf{B} can be interpreted as the expected number of edges between blocks, we define the block in-degree and block out-degree to be the total number of incoming edges and outgoing

²This prevents scenarios where edges are unlikely within blocks and more likely between blocks. In such scenarios, local clustering needs to be reimagined cautiously. See Supplementary Materials S2 for additional details about generalizations.

edges respectively, that is, $\mathbf{d}_j^{\text{in}} = \sum_{i=1}^K \mathbf{B}_{ij}$, and $\mathbf{d}_i^{\text{out}} = \sum_{j=1}^K \mathbf{B}_{ij}$.

3 Population Analysis of PageRank

In this section, we analyze the PPR vector of the expected adjacency matrix under the DC-SBM. This provides a simple representation of the PPR vector that motivates (1) the bias adjustment and (2) the generalization of Algorithm 1 and 2 to directed graphs.

We use three distinct typefaces to denote three classes of objects. Calligraphic typeface is given to the population version of any observable quantities in random graphs, such as graph adjacency matrix and node degrees (e.g. Equation (3)). Normal typeface is given to unobserved model parameters, such as block membership and degree parameters θ_i . Bold face is given to all block-level quantities and parameters like \mathbf{B} and $\mathbf{d}_i^{\text{out}}$.

Define the population graph adjacency matrix,

$$\mathcal{A} = \mathbb{E}(A \mid z(1), z(2), \dots, z(N)), \quad (3)$$

to be the expectation of random adjacency matrix A . Let $Z \in \{0, 1\}^{N \times K}$ be the block membership matrix with $Z_{vi} = 1$ if and only if vertex v belongs to block i , and define diagonal matrices Θ^{in} and Θ^{out} with entries θ^{in} 's and θ^{out} 's respectively. Then, under the directed DC-SBM with K blocks and parameters $\{\mathbf{B}, Z, \Theta^{\text{in}}, \Theta^{\text{out}}\}$, $\mathcal{A} \in \mathbb{R}^{K \times K}$ can be compactly expressed as

$$\mathcal{A} = \Theta^{\text{out}} Z \mathbf{B} Z^{\top} \Theta^{\text{in}}.$$

Accordingly, we define the population node degrees and the population transition matrix, $\mathcal{d}_u^{\text{in}} = \sum_{v \in V} \mathcal{A}_{uv}$, $\mathcal{d}_v^{\text{out}} = \sum_{u \in V} \mathcal{A}_{uv}$, and $\mathcal{P} = [\mathcal{D}^{\text{out}}]^{-1} \mathcal{A}$, where \mathcal{D}^{in} and \mathcal{D}^{out} are the diagonal matrices of the population node in-degrees $\mathcal{d}_u^{\text{in}}$'s and out-degrees $\mathcal{d}_v^{\text{out}}$'s respectively. Let $\boldsymbol{\rho}$ be the population PPR vector (i.e., the solution to equation $\boldsymbol{\rho}^{\top} = \alpha \boldsymbol{\pi}^{\top} + (1 - \alpha) \boldsymbol{\rho}^{\top} \mathcal{P}$) and let $\boldsymbol{\rho}^* = [\mathcal{D}^{\text{in}}]^{-1} \boldsymbol{\rho}$ be the population aPPR vector.

In addition, define the *block transition matrix* $\mathbf{P} \in \mathbb{R}^{K \times K}$ as

$$\mathbf{P} = [\mathbf{D}^{\text{out}}]^{-1} \mathbf{B}, \quad (4)$$

where $\mathbf{D}^{\text{in}} \in \mathbb{R}^{K \times K}$ and $\mathbf{D}^{\text{out}} \in \mathbb{R}^{K \times K}$ are diagonal matrices of the block in-degrees \mathbf{d}_i^{in} 's and out-degrees $\mathbf{d}_i^{\text{out}}$'s.

3.1 A representation of PPR vectors

This section provides a simple and interpretable form for PPR vectors under the population DC-SBM. To this end, we define the “*block-wise*” PPR vector $\mathbf{p} \in \mathbb{R}^K$ to be the unique solution to linear system

$$\mathbf{p}^{\top} = \alpha \boldsymbol{\pi}^{\top} + (1 - \alpha) \mathbf{p}^{\top} \mathbf{P}, \quad (5)$$

where $\boldsymbol{\pi} = Z^{\top} \boldsymbol{\pi} \in \mathbb{R}^K$ is the block-wise preference vector and \mathbf{P} is the block transition matrix in Equation (4). This treats the block connectivity matrix \mathbf{B} as a weighted adjacency matrix of blocks and the block of seed node as a seed block. To build up the relationship between PPR and the block-wise PPR, the next theorem gives an explicit form for PPR vectors which also reveals the sources of bias for local clustering.

Theorem 1 (Explicit form of PPR vectors). *Under the population directed DC-SBM with K blocks and parameters $\{\mathbf{B}, Z, \Theta^{\text{in}}, \Theta^{\text{out}}\}$,*

(a) *the population PPR vector $\boldsymbol{\rho} \in \mathbb{R}^N$ has elements*

$$\rho_u = \theta_u^{\text{in}} \mathbf{p}_{z(u)}$$

where \mathbf{p} is the block-wise PPR vector in Equation (5),

(b) *and the population aPPR vector $\boldsymbol{\rho}^* \in \mathbb{R}^N$ has elements*

$$\rho_u^* = \mathbf{p}_{z(u)}^* \tag{6}$$

where $\mathbf{p}^ = [\mathbf{D}^{\text{in}}]^{-1} \mathbf{p}$.*

Theorem 1 demonstrates that the PPR vector $\boldsymbol{\rho}$ decomposes into block-related information (\mathbf{p}) and node specific information (Θ). Within each block, the PPR values are proportional to the node degree parameters θ_v 's and sum up to the block-wise PPR value of the block. The proof of Theorem 1 (Appendix A) relies on a key observation (Appendix A.3) that the powers of population transition matrix, \mathcal{P}^s for $s = 1, 2, \dots$, have a similarly simple form and the node specific information components (i.e., $z(v)$ and θ_v) are invariant in s .

In order to justify the adjustment (Step 2) in Algorithm 2, we observe that the seed always has the highest population aPPR score. This turns out to be a key feature that facilitates the aPPR vector to recover a local cluster correctly, so we state it in the following lemma.

Lemma 1 (The largest entry of aPPR vector). *Under the population DC-SBM, assume that the minimum expected degree is positive, that is, $\min_{v \in V} \mathcal{d}_v > 0$. Then, for any fixed $\alpha > 0$, the population aPPR vector $\boldsymbol{\rho}^*$ has the strictly largest entry corresponding to the seed node,*

$$\rho_{v_0}^* > \rho_v^*, \text{ for any } v \neq v_0.$$

On the other hand, this is not generally true for a PPR vector.

When $\alpha = 0$ (i.e., no teleportation), the PPR vector becomes the limiting distribution of a standard random walk and all entries of the aPPR vector are equal (Appendix A). Lemma 1 (applied to block-wise PPR vectors) and Theorem 1 together identify two sources of bias for PPR vectors and suggest a justification for the degree adjustment, which we discuss in order:

- (i) Both node degree heterogeneity (Θ) and block size imbalance (\mathbf{D}) confound the identification of local cluster by the PPR vector. In particular, suppose vertex v belongs to a block $z(v) = i$ other than 1. PPR vector assigns it a score $\theta_v \mathbf{p}_i$, where \mathbf{p}_i is the block-wise PPR of block i , and θ_v is the parameter specifically controlling the degree of v . Then, node v may rank at the top, if θ_v is large enough. Furthermore, Lemma 1 implies that \mathbf{p}_1 is not necessarily the largest due to block degree heterogeneity. Specifically, if block i has an exceedingly high block degree, it is likely that $\boldsymbol{\rho}$ fails to down-rank node v vis-a-vis those nodes of block 1.
- (ii) Adjusted personalized PageRank removes the node and the block degree heterogeneity simultaneously, and perfectly recovers the local cluster. To see this, note that \mathbf{p}^* is the adjusted version of block-wise PPR vector. From Lemma 1, \mathbf{p}_1^* is the largest entry of \mathbf{p}^* . From Equation 6, the aPPR vector assigns

any vertex v a score $\mathbf{p}_{z(v)}^*$. Hence, nodes with the highest value of ρ^* belong to block 1, which is precisely the desired local cluster.

Note that the PPR vector can still be biased for local clustering even under the classic SBM. To see this, set the matrix Θ to the identity matrix in Theorem 1. In this case, the heterogeneous block degrees still confound the PPR vector (Section 5.2); there is generally no guarantee for \mathbf{p}_1 to appear on the top (due to Lemma 1), unless there are further symmetry conditions. Kloumann et al. [2017] uses such one scenario. As a byproduct of our analysis, we extend their results under the DC-SBM with the symmetric conditions (see Supplementary Materials S3 to the paper).

3.2 Local clustering on directed graphs

In light of the clean form of PPR vectors under the DC-SBM, one can modify Algorithm 1 and 2 to operate on a directed graph accordingly. To this end, note that the transition matrix of a directed graph requires node out-degrees, hence Algorithm 1 examines only the edges leaving visited nodes. Consequently it suffices to replace d_u 's in Algorithm 1 by d_u^{out} 's (Algorithm 3). Proposition 2 applies to Algorithm 3 as well, and one can approximate the PPR vector provided the out-degrees of visited nodes can be observed and the tolerance parameter $\epsilon > 0$ is sufficiently small.

To perform local clustering on a directed graph, Algorithm 4 adjusts the approximate PPR vectors from Algorithm 3 by node in-degrees, that is,

$$p_v^* = \frac{p_v}{d_v^{\text{in}}}, \text{ for } v = 1, 2, \dots, N.$$

Another option is regularized adjustment, which produces the *regularized* PPR (rPPR) vector,

$$p_v^\tau = \frac{p_v}{d_v^{\text{in}} + \tau}, \text{ for } v = 1, 2, \dots, N,$$

where $\tau > 0$ is the regularization parameter. The regularized adjustment greatly stabilize the PPR clustering in practice, by removing nodes with extremely low in-degrees (see Section 6 for more details). Adjusted PPR for directed graphs is a local algorithm so long as d^{in} is available with a local query, for example, the Twitter friendship graph.

Algorithm 3 Approximate PPR Vector (directed)

Require: Directed graph G , preference vector π , teleportation constant α , and tolerance ϵ .

Initialize $p \leftarrow 0$, $r \leftarrow \pi$, $\alpha' \leftarrow \alpha/(2 - \alpha)$.

while $\exists u \in V$ such that $r_u \geq \epsilon d_u^{\text{out}}$ **do**

Sample a vertex u uniformly at random, satisfying $r_u \geq \epsilon d_u^{\text{out}}$.

$p_u \leftarrow p_u + \alpha' r_u$.

for $v : (u, v) \in E$ **do**

$r_v \leftarrow r_v + (1 - \alpha') r_u / (2 d_u^{\text{out}})$.

end for

$r_u \leftarrow (1 - \alpha') r_u / 2$.

end while

Return: ϵ -approximate PPR vector p .

Algorithm 4 PPR Clustering (directed)

Require: Directed graph G , seed node v_0 , the desired size of local cluster n , and an optional regularization parameter τ .

- 1: Calculate the approximate PPR vector p (Algorithm 3).
- 2: Adjust the PPR vector p with:
 - Option (a): node in-degrees, $p_v^* \leftarrow p_v/d_v^{\text{in}}$,
 - Option (b): regularized node in-degrees, $p_v^\tau \leftarrow p_v/(d_v^{\text{in}} + \tau)$.
- 3: Rank all vertices according to the aPPR vector p^* or p^τ .

Return: local cluster – n top-ranking nodes.

4 Personalized PageRank in Random Graphs

This section establishes several concentration results for the local clustering algorithm using the adjusted PPR vector (Algorithm 2 and 4) under the DC-SBM. The results show that if the graph is generated from the DC-SBM, then PPR clustering returns the desired local cluster with high probability. Since in Algorithm 4, the calculation for PPR vectors only relies on node out-degrees and the adjustment step solely utilizes node in-degrees, it is not difficult to distinguish d^{in} and d^{out} . Thus, we state the results in undirected graphs for simplicity. One can draw the analogous conclusions for directed graphs by tracing the proof step by step.

We first present a useful tool that controls the entrywise errors of a PPR vector in random graphs. Recall that $\boldsymbol{\rho}$ is the stationary distribution of probability transition matrix $\mathcal{Q} = \alpha\Pi + (1 - \alpha)\mathcal{P}$. For any vector $x \in \mathbb{R}^n$, define the vector infinity norm as $\|x\|_\infty = \max_i |x_i|$. The following theorem bounds the entrywise error of the stationary distribution of \mathcal{Q} .

Theorem 2 (Concentration of the PPR vectors). *Let $G = (V, E)$ be a graph of N vertices generated from the DC-SBM with K blocks and parameters $\{\mathbf{B}, Z, \Theta\}$. Let p and $\boldsymbol{\rho}$ be the PPR vector corresponding to random transition matrix P and its population version \mathcal{P} respectively, with the same teleportation constant α . Let $p^*, \boldsymbol{\rho}^* \in [0, 1]^N$ be the adjusted PPR vector of p and $\boldsymbol{\rho}$. Let δ be the average expected node degrees, that is, $\delta = \frac{1}{N} \sum_{v \in V} d_v$. Assume that $\rho = \frac{\max_{v \in V} d_v}{\min_{v \in V} d_v}$ is bounded by some finite constant and that*

$$\delta > c_0(1 - \alpha)^2 \log N, \tag{7}$$

for some sufficiently large constant $c_0 > 0$. Then, with probability at least $1 - \mathcal{O}(N^{-5})$,

$$\frac{\|p - \boldsymbol{\rho}\|_\infty}{\|\boldsymbol{\rho}\|_\infty} \leq c_1(1 - \alpha) \sqrt{\frac{\log N}{\delta}}, \quad \text{and} \quad \frac{\|p^* - \boldsymbol{\rho}^*\|_\infty}{\|\boldsymbol{\rho}^*\|_\infty} \leq c_2(1 - \alpha) \sqrt{\frac{\log N}{\delta}},$$

for some sufficiently large constant $c_1, c_2 > 0$.

The proof of Theorem 2 invokes the elementary eigenvector perturbation bound for asymmetric matrices, an analog to the celebrated Davis-Kahan $\sin \Theta$ theorem [Davis and Kahan, 1970], and the novel leave-one-out technique due to Chen et al. [2019]. The detailed proof is given in the Supplementary Materials S1 to the paper.

Theorem 2 demonstrates that if the expected average degree δ exceeds $(1 - \alpha)^2 \log N$ to some sufficiently large extent, then with high probability, the random aPPR vector concentrates around the population aPPR vector in terms of all entries. In fact, the concentration statement holds for any valid preference vector π . Hence, the classic PageRank vector and some other variants also enjoy the entrywise error bounds, so long as they can be written as the solution to the linear system (1).

Next, we introduce a separation measure of the DC-SBM. Recall that one can conduct a local clustering task by selecting nodes ranked by the adjusted PPR vector p^* . In the population version, it is equivalent to distinguishing between \mathbf{p}_1^* and \mathbf{p}_k^* , for all $k = 2, 3, \dots, K$, which also characterizes the distance from the desired local cluster (block 1) to its complement set (the other blocks). Only if they are sufficiently separated, can the local cluster be identifiable in the sample. Due to Lemma 1, we assume without loss of generality that the second block has the second highest value in the “block-wise” aPPR vector, that is, $\mathbf{p}_1^* > \mathbf{p}_2^* \geq \mathbf{p}_k^*$ for $k = 3, 4, \dots, K$. Then, we define the *separation measure* $\Delta_\alpha \in (0, 1]$,

$$\Delta_\alpha = \frac{\mathbf{p}_1^* - \mathbf{p}_2^*}{\mathbf{p}_1^*},$$

which turns out to be crucial in determining the sample complexity required to guarantee the exact recovery. We remark that Δ_α is an increasing function of the teleportation constant, hence the subscript α .

With Theorem 2 and the separation measure, we then give following corollary that bounds the accuracy of Algorithm 2, in terms of graph edge density.

Corollary 1 (Exact recovery by adjusted PPR vector). *For any seed nodes, let $C \subset V$ be the local cluster of n nodes returned by Algorithm 2 with teleportation constant α and tolerance ϵ , and $\mathcal{C} \subset V$ be the nodes in the seed node’s block. Assume that $\rho < c_0$, $\epsilon \leq c_1(1 - \alpha)\mathbf{p}_1^*\sqrt{\log N/\delta}$, and that*

$$\delta > 16c_2 \left(\frac{1 - \alpha}{\Delta_\alpha} \right)^2 \log N, \quad (8)$$

for some sufficiently large constants $c_0, c_1, c_2 > 0$. If the desired size of the local cluster $n = |\mathcal{C}|$, then with probability at least $1 - \mathcal{O}(N^{-5})$, we have $C = \mathcal{C}$.

The proof of Corollary 1 is presented in Appendix A. We make a few remarks:

- (i) Corollary 1 demonstrates that Algorithm 2 works under a sparse scenario, where the number of edges is exceedingly small in proportion to the number of possible edges in the network. To reach the entrywise control of the aPPR vector and the sufficient separation of local cluster from others, the theorem calls for the expected node degree δ to grow with only a fraction (for any fixed teleportation constant α) of the logarithm of the size of the network, $\log N$. In other words, Algorithm 2 requires a sample complexity (the number of edges) of order

$$\left(\frac{1 - \alpha}{\Delta_\alpha} \right)^2 N \log N.$$

- (ii) The results show that α leverages between the sampling complexity and statistical performance of PPR clustering. To see this, rearrange condition (8),

$$\left(\frac{1 - \alpha}{\Delta_\alpha} \right)^2 < \frac{c'\delta}{\log N},$$

for some small enough constant $c' > 0$. As α increases, the left hand side is decreasing to zero thus making the condition more likely to hold. On the other hand, as α increases, the tolerance ϵ must decrease at rate $\mathcal{O}(1 - \alpha)$ in order to guarantee an entrywise control of p^ϵ analogous to the form in Theorem 2 (Appendix A). More intuitively, if ϵ does not decrease, then as α goes to one, Algorithm

1 may terminate early without reaching all vertices in the desired local cluster. In sum, Algorithm 1 and 3 need at least $\mathcal{O}\left(\frac{1}{\alpha(1-\alpha)}\right)$ queries (see Supplementary Materials S2 for an example). This implies that one can approach the conditions in Corollary 1 by setting the teleportation constant sufficiently large, while the computational burden can increase as $\alpha \rightarrow 1$.

5 Simulation Studies

This section compares the PPR vector and the aPPR vector. The results show the effectiveness and robustness of aPPR vector in detecting a local cluster. Experiment 1 utilizes the DC-SBM with a power-law degree distribution and investigates the effects of heterogeneous node degrees. Experiment 2 uses the SBM with unequal block sizes to study the influences of heterogeneous block degrees. Experiment 3 generates networks from the SBM with equal block sizes and varying edge density to examine the efficacy of PPR methods in sparse graphs.

In all simulations, we employ the block connectivity matrix \mathbf{B} with homogeneous diagonal elements, $\mathbf{B}_{ii} = b_1$, and homogeneous off-diagonal elements, $\mathbf{B}_{ij} = b_2$ for any $i \neq j$. Define the signal-to-noise ratio (SNR) to be the expected number of in-block edges divided by the expected number of out-block edges, that is, $b_1/(b_2(K-1))$, where K is the number of blocks. In particular, we set the SNR to 1.5 and choose the teleportation constant of $\alpha = 0.15$ throughout the section. Additional simulation results (illustrating the Theorem 2) are available from Supplementary Materials S2.

5.1 Experiment 1

This experiment illustrates how node degree heterogeneity affects the discriminant power in identifying local cluster using a PPR vector or an aPPR vector. The results also illustrate the advantages of having multiple seed nodes. The Θ parameters from the DC-SBM are drawn from the power law distribution with lower bound $x_{\min} = 1$ and shape parameter $\beta = 2.5$. A random networks were sampled from the DC-SBM with $K = 3$, $N = 1500$ and equal block sampling proportions,

$$z(v) \stackrel{\text{i.i.d.}}{\sim} \text{Multinomial}\left(\frac{1}{3}, \frac{1}{3}, \frac{1}{3}\right),$$

for vertex $v = 1, 2, \dots, N$, whose expected average degree (δ) is set to 105. The PPR vector is calculated with one or ten seeds randomly chosen from block one.

Figure 1 plots PPR values (left two panels) and aPPR values (right two panels) of a random graph generated from the DC-SBM, excluding seed node(s). The upper two panels in Figure 1 contrast PPR and aPPR when there is only one seed node and the bottom two panels compare two vectors when ten seed nodes are used. The vertices from the local block in the SBM are colored in blue and the others are in yellow. The nodes are ordered first by block, then by node degree parameters θ (left is larger). A horizontal line is drawn for each block indicating the median of the aPPR values within that block.

With one seed node (upper two panels), the scatter plots has two clouds within each block. The upper cloud contains the immediate neighbors of the seed node. This separation disappears when multiple seed nodes are used (bottom two panels). To see the effect of node heterogeneity, the skewed distribution of PPR values in each block demonstrates its bias towards high degree node inside and outside of the seed nodes block in the SBM. In contrast, aPPR values are evenly distributed within blocks, verifying that aPPR vector removes the effects of node degree heterogeneity.

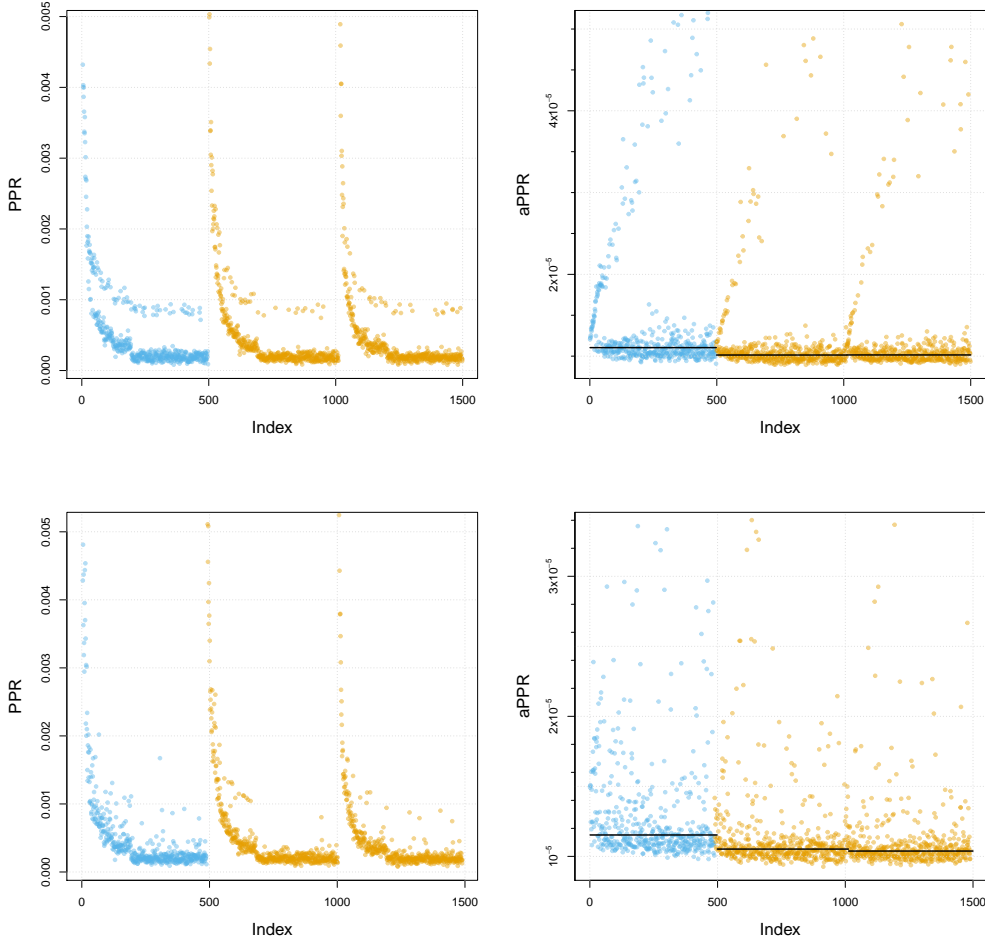


Figure 1: Comparison of PPR (left two panels) and aPPR (right two panels) under the DC-SBM with one seed node (upper two panels) and ten seed nodes (bottom two panels). Local cluster is in blue and other clusters are colored in yellow. Solid horizontal lines on right panels indicate the median of aPPR values within each cluster.

5.2 Experiment 2

This experiment compares PPR and aPPR under the SBM with block degree heterogeneity. A number of random networks were sampled from the SBM with $K = 3$, $N = 900$, and geometric block sampling proportions,

$$z(v) \stackrel{\text{i.i.d.}}{\sim} \text{Multinomial}(1, b, b^2), \quad (9)$$

where $b \in \{1.0, 1.2, 1.4, 1.6, 1.8, 2.0\}$. When b is larger, the population of nodes in each block becomes more unbalanced and thus inducing greater block degree heterogeneity. The block connectivity matrix \mathbf{B} is configured as described in the beginning of this section. The expected average degree (δ) is set to 70. For each sampled network, the size of the first block is assumed known to Algorithm 2. The PPR vector is calculated exactly in place of the approximation PPR vector (Step 1), with one seed randomly chosen from the first block.

The top panels of Figure 2 displays the PPR vector on an example network with $b = 1.4$, demonstrating

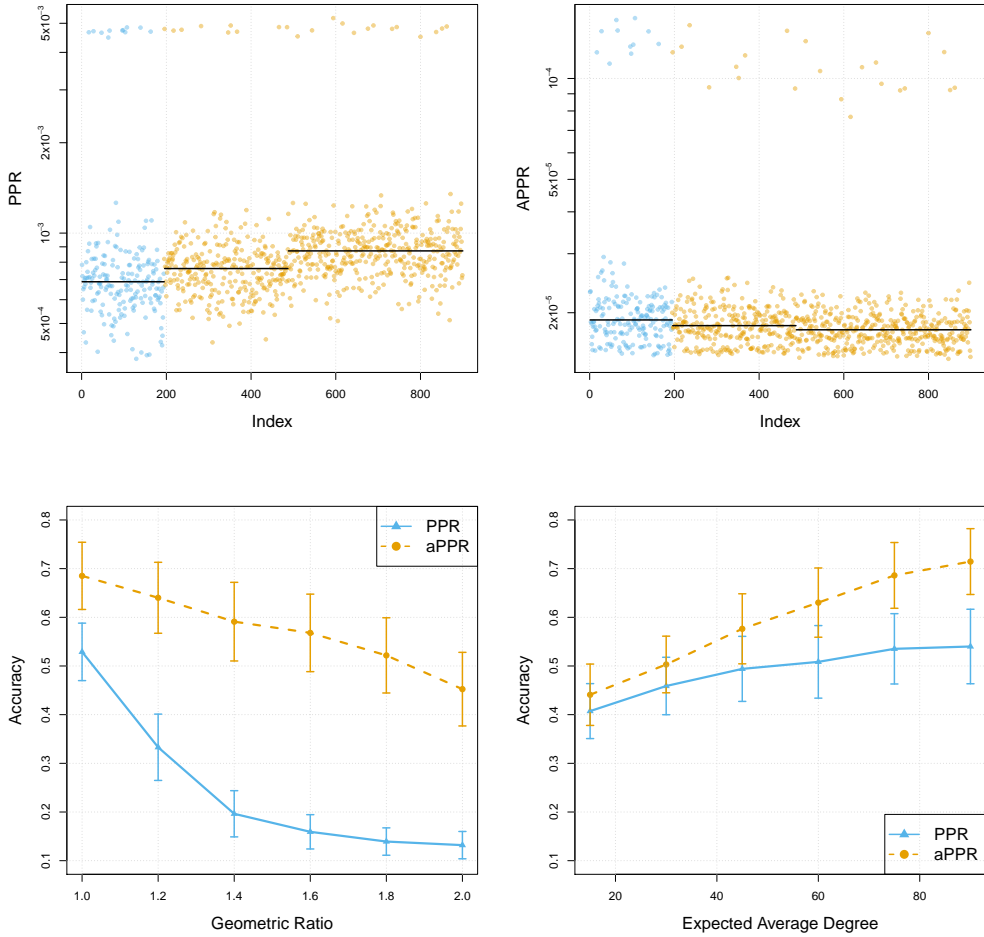


Figure 2: (Top) Simulated network generated from the classic SBM of 3 blocks with block degree heterogeneity. Three horizontal lines indicate the median of PPR and aPPR values within each cluster. (Bottom Left) Comparison of performance for PPR (triangles with solid line) and aPPR (circles with dashed line) under the SBM with different levels of block degree heterogeneity. (Bottom Right) Comparison of performance for PPR and aPPR under the four-parameters SBM with different sparsity. Error bars are drawn using standard deviation.

its preference toward the high degree block (the third block) over local cluster. Given the size of the first block, we measure the accuracy by the proportion of vertices belonging to the first block in the returned cluster. The bottom left panel of Figure 2 shows the accuracy of PPR and aPPR for six different values of b (i.e., the geometric ratio in distribution (9)) where each point is the average of 100 sampled network. The comparison demonstrates that the adjusted PPR vector corrects the bias of PPR caused by block heterogeneity. Moreover, block degree heterogeneity degrades the performance of both PPR and aPPR. Note that aPPR outperforms PPR even when $b = 1$; this is likely due to the fact that even when nodes have equal expected degrees in the SBM, the actual node degrees will be heterogeneous due to the randomness in the sampled graph. In a finite graph, this variability is enough to give aPPR an advantage over PPR. Asymptotically, this advantage should fade away [Kloumann et al., 2017].

5.3 Experiment 3

This experiment investigates the performance of PPR and aPPR under the SBM where there is no heterogeneity in the expected node degrees or block degrees. A number of random networks were sampled from the four-parameter stochastic block model, $\text{SBM}(K = 3, N = 900, b_1 = 0.6, b_2 = 0.2)$ [Rohe et al., 2011]. Under the four-parameter SBM, each of K blocks has equal size in expectation, N/K , and the probability of a connection between two nodes is b_2 if they are in two separate blocks, or b_1 if in the same one. In addition, the expected average degree varies, $\delta \in \{15, 30, 45, 60, 75, 90\}$. For every setting, the results are averaged over 100 samples of the network. The PPR vector is calculated with one seeds randomly chosen from block one. The bottom right panel of Figure 2 contrasts the accuracy of PPR and aPPR against six different values of expected average degree, showing that when the sampled graph has minimal degree heterogeneity, the adjusted PPR vector has only slightly higher accuracy than the PPR vector.

6 A Sample of Twitter

In this section, we provide a more detailed case study to illustrate the properties of different PPR vectors. We obtain a local cluster of nodes around the seed node @NBCPolitics (NBC Politics) in the Twitter friendship graph. In the Twitter graph, the nodes are called handles or accounts (e.g. @NBCPolitics) and if Twitter handle i follows Twitter handle j , then we define this as a directed edge (i, j) pointing from i to j . Affiliated with NBC news, NBC Politics specializes in political news coverage and has over 470k followers on Twitter (in-degree) and follows 145 handles (out-degree) as of December 2018. A brief look through @NBCPolitics’ following list reveals that it follows a wide range of accounts, from TV programs, reporters and editors affiliated with NBC, to media accounts and journalists of other news outlets as well as politicians.

Data on following and handle profile information were collected through the Standard Twitter Search API. We queried the Twitter friendship graph starting from the seed node @NBCPolitics, using Algorithm 3 with teleportation constant $\alpha = 0.15$ and termination parameter $\epsilon = 10^{-7}$, ending up with 5840 surrounding handles. Through this exercise, we intend to illustrate the properties and applications of local clustering using PPR, aPPR and rPPR vectors, where we set the regularization parameter τ to 100.

We first present the results of PPR. As Table 3 shows, the top 30 handles (except @NBCPolitics) with the highest PPR values are a combination of (i) NBC’s news related programs such as NBC News, TODAY and Meet the Press; (ii) NBC’s political reporters, anchors and editors, from well-known figures like Chuck Todd and Andrea Mitchell to less-known ones like Pete Williams (justice correspondent) and Mark Murray (senior political editor); (iii) other mainstream news outlets such as The Wall Street Journal, POLITICO, and TIME; and (iv) prominent public figures and politicians like Melania Trump, Bill Clinton and John McCain. In light of NBC’s status as a mainstream news outlet and the political focus of @NBCPolitics, such results make sound sense. It must also be noted that all the top 30 handles are direct friends of @NBCPolitics’s and have at least tens of thousands of followers. The median follower count is 1.4 million, suggesting high in-degrees. In fact, the pattern observed in the top 30 extends to the top 200 handles with the highest PPR values, which include NBC’s own programs, journalists, editors and staff; fellow mainstream media outlets and their staff; and prominent public figures, politicians and government institutions (see Supplementary Materials S4). The median in-degree of top 200 handles is around 184k, though there are four handles with less than one thousand followers. One important thing to notice is that among the top 200 handles, the first 139 are all directly followed by @NBCPolitics, with handles having high in-degrees generally ranked higher than those having low in-degrees (although @NBCPolitics follows 145 handles, 6 of them might have

Table 3: Top 30 handles of PPR with seed node @NBCPolitics and the teleportation constant $\alpha = 0.15$ in December 2018.

	Name	Followers	Description
1	Melania Trump	11242283	This account is run by the Office of First Lady Melania Trump...
2	The White House	17625630	Welcome to @WhiteHouse! Follow for the latest from President...
3	Chuck Todd	2032038	Moderator of @meetthepress and @nbcnews political director; ...
4	NBC News	6280551	The leading source of global news and info for more than 75 ...
5	NBC Nightly News	962290	Breaking news, in-depth reporting, context on news from ...
6	Andrea Mitchell	1737764	NBC News Chief Foreign Affairs Correspondent/anchor, Andrea ...
7	Savannah Guthrie	881669	Mom to Vale & Charley, TODAY Co-Anchor, Georgetown Law. ...
8	Joe Scarborough	2521215	With Malice Toward None
9	MSNBC	2261911	The place for in-depth analysis, political commentary and ...
10	Rachel Maddow MSNBC	9498076	I see political people...
11	Breaking News	9223158	
12	NBC News First Read	53847	The first place for news and analysis from the @NBCNews Poli...
13	TODAY	4276453	America's favorite morning show Snapchat: todayshow
14	Meet the Press	566713	Meet the Press is the longest-running television show in history ...
15	The Wall Street Journal	16188842	Breaking news and features from the WSJ.
16	Pete Williams	70062	NBC News Justice Correspondent. Covers US Supreme Court, ...
17	Mark Murray	97571	Mark Murray is the senior political editor for NBC News, ...
18	POLITICO	3695835	Nobody knows politics like POLITICO. Got a news tip for us? ...
19	Katy Tur	587474	MSNBC anchor @2pm, NBC News correspondent, author of NYT ...
20	Bill Clinton	10697521	Founder, Clinton Foundation and 42nd President of the United...
21	Kasie Hunt	381704	@NBCNews Capitol Hill Correspondent. Host, @KasieDC, Sundays...
22	TIME	15584815	Breaking news and current events from around the globe. Host...
23	Kelly O'Donnell	195765	White House Correspondent @NBCNews Veteran of Cap Hill & ...
24	John McCain	3181773	Memorial account for U.S. Senator John McCain, 1936-2018. To...
25	Peter Alexander	283522	@NBCNews White House Correspondent / Weekend @TODAYshow ...
26	Hallie Jackson	359099	Chief White House Correspondent / @NBCNews / @MSNBC Anchor ...
27	Kristen Welker	182244	@NBCNews White House Correspondent. Links and retweets ...
28	Carrie Dann	37119	..@NBCNews / @NBCPolitics. RTs not endorsements.
29	Willie Geist	807536	Host @NBC #SundayTODAY, Co-Host @Morning_Joe, Sunday ...
30	Morning Joe	563650	Live tweet during the show! Links to must-read op-eds ...

Through the PPR vector, the top 30 handles returned to @NBCPolitics include NBC's news related programs and celebrity reporters, comparable mainstream media outlets, as well as prominent political and public figures and institutions. Such results line up with its status as a mainstream political news source, demonstrating clustering effectiveness. Those Twitter handles tend to have millions of followers, showing the PPR vector's bias toward high in-degree.

privacy protection that has prevented us from accessing their information). The remaining handles on the list, although not directly followed by @NBCPolitics, include five handles associated with NBC, from its news anchor Lester Holt to its News International President. However, the majority of those indirectly followed by @NBCPolitics are mainly high profile political and public figures (like President Trump, Vice President Pence, Hillary Clinton, and Stephen Colbert), government organizations (like WhiteHouse Office of Cabinet Affairs and National Security Council), and mainstream news outlets (like New York Times, CNN and AP) and well-known journalists (like John Dickerson and Anderson Cooper). We can thus conclude that the PPR vector is biased toward popular accounts followed directly by the seed node or indirectly by its friends, reflecting the popular Twitter handles followed by them. This property of the PPR vector can be harnessed by researchers interested in identifying the upstream of a handle, i.e., those Twitter elites who are followed by and might influence the seed node and by extension its followers.

In contrast, the aPPR vector up-weights handles that are much less popular (i.e., those with low in-degrees). As shown in Table 2, the 30 handles with the highest aPPR values include NBC's reporters, writers, editors, producers, and programs, all of whom have a few hundred to a few thousand followers. The 30 handles also include those unaffiliated with NBC, such as director of a non-profit (Enroll America), director of digital programming at National Geographic, and @CNNPolitics' editor. All of them are professionally related to the seed node. This testifies to the applicability of aPPR for locating an idiosyncratic local cluster around a seed node. However, more than half (17) of the 30 handles are obscure and not directly followed by @NBCPolitics. The reason they appear on the list is probably that they have just one and at most a dozen

Table 4: Top 30 handles of aPPR with seed node @NBCPolitics and the teleportation constant $\alpha = 0.15$ in December 2018.

	Name	Followers	Description
1	Stephanie Palla	198	Enroll America National Regional Director...
2	Jennifer Sizemore	386	
3	Alissa Swango	441	Director of Digital Programming at @natgeo. All things ...
4	Making a Difference	670	@NBCNightlyNews' popular feature profiles ordinary ...
5	Ron Whittemore	1	
6	Svante Stockselius	3	
7	Greg Martin	1161	Political Booking Producer at @nbcnews @todayshow
8	Area Man	1	I am Area Man. I pwn your news feed.
9	CELESTIA ROBINSON	2	
10	NBC Field Notes	1390	NBC News correspondents and http://t.co/1eSopOQt8s ...
11	rob adams	2	
12	JL	2	
13	David Kelsey	1	
14	Hank Morris	1	
15	Jesse Marks	1	
16	Brayden Rainey	1	
17	child of the tiger	3	yet another activist twitter, fighting all those fun...
18	Julie Swango	4	
19	Author Dianne Kube	7	Dianne Kube is an Author with a passion, for family,...
20	Consider the Source	7	
21	Adam Edelman	2341	Political reporter @nbcnews. Wisconsin native, ...
22	Phil McCausland	2519	@NBCNews Digital reporter focused on the rural-urban...
23	Corky Siemaszko	2538	Senior Writer at NBC News Digital (former NY Daily ...
24	Sam Petulla	2588	Editor @cnnpolitics Usually looking for datasets. ...
25	Ken Strickland	2693	NBC News Washington Bureau Chief
26	Mike Mullen	7	
27	Elyse PG	2697	White House producer @nbcnews @USCAnnenberg alum ...
28	A. Johnson	2	Change your thoughts & you change your world. -Normal...
29	Steve Fenton	4	
30	Dobe Pitty Mami	13	

Through the aPPR vector, the top 30 handles returned to @NBCPolitics include some relevant handles (NBC's news team and their counterparts in other mainstream news organizations) and many obscure ones (handles with few followers and no profile descriptions). This results from the aPPR vector's bias toward extreme low degree and introduces noise to the clustering results.

followers (recall that aPPR divides by in-degree). In fact, 160 of the top 200 handles are not direct friends of @NBCPolitics; the median in-degree of the top 200 handles is merely 8 (Supplementary Materials S4). Those handles might have ended up on the list due to a combination of luck and, more importantly, their extremely low in-degrees. In this regard, noise can be introduced by the aPPR vector because it prioritizes handles with extremely low in-degrees that are possibly several degrees separated from the seed node.

To reduce noise, we applied a regularization step to the aPPR vector to remove those “distant” and small nodes while preserving the close and relevant ones. In Table 3, the majority of the top 30 handles with the highest regularized aPPR (i.e., rPPR) values have three- or four-digit numbers of followers. Similar to the aPPR results, they include NBC's news crew. But the difference is that the overwhelming majority (18) of the top 30 handles work at NBC. Some handles who work for other news organizations (e.g., Sam Petulla at @cnnpolitics and Emmanuelle Saliba at @Euronews) might have previously worked at NBC or have close connection with its news team. Even the four handles that are not directly followed by @NBCPolitics are interesting – they are non-profit organizations (NYC Clothing Bank and Voices United) and news-related individual or organization (James Miklaszewski and Social Headlines). This pattern can also be observed in the top 200 handles, 72 of whom are directly followed by @NBCPolitics. The overwhelming majority of those directly followed by it are affiliated with NBC, comprising its day-to-day news team, who enjoy much less publicity than the celebrity reporters. The remaining 128 of them, who are not directly followed by @NBCPolitics, actually also include 20 NBC's journalists and staff, such as Ray Farmer (NBC News photographer) and Jim Miklaszewski (chief Pentagon correspondent for NBC News). Others are non-profits like Vets Helping Heroes and professionals from other news organizations or companies such as WSJ, NFL

Table 5: Top 30 handles of rPPR with seed node @NBCPolitics and the teleportation constant $\alpha = 0.15$ in December 2018.

	Name	Followers	Description
1	Stephanie Palla	198	Enroll America National Regional Director http://t.co/X6jJIE...
2	Jennifer Sizemore	386	
3	Alissa Swango	441	Director of Digital Programming at @natgeo. All things food....
4	Making a Difference	670	@NBCNightlyNews' popular feature profiles ordinary people do...
5	Greg Martin	1161	Political Booking Producer at @abcnews @todayshow
6	NBC Field Notes	1390	NBC News correspondents and http://t.co/1eSopOQt8s reporters...
7	Adam Edelman	2341	Political reporter @abcnews. Wisconsin native, Bestchester ...
8	Phil McCausland	2519	@NBCNews Digital reporter focused on the rural-urban divide....
9	Corky Siemaszko	2538	Senior Writer at NBC News Digital (former NY Daily News ...
10	Sam Petulla	2588	Editor @cnnpolitics Usually looking for datasets. You can ...
11	Ken Strickland	2693	NBC News Washington Bureau Chief
12	Elyse PG	2697	White House producer @abcnews @USCAnnenberg alum LA kid ...
13	Hasani Gittens	3002	Level 29 Mage. Senior News Ed. @NBCNews. Sheriff of Nattahna...
14	Scott Foster	3464	Senior Producer, Washington @NBCNEWS @TODAYshow
15	Zach Haberman	3693	Lead Breaking News Editor, @NBCNews. Previously had other jobs...
16	Emmanuelle Saliba	4004	Head of Social Media Strategy @Euronews Launched #THECUBE ...
17	Alex Johnson	4371	News, data and analysis for @NBCNews; data geek; ...
18	Savannah Sellers	4637	News junkie. Host of NBC's "Stay Tuned" on Snapchat. Storyte...
19	NYC Clothing Bank	154	We distribute new, never-worn clothing and merchandise...
20	Shaquille Brewster	5362	@NBCNews Producer/Politics @HowardU Alum Journalist Pol...
21	Joey Scarborough	6277	NBC News Social Media Editor. New York Daily News Alum. RTs ...
22	Jane C. Timm	6478	@abcnews political reporter and fact checker. More fun than ...
23	Anthony Terrell	6827	Emmy Award winning journalist. Political observer. Covered ...
24	NBC News Videos	7838	The latest video from http://t.co/xPyvMOTEF6
25	Libby Leist	7946	Executive Producer @todayshow
26	Voices United	310	Voices United is a non profit educational organization ...
27	Social Headlines	344	Daily roundup of top social media and networking stories.
28	James Miklaszewski	337	Writer, Photographer, Editor, Director, Producer, Newshound ...
29	Courtney Kube	9494	NBC News National Security & Military Reporter...
30	Bob Corker	10042	Serving Tennesseans in the U.S. Senate

Through the rPPR vector, the top 30 handles returned to @NBCPolitics include much fewer low in-degree and obscure ones and many more moderately connected nodes that are relevant to @NBCPolitics, including its reporters and editors and media professionals from other organizations.

Network, and Microsoft, who might have worked for NBC or have close connection with it. Although there still appear to be obscure handles with few followers, they decrease significantly in number – the median in-degree of the top 200 handles is 340 (Supplementary Materials S4), a precipitous drop from that of the top PPR handles yet not too small as compared to that of the top aPPR handles. We thus conclude that the regularized aPPR vector returns a local cluster with little noise, reflecting a seed node’s close circles, either directly or indirectly related.

In order to evaluate the influence of the desired cluster size n on the results based on different PPR vectors, we compare the local clusters of PPR, aPPR, and rPPR by varying sample size. Define the *in-and-out ratio* of local cluster $C \subset V$ as the proportion of edges inside C among all edges connected to C ,

$$\frac{2 \times \sum_{u,v \in C} A_{uv}}{\sum_{u \in C} d_u^{\text{in}} + d_u^{\text{out}}}$$

A higher in-and-out ratio indicates a more internally connected sample. Figure 3 (Right) shows the effectiveness of aPPR and rPPR in producing a compact local cluster. When the sample size is bigger than 100, the connectedness of the local cluster produced by rPPR stabilizes; the greater the sample size, the more densely connected a cluster aPPR would produce. However, PPR is easily susceptible to the inclusion of popular nodes. In this case, a sharp drop of in-and-out ratio for PPR when the sample size reaches around 140 is caused by inclusions of highly popular accounts @POTUS (President Trump) and @realDonaldTrump (Donald J. Trump).

The PPR clustering is fairly robust to the choice of teleportation constant, despite the size of local

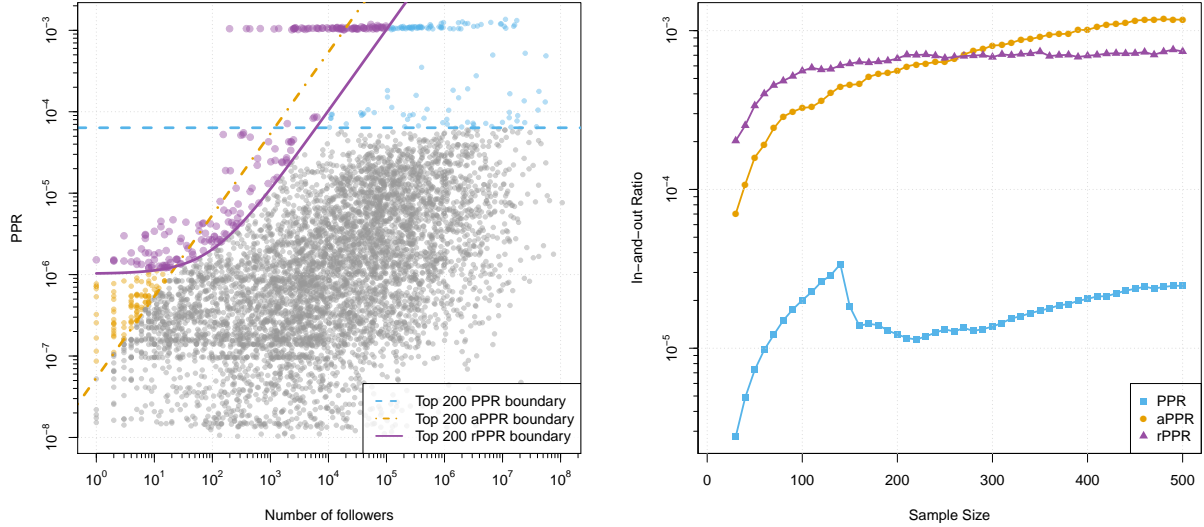


Figure 3: Left: an illustration of 5840 Twitter handles examined by Algorithm 3 and three samples of size 200 by PPR, aPPR, and rPPR. Each dot represents a user in Twitter. The blue dashed line delimits the top 200 handles by PPR vector; vertices above the line are PPR’s sample. Similarly, the yellow dotdash line determines the sample returned by Algorithm 4 given $n = 200$; vertices above this boundary correspond to aPPR’s sample. In particular, dots in purple stand for the sample of rPPR; the purple solid line shows the boundary of this sample. Right: The in-and-out ratio of local clusters identified by PPR, aPPR, and rPPR, as the sample sizes vary. A higher in-and-out ratio indicates a more internally connected cluster.

cluster. To illustrate this, we also performed the same pipeline of analysis with the seed @NBCPolitics while varying the value of α (e.g., 0.05, 0.25, and 1/3) in parallel. We observed that those local clusters returned by Algorithm 4 all share a great portion of members in common. For example, there are 280 (93.3%) overlapping members between two targeted samples of size $n = 300$, using $\alpha = 0.15$ and 0.25 respectively. These suggest a low sensitivity to the teleportation constant (see Supplementary Materials S2).

The left panel of Figure 3 depicts the behaviors of PPR, aPPR and rPPR. Each handle queried in this sampling is displayed as a dot, with y-axis representing the PPR value and x-axis the number of followers (i.e., in-degree). Top handles with the highest PPR values are above blue dashed line, which tend to concentrate on the right end of the x-axis and thus are biased toward high in-degrees. Top handles with highest aPPR values are dots to the left of the yellow dotdash line, which gather on the left end of the x-axis and thus in favor of low in-degrees. Regularized aPPR, by purple dots, excludes the very low degree nodes and very high degree nodes. As the empirical results show, these three vectors can be thought of as lenses through which we view the local structure of a given Twitter handle with varying foci, rendering high, moderate, and low in-degree blocks and serving different needs and purposes.

7 Discussion

This paper studies the PPR vector under the degree-corrected stochastic block model and PPR clustering in massive block model graphs. We establish some consistency results for this method, and examine its performance through analysis of Twitter friendship graph. As shown in the results, the PPR vectors with

and without adjustment have distinct properties and can be used to effectively sample a massive graph for various purposes. However, there are limitations worthy of future investigations.

In Section 3, we provide a representation of the PPR vector under the DC-SBM and its extension into directed graphs. The result does not impose extra structural restrictions on the model parameters, except that \mathbf{B} corresponds to a strongly connected “block-wise” graph. We consider a positive definite connectivity matrix particularly so that it is intuitive to conceive the notion of local cluster. In practice (and many of our experiments, see Supplementary Materials S2), however, a PPR-type algorithm appears to continue working for a broader range of \mathbf{B} (e.g., singular or indefinite), provided that the teleportation constant is sufficiently large (e.g. $\alpha > 0.1$). It is unclear yet what is the minimum constraint needed on \mathbf{B} in order for the PPR clustering to function. In addition, DC-SBM does have its limits. For example, the model fails to capture either mixed block membership or popularity features which are potentially informative in real world networks. The behavior of a PPR vector under other extensions of stochastic block model, such as mixed membership stochastic block model and popularity-adjusted block model, remains unknown [Airoldi et al., 2008, Sengupta and Chen, 2018]. Future studies on the PPR vector under these models could shed further light on the PPR clustering and offer more practical guidelines on their application.

In Section 4, we proved the consistency of the PPR clustering, requiring the average expected node degree to grow in order of $\log N$, which hits the boundary between the theoretical guarantees and the realistic observation. In contrast, scale-free networks such as the preferential attachment model [Barabási and Albert, 1999] have finite expected node degrees. Future investigations into variants of PPR that could possibly overcome this limitation yet ensure a fine local cluster discovery would be particularly interesting and useful.

In Section 6, we introduce the regularized version of adjusted PPR (rPPR) vector, with a series of empirical evidence showing its efficacy in targeted sampling. While the results appear promising, theoretical guarantees for this technique remain unexplored. In order for some mathematical analyses, one may resort to the techniques used in Le et al. [2016]. It is previously shown that the regularized graph Laplacian (or transition matrix) enjoys “nice” finite sample properties, which facilitate the consistency of many regularized spectral methods. It thus is reasonable conjecture that rPPR vectors are also suitable for local clustering.

An R implementation of the PPR clustering is available at author’s GitHub ([https://github.com/](https://github.com/RoheLab/aPPR)RoheLab/aPPR).

Acknowledgments

This research is supported by NSF Grants DMS-1612456 and DMS-1916378 and ARO Grant W911NF-15-1-0423. Thank you to Yuling Yan and E. Auden Krauska for the helpful comments. Thank you to Alex Hayes for kindly advising on the software development.

A Technical Proofs

A.1 Proof of Proposition 1

Proof. We apply Perron-Frobenius theorem for the first part [Perron, 1907, Frobenius et al., 1912], and complete the proof by construction.

- (a) First, notice that Q is a Markov transition matrix by modifying $G = (V, E)$ a little. To this end, (i)

shrink the weights of every existing edge by factor $1 - \alpha$, and (ii) add an edge weighted α between seed node v_0 and all nodes in the graph. Then Q represents the new graph $G'(V, E')$, which is strongly connected by construction. Hence Q is irreducible.

The PPR vector p is all-positive. To see this, note that the equation $p^\top = p^\top Q$ implies that p is a stationary distribution for the standard random walk on G' . Since G' is strongly connected, it follows that the stationary distribution must be all-positive.

From the Perron-Frobenius theorem, the only all-positive eigenvector of a non-negative irreducible matrix is associated with the leading eigenvalue, which is 1 in our case. Since the leading eigenvalue of non-negative irreducible matrix is simple, we conclude that p is unique.

- (b) We finish the proof by constructing an explicit form of the PPR vector. Let $R_\alpha = \alpha \sum_{s=0}^{\infty} (1 - \alpha)^s P^s$. The infinite sum converges for $\alpha \in (0, 1]$. Then, $p = R_\alpha^\top \pi$ satisfies the definition of personalized PageRank vector,

$$\begin{aligned} \alpha \pi^\top + (1 - \alpha) \pi^\top R_\alpha P &= \alpha \pi^\top + (1 - \alpha) \pi^\top \left(\alpha \sum_{s=0}^{\infty} (1 - \alpha)^s P^s \right) P \\ &= \alpha \pi^\top + \alpha \sum_{s=1}^{\infty} (1 - \alpha)^s \pi^\top P^s \\ &= \pi^\top R_\alpha. \end{aligned}$$

Since the solution is unique, we have $p = R_\alpha^\top \pi$. □

A.2 Proof of Proposition 2

Proof. Algorithm 1 maintains two vectors, p^ϵ and r , by transporting probability mass from r to p^ϵ at each updating step. Note that the termination criterion implies that $r_u < \epsilon d_u$ for any u sampled, thus it suffices to prove that

$$|p_u - p_u^\epsilon| \leq r_u.$$

For a fixed α , let $p(x)$ be the PPR vector with preference vector $x \in \mathbb{R}^N$ satisfying $x_i \geq 0$ and $\|x\|_1 \leq 1$. Then $p(\pi)$ is the exact PPR vector as in Equation (2). Since $p(x)^\top P = p(x^\top P)$, we have [Jeh and Widom, 2003]

$$p(x) = \alpha x + (1 - \alpha) p(P^\top x). \tag{10}$$

We argue that $p^\epsilon + p(r)$ is invariant in updating steps. To see this, suppose $(p^\epsilon)'$ and r' are the results of performing one update on p^ϵ and r after sampling node u . We have

$$\begin{aligned} (p^\epsilon)' &= p^\epsilon + \alpha r_u e_u, \\ r' &= r - r_u e_u + (1 - \alpha) r_u P^\top e_u. \end{aligned}$$

where e_u is the unit vector on the direction of u . Then,

$$\begin{aligned}
p(r) &= p(r - r_u e_u) + p(r_u e_u) \\
&\stackrel{(i)}{=} p(r - r_u e_u) + \alpha r_u e_u + (1 - \alpha) p(r_u P^\top e_u) \\
&\stackrel{(ii)}{=} p(r - r_u e_u + (1 - \alpha) r_u P^\top e_u) + \alpha r_u e_u \\
&= p(r') + (p^\epsilon)' - p^\epsilon,
\end{aligned}$$

where (i) is applying Equation (10) at $x = r_u e_u$ and (ii) comes from the linearity of PPR vector in the preference vector.

The desired result follows from recognizing that $p^\epsilon + p(r)$ is initially $\vec{0} + p(\pi)$ and that when the algorithm terminates, $[p(r)]_u \leq r_u$ for any sampled u . \square

REMARK. If $\epsilon d_1 > 1$, Algorithm 1 terminates after the first round and simply output $p = \vec{0}$. Under this circumstance, Proposition 2 still holds, because $|p_u - p_u^\epsilon| \leq |p_u| + |p_u^\epsilon| \leq 1$.

A.3 Lemmas for the DC-SBM

Lemma 2 (Properties of the DC-SBM). *Under the population directed DC-SBM with K blocks and parameters $\{\mathbf{B}, Z, \Theta^{\text{in}}, \Theta^{\text{out}}\}$,*

(a) $\mathbf{D}^{\text{in}} = Z^\top \mathcal{D}^{\text{in}} Z$, and $\mathbf{D}^{\text{out}} = Z^\top \mathcal{D}^{\text{out}} Z$, and

(b) $\mathcal{d}_v^{\text{in}} = \theta_v^{\text{in}} \mathbf{d}_{z(v)}^{\text{in}}$, and $\mathcal{d}_v^{\text{out}} = \theta_v^{\text{out}} \mathbf{d}_{z(v)}^{\text{out}}$.

Proof. (a) is an alternative way of writing the definition. For (b), we prove the first equation. Recall that for any i , $\sum_{u:z(u)=i} \theta_u^{\text{out}} = 1$, then by definition,

$$\mathcal{d}_v^{\text{in}} = \sum_u \theta_u^{\text{out}} \theta_v^{\text{in}} B_{z(u)z(v)} = \theta_v^{\text{in}} \sum_{j=1}^K \left(\mathbf{B}_{jz(v)} \sum_{u:z(u)=j} \theta_u^{\text{out}} \right) = \theta_v^{\text{in}} \mathbf{d}_{z(v)}^{\text{in}}.$$

\square

REMARK. Since $Z^\top \Theta^{\text{in}} Z = I_K$, (a) implies $[\mathcal{D}^{\text{in}}]^{-1} \Theta^{\text{in}} Z = Z [\mathbf{D}^{\text{in}}]^{-1}$.

Lemma 3 (Explicit form of \mathcal{P} and its powers). *Under the population directed DC-SBM with K blocks and parameters $\{\mathbf{B}, Z, \Theta^{\text{in}}, \Theta^{\text{out}}\}$, the population graph transition is the product*

$$\mathcal{P} = Z \mathbf{P} Z^\top \Theta^{\text{in}}.$$

and its matrix powers are

$$\mathcal{P}^k = Z \mathbf{P}^k Z^\top \Theta^{\text{in}}.$$

Proof. By definition and Lemma 2(b), for any $u, v \in V$,

$$\mathcal{P}_{uv} = \left(\theta_u^{\text{out}} \mathbf{d}_{z(u)}^{\text{out}} \right)^{-1} \theta_u^{\text{out}} \theta_v^{\text{in}} \mathbf{B}_{z(u)z(v)} = \theta_v^{\text{in}} \mathbf{B}_{z(u)z(v)} / \mathbf{d}_{z(u)}^{\text{out}} = \theta_v^{\text{in}} \mathbf{P}_{z(u)z(v)}.$$

For the powers of \mathcal{P} , noticing that $Z^\top \Theta^{\text{in}} Z = I_K$,

$$\mathcal{P}^2 = Z \mathbf{P} Z^\top \Theta^{\text{in}} Z \mathbf{P} Z^\top \Theta^{\text{in}} = Z \mathbf{P}^2 Z^\top \Theta^{\text{in}}.$$

The desired result follows from the principle of induction on k -th power. \square

A.4 Proof of Theorem 1

Proof. By Proposition 1 and Lemma 3, we have

$$\begin{aligned} \boldsymbol{\rho} &= \alpha \sum_{s=0}^{\infty} (1-\alpha)^s (\mathcal{P}^s)^\top \boldsymbol{\pi} \\ &= \alpha \sum_{s=0}^{\infty} (1-\alpha)^s \Theta^{\text{in}} Z (\mathbf{P}^s)^\top Z^\top \boldsymbol{\pi} \\ &= \Theta^{\text{in}} Z \left(\alpha \sum_{s=0}^{\infty} (1-\alpha)^s (\mathbf{P}^s)^\top \boldsymbol{\pi} \right) \\ &= \Theta^{\text{in}} Z \mathbf{p}, \end{aligned}$$

In addition, it follows from Lemma 2(a) that

$$\boldsymbol{\rho}^* = [\mathcal{D}^{\text{in}}]^{-1} \boldsymbol{\rho} = [\mathcal{D}^{\text{in}}]^{-1} \Theta^{\text{in}} Z \mathbf{p} = Z [\mathbf{D}^{\text{in}}]^{-1} \mathbf{p} = Z \mathbf{p}^*.$$

This completes the proof. \square

A.5 Proof of Lemma 1

Proof. For any $\alpha > 0$, the PPR vector with seed node $v_0 = 1$ is the solution to the equation $\boldsymbol{\rho}^\top = \boldsymbol{\rho}^\top \mathcal{Q}$, where $\mathcal{Q} = \alpha \Pi + (1-\alpha)\mathcal{P}$. Define a sequence of probability distribution $\boldsymbol{\rho}^s \in \mathbb{R}^N$ such that $\boldsymbol{\rho}^s = (\mathcal{Q}^s)^\top \boldsymbol{\rho}^0$, where $\boldsymbol{\rho}^0$ is an arbitrary initial probability distribution. Then, $\lim_{s \rightarrow \infty} \boldsymbol{\rho}^s = \boldsymbol{\rho}$. For simplicity, we assume $\boldsymbol{\rho}^0$ is close to $\boldsymbol{\rho}$, that is, for any $\varepsilon > 0$ and $s \geq 0$,

$$\|\boldsymbol{\rho}^s - \boldsymbol{\rho}\|_\infty < \varepsilon/2. \quad (11)$$

This can be achieved by finding an integer $S(\varepsilon)$ large enough and setting $\boldsymbol{\rho}^0 = \boldsymbol{\rho}^S$.

We first claim that

$$\max_{u \neq 1} \frac{\rho_u^{s+1}}{d_u} \leq (1-\alpha) \max_{u \in V} \frac{\rho_u^s}{d_u}. \quad (12)$$

In fact, for any $u \neq 1$,

$$\begin{aligned} \rho_u^{s+1} &= \alpha \mathbf{1}_{\{u=1\}} + (1-\alpha) \sum_{v \in V} \frac{\mathcal{A}_{vu}}{d_v} \rho_v^s \\ &\leq (1-\alpha) \left(\sum_{v \in V} \mathcal{A}_{vu} \right) \max_{v \in V} \frac{\rho_v^s}{d_v} \\ &= (1-\alpha) d_u \max_{v \in V} \frac{\rho_v^s}{d_v}. \end{aligned}$$

We then show $\frac{\rho_1^s}{d_1} > \frac{\rho_v^s}{d_v}$ for any $v \neq 1$ by contradiction. Suppose otherwise that $\frac{\rho_1^s}{d_1} \leq \max_{u \neq 1} \frac{\rho_u^s}{d_u}$, then Equation (11) implies for any s' ,

$$\frac{\rho_1^{s'}}{d_1} \leq \frac{\rho_1^s + \varepsilon}{d_1} \leq \max_{u \neq 1} \frac{\rho_u^s}{d_u} + \frac{\varepsilon}{d_1} \leq \max_{u \neq 1} \frac{\rho_u^{s'} + \varepsilon}{d_u} + \frac{\varepsilon}{d_1} \leq \max_{u \neq 1} \frac{\rho_u^{s'}}{d_u} + \frac{2\varepsilon}{d_{\min}},$$

where $d_{\min} = \min_{v \in V} d_v$. Hence, $\max_{u \in V} \frac{\rho_u^{s'}}{d_u} \leq \max_{u \neq 1} \frac{\rho_u^{s'}}{d_u} + \frac{2\varepsilon}{d_{\min}}$. In addition, applying Equation (12) recursively we have

$$\begin{aligned} \max_{u \in V} \frac{\rho_u^s}{d_u} &= \max_{u \neq 1} \frac{\rho_u^s}{d_u} \\ &\leq (1 - \alpha) \max_{u \in V} \frac{\rho_u^{s-1}}{d_u} \\ &\leq (1 - \alpha) \left(\max_{u \neq 1} \frac{\rho_u^{s-1}}{d_u} + \frac{2\varepsilon}{d_{\min}} \right) \\ &\leq (1 - \alpha)^s \max_{u \in V} \frac{\rho_u^0}{d_u} + \frac{2\varepsilon}{d_{\min}} \sum_{t=1}^{s-1} (1 - \alpha)^t. \end{aligned}$$

The inequality means that if $d_{\min} > 0$ is fixed, ρ_u^s can be arbitrarily small when $s \rightarrow \infty$, which contradicts the fact that ρ is a probability distribution. This completes the proof.

REMARK. When the teleportation constant is zero, the PPR vector becomes the stationary probability distribution of a standard random walk,

$$\left(\frac{d_1}{\sum_i d_i}, \frac{d_2}{\sum_i d_i}, \dots, \frac{d_N}{\sum_i d_i} \right).$$

After adjusting by node degrees, every entry becomes identical ($1/\sum_i d_i$). The lemma is intuitive, recognizing that the teleportation introduces a particular favor of the seed node.

REMARK. When the edges are weighted (non-negative), the stationary distribution of a random walk is still proportional to node degrees, if one defines the degree as sum of edge weights incident to the node [Lovász, 1996]. Note also that the stationary distribution of a random walk in a directed graph is characterized by the in-degree of nodes [Ghoshal and Barabási, 2011, Lu et al., 2013]. The conclusion and a modified proof apply to directed or weighted graphs. \square

A.6 Proof of Corollary 1

Proof. The algorithm ranks all vertices according to $p^{\varepsilon*}$, and the population local cluster can be explicitly written as

$$\mathcal{C} = \{v \in V : \rho_v^* = \mathbf{p}_1^*\}.$$

It suffices to show that

$$p_v^{\varepsilon*} > p_u^{\varepsilon*}, \text{ for } \forall v \in \mathcal{C}, u \in V \setminus \mathcal{C},$$

where $p_v^{\epsilon^*} = p_v^\epsilon/d_v$. To this end, we apply triangle inequality and get

$$\begin{aligned} \frac{p_v^{\epsilon^*} - p_u^{\epsilon^*}}{\|\mathcal{P}^*\|_\infty} &\geq \frac{\mathcal{P}_v^* - \mathcal{P}_u^*}{\|\mathcal{P}^*\|_\infty} - \frac{|p_v^* - \mathcal{P}_v^*|}{\|\mathcal{P}^*\|_\infty} - \frac{|p_u^* - \mathcal{P}_u^*|}{\|\mathcal{P}^*\|_\infty} - \frac{|p_u^{\epsilon^*} - p_u^*|}{\|\mathcal{P}^*\|_\infty} - \frac{|p_v^{\epsilon^*} - p_v^*|}{\|\mathcal{P}^*\|_\infty} \\ &\geq \Delta - \frac{2\|p^* - \mathcal{P}^*\|_\infty}{\|\mathcal{P}^*\|_\infty} - \frac{2\|p^{\epsilon^*} - p^*\|_\infty}{\|\mathcal{P}^*\|_\infty}. \end{aligned}$$

Since $\Delta_\alpha \leq 1$, assumption (8) contains condition (7) in Theorem 2, which together with Proposition 2 implies that

$$\frac{\|p^* - \mathcal{P}^*\|_\infty}{\|\mathcal{P}^*\|_\infty} < \frac{1}{4}\Delta, \quad \frac{\|p^{\epsilon^*} - p^*\|_\infty}{\|\mathcal{P}^*\|_\infty} < \frac{1}{4}\Delta,$$

if $\Delta^2\delta/\log N$ is large enough. These collectively imply $p_v^* > p_u^*$ as desired. \square

Supplementary Materials

Abstract

This document provides several supplementary materials to “Targeted sampling from massive block model graphs with personalized PageRank”. Section S1 contains a proof for the entrywise error control (Theorem 2). Section S2 gives additional information about some model parameters, including \mathbf{B} , \mathcal{P} , α , and N . Section S3 extends the results in Kloumann et al. [2017] to the DC-SBM from a linear discriminant analysis perspective. Section S4 supplies three targeted Twitter samples about the seed @NBCPolitics described in the paper. The PPR clustering is implemented in R and all source codes are available at author’s GitHub (<https://github.com/RoheLab/aPPR>).

S1 A proof for the entrywise error control

We start with a few lemmas to prepare for the proof of Theorem 2. For completeness, Section S1.3 lists a few inequalities that are used throughout the proofs.

S1.1 Some definitions and lemmas

In this section, we introduce a few notations used in Lemma S3 and list a few properties of vector norm and matrix norm [Brémaud, 2013].

For any strictly positive probability distribution vector $p \in \mathbb{R}^N$, the inner product space indexed by p is a real vector space \mathbb{R}^N endowed with the inner product

$$\langle x, y \rangle_p = \sum_{v=1}^N p_v x_v y_v.$$

The corresponding vector norm and the induced matrix norm are defined respectively as

$$\|x\|_p = \sqrt{\langle x, x \rangle_p} \quad \text{and} \quad \|A\|_p = \sup_{\|x\|_p=1} \|A^\top x\|_p.$$

Lemma S1. *If $0 \leq p_{\min} \leq p_v \leq p_{\max}$ for all $v = 1, 2, \dots, N$, then the following inequalities hold*

$$\sqrt{p_{\min}} \|x\|_2 \leq \|x\|_p \leq \sqrt{p_{\max}} \|x\|_2 \quad \text{and} \quad \sqrt{\frac{p_{\min}}{p_{\max}}} \|A\|_2 \leq \|A\|_p \leq \sqrt{\frac{p_{\max}}{p_{\min}}} \|A\|_2.$$

The following lemma provides concentration of the node degrees in a graph generated from the DC-SBM.

Lemma S2 (Degree concentration). *Let $G = (V, E)$ be a graph of N vertices generated from the DC-SBM with K blocks and parameters $\{\mathbf{B}, Z, \Theta\}$. Let d_{\min} and d_{\max} be the smallest and the largest node degree observed. Let δ be the average expected node degree, and define $\rho = d_{\max}/d_{\min}$. If $\delta \geq c_0(1 - \alpha) \log N$ for some sufficiently large constant $c_0 > 0$, then with probability at least $1 - \mathcal{O}(N^{-10})$, it holds that*

$$\frac{\delta}{2\rho} \leq d_{\min} \leq d_{\max} \leq \frac{3\rho\delta}{2}. \tag{13}$$

Proof. Note that the definition of ρ immediately implies that

$$\frac{\delta}{\rho} \leq d_{\min} \leq d_{\max} \leq \delta\rho.$$

The lemma follows from the standard Chernoff's bound, hence is omitted. \square

The following useful lemma concerns the eigenvector perturbation for probability transition matrices, promoted from the celebrated Davis-Kahan $\sin \Theta$ Theorem [Davis and Kahan, 1970].

Lemma S3 (Eigenvector perturbation). *Suppose that Q , \hat{Q} , and \mathcal{Q} are probability transition matrices with stationary distributions p , \hat{p} , and $\boldsymbol{\rho}$ respectively. Assume that \mathcal{Q} represents a reversible Markov chain. Then,*

$$\|p - \hat{p}\|_{\boldsymbol{\rho}} \leq \frac{\|(Q - \hat{Q})^\top p\|_{\boldsymbol{\rho}}}{1 - \max\{\lambda_2(\mathcal{Q}), -\lambda_N(\mathcal{Q})\} - \|\hat{Q} - \mathcal{Q}\|_{\boldsymbol{\rho}}}.$$

The proof the Lemma S3 can be found in Chen et al. [2019] Section 3, thus omitted.

S1.2 Proof of Theorem 2

Proof. The proof processes as follows. We first bound the entrywise error rate of p ,

$$\frac{\|p - \boldsymbol{\rho}\|_{\infty}}{\|\boldsymbol{\rho}\|_{\infty}} \leq c_0 \sqrt{\frac{\log N}{\delta}},$$

by invoking the novel leave-one-out techniques [Chen et al., 2019], The entrywise error bounds of p^* follows immediately.

Recall that both p and $\boldsymbol{\rho}$ are stationary distribution, which means

$$p = Q^\top p \quad \text{and} \quad \boldsymbol{\rho} = \mathcal{Q}^\top \boldsymbol{\rho}.$$

Due to this, for any $w = 1, 2, \dots, N$, we can decompose

$$\begin{aligned} p_w - \boldsymbol{\rho}_w &= Q_{\cdot w}^\top p - \mathcal{Q}_{\cdot w}^\top \boldsymbol{\rho} \\ &= \underbrace{(Q_{\cdot w} - \mathcal{Q}_{\cdot w})^\top \boldsymbol{\rho}}_{:=I_1^w} + \underbrace{Q_{\cdot w}^\top (p - \boldsymbol{\rho})}_{:=I_2^w}, \end{aligned}$$

where $Q_{\cdot w}$ denotes the w -th column of Q .

(a) We start with the first term I_1^w . Note that

$$\begin{aligned} I_1^w &= (1 - \alpha) \sum_{v=1}^N \left[\frac{A_{vw}}{d_v} - \frac{\mathcal{A}_{vw}}{d_v} \right] \boldsymbol{\rho}_v \\ &= \underbrace{(1 - \alpha) \sum_{v=1}^N \left[(A_{vw} - \mathcal{A}_{vw}) \frac{1}{d_v} \right] \boldsymbol{\rho}_v}_{:=I_{11}^w} + \underbrace{(1 - \alpha) \sum_{v=1}^N A_{vw} \left(\frac{1}{d_v} - \frac{1}{d_v} \right) \boldsymbol{\rho}_v}_{:=I_{12}^w}. \end{aligned}$$

Recall that A_{vw} 's correspond to independent Bernoulli random variables, we can easily bound the first

term using Bernstein's inequality (Lemma S6), with probability at least $1 - \mathcal{O}(N^{-8})$,

$$\begin{aligned}
|I_{11}^w| &\leq (1 - \alpha) \left| \sum_{v=1}^N (A_{vw} - \mathcal{A}_{vw}) \right| \frac{\|p\|_\infty}{\delta} \\
&\leq (1 - \alpha) \left(\sqrt{16 \log N \sum_{v=1}^N \mathcal{A}_{vw}} + \frac{16 \log N}{3} \right) \frac{\|p\|_\infty}{\delta} \\
&\stackrel{(i)}{\leq} (1 - \alpha) \left(4 \sqrt{\frac{\rho \log N}{\delta}} + \frac{16 \log N}{3\delta} \right) \|p\|_\infty,
\end{aligned}$$

where (i) follows from the fact that $\rho\delta \leq \mathcal{d}_{\max}$.

Note that the second term is

$$I_{12}^w = (1 - \alpha) \sum_{v=1}^N \mathbb{1}_{(v,w) \in E} \left(\frac{1}{d_v} - \frac{1}{\mathcal{d}_v} \right) \mathcal{P}_v,$$

to which we can apply the Hoeffding's inequality (Lemma S4) and obtain

$$\mathbb{P} \left(|I_{12}^w| \leq \rho(1 - \alpha) \sqrt{\frac{\rho \log N}{\delta}} \|p\|_\infty \right) \geq 1 - 2N^{-8}.$$

In sums, we have high probability event

$$|I_1^w| \leq (1 - \alpha) \left((4 + \rho) \sqrt{\rho} + 3 \sqrt{\frac{\log N}{\delta}} \right) \sqrt{\frac{\log N}{\delta}} \|p\|_\infty. \quad (14)$$

- (b) The statistical dependency between p and Q introduces difficulty in sharply bounding I_2^w . Nevertheless, we can invoke the leave-one-out techniques to decouple the dependency. To this end, we define, for each $w = 1, 2, \dots, N$, a new transition matrix $Q^{(w)} = \alpha\Pi + (1 - \alpha)P^{(w)}$ that bridges between Q and \mathcal{Q} . $P^{(w)}$ has almost the same entries as P except for replacing those in w -th row or column by their expectations; that is, for any $u \neq v$,

$$P_{uv}^{(w)} = \begin{cases} P_{uv}, & u \neq w \text{ and } v \neq w, \\ \mathcal{P}_{uv}, & u = w \text{ or } v = w, \end{cases}$$

and for any $u = 1, 2, \dots, N$,

$$P_{uu}^{(w)} = 1 - \sum_{v:v \neq u} P_{uv}^{(w)},$$

in order to ensure that $P^{(w)}$ and $Q^{(w)}$ are transition matrices. In addition, define $p^{(w)}$ to be the stationary distribution corresponding to $Q^{(w)}$. As demonstrated in Chen et al. [2019], $p^{(w)}$ helps us well approximate p , yet it is statistically independent of $Q_{\cdot w}$.

Now we decompose I_2^w as follows:

$$\begin{aligned} I_2^w &= \sum_{v=1}^N Q_{vw} (p_v - \rho_v) \\ &= \underbrace{\sum_{v=1}^N Q_{vw} (p_v - p_v^{(w)})}_{:=I_{21}^w} + \underbrace{\sum_{v=1}^N Q_{vw} (p_v^{(w)} - \rho_v)}_{:=I_{22}^w}. \end{aligned}$$

- (c) In this part, we focus on the first term I_{21}^w , where we would need another intermediate quantity to facilitate our estimation. To be specific, consider the leave-one-out version of Q conditioning on the graph $G = (V, E)$, $Q^{(w,G)} = \alpha\Pi + (1 - \alpha)P^{(w,G)}$, which is almost the same as Q except for replacing the non-zero entries in w -th row or column by their expectations. Concretely, for and $u \neq v$,

$$P_{uv}^{(w,G)} = \begin{cases} P_{uv}, & u \neq w \text{ and } v \neq w, \\ \mathbf{1}_{(u,v) \in E} \mathcal{P}_{uv}, & u = w \text{ or } v = w, \end{cases}$$

and for any $u = 1, 2, \dots, N$, define

$$P_{uu}^{(w,G)} = 1 - \sum_{v:v \neq u} P_{uv}^{(w,G)},$$

so that $P^{(w,G)}$ is a probability transition matrix.

With $Q^{(w,G)}$ in mind, we now apply Cauchy-Schwarz inequality on I_{21}^w to reach

$$\begin{aligned} |I_{21}^w| &= \left| \sum_{v=1}^N Q_{vw} (p_v - p_v^{(w)}) \right| \\ &\leq \left(\sum_{v=1}^N Q_{vw}^2 \right)^{\frac{1}{2}} \|p - p^{(w)}\|_2 \\ &\stackrel{(i)}{\leq} \sqrt{\alpha + \frac{1}{d_{\min}}} \sqrt{\frac{\rho_{\max}}{\rho_{\min}}} \|p - p^{(w)}\|_{\rho} \\ &\stackrel{(ii)}{\leq} \sqrt{\alpha + \frac{1}{d_{\min}}} \sqrt{\frac{\rho_{\max}}{\rho_{\min}}} \frac{1}{\gamma} \left\| (Q - Q^{(w)})^\top p^{(w)} \right\|_2 \\ &\stackrel{(iii)}{\leq} \sqrt{\alpha + \frac{2\rho}{\delta} \frac{\sqrt{\kappa}}{\gamma}} \left(\underbrace{\left\| (Q - Q^{(w,G)})^\top p^{(w)} \right\|_2}_{:=I_{211}^w} + \underbrace{\left\| (Q^{(w,G)} - Q^{(w)})^\top p^{(w)} \right\|_2}_{:=I_{212}^w} \right). \end{aligned}$$

where (i) follows from Lemma S1 and the fact that $P_{vw} \leq \frac{1}{d_{\min}}$, (ii) comes from Lemma S3, and (iii) results from Lemma S2 and the triangle inequality, and recognizing $\kappa = \rho_{\max}/\rho_{\min}$ (from the proof of Proposition 1, it is bounded), and ‘‘w.h.p.’’ is short for ‘‘with high probability’’. Note that Π adds at most 1 to the rank of \mathcal{Q} , and because we presume B is positive definite \mathcal{P} has exactly K positive eigenvalues among other zeros (Section S2.2). Here, $\gamma = 1 - \max\{\lambda_2(\mathcal{Q}), -\lambda_N(\mathcal{Q})\} - \|Q^{(w,G)} - \mathcal{Q}\|_{\rho}$ is the spectral gap and is lower bounded by some positive constant (due to Khanna et al. [2017]). Then, it boils down to controlling I_{211}^w and I_{212}^w .

For I_{211}^w , the w -th entry inside the vector norm is

$$\begin{aligned} \left[\left(Q - Q^{(w,G)} \right)^\top p^{(w)} \right]_w &= \left[(Q - \mathcal{Q})^\top p^{(w)} \right]_w \\ &= (1 - \alpha) \sum_{v=1}^N (P_{vw} - \mathcal{P}_{vw}) p_v^{(w)}. \end{aligned}$$

Note that $p_v^{(w)}$ is statistically independent of P_w . Then, by Hoeffding's inequality (Lemma S4) and Lemma S2, we have with probability at least $1 - 2N^{-8}$,

$$\left[\left(Q - Q^{(w,G)} \right)^\top p^{(w)} \right]_w \leq 4\rho(1 - \alpha) \sqrt{\frac{\rho \log N}{\delta}} \|p^{(w)}\|_\infty. \quad (15)$$

As for any $u \neq w$, applying Hoeffding's inequality again yields

$$\begin{aligned} \left[\left(Q - Q^{(w,G)} \right) p^{(w)} \right]_u &= (1 - \alpha) \sum_{v=1}^N (P_{vu} - \mathcal{P}_{vu}) p_v^{(w)} \\ &= (1 - \alpha) \left(P_{uu} - P_{uu}^{(w,G)} \right) p_u^{(w)} \\ &\quad + (1 - \alpha) \left(P_{uw} - P_{uw}^{(w,G)} \right) p_w^{(w)} \\ &= -(1 - \alpha) \left(P_{uw} - P_{uw}^{(w,G)} \right) p_u^{(w)} \\ &\quad + (1 - \alpha) \left(P_{uw} - P_{uw}^{(w,G)} \right) p_w^{(w)}. \end{aligned}$$

Recognizing that

$$\left| P_{uw} - P_{uw}^{(w,G)} \right| = \begin{cases} A_{uw} d_{uw}^{-1} - \mathcal{A}_{uw} \mathcal{d}_{uw}^{-1}, & (u, w) \in E, \\ 0, & (u, w) \notin E, \end{cases}$$

we apply again the Hoeffding's inequality (Lemma S4) together with (13), and obtain with probability at least $1 - \mathcal{O}(N^{-8})$,

$$\left| \left[\left(Q - Q^{(w,G)} \right)^\top p^{(w)} \right]_u \right| \leq \begin{cases} 4\rho(1 - \alpha) \frac{\sqrt{\log N}}{\delta} \|p^{(w)}\|_\infty, & (u, w) \in E, \\ 0, & (u, w) \notin E. \end{cases} \quad (16)$$

Combining (15) and (16) yields

$$\begin{aligned} I_{211}^w &\leq 4\rho(1 - \alpha) \left(1 + \sqrt{\sum_{u:u \neq w} \mathbb{1}_{(u,w) \in E}} \right) \sqrt{\frac{\rho \log N}{\delta}} \|p^{(w)}\|_\infty \\ &\stackrel{(i)}{\leq} \stackrel{\text{w.h.p.}}{\leq} 8\rho^2 \sqrt{\rho}(1 - \alpha) \sqrt{\frac{\log N}{\delta}} \|p^{(w)}\|_\infty, \end{aligned}$$

where (i) follows from the high probability event that $d_{\max} \leq 3\rho\delta/2$.

Regarding I_{212}^w , since $(Q^{(w,G)} - Q^{(w)})\boldsymbol{\rho} = \vec{0}$, we can rewrite this as

$$I_{212}^w = \left\| \left(Q^{(w,G)} - Q^{(w)} \right)^\top \left(p^{(w)} - \boldsymbol{\rho} \right) \right\|_2.$$

Similarly, note that $P_{vw}^{(w)} - P_{vw}^{(w,G)} = \frac{\mathcal{A}_{vw}}{\mathcal{d}_v} \mathbf{1}_{(w,v) \notin E}$, we apply Bernstein's inequality on w -th term inside the vector norm to obtain that with probability at least $1 - 2N^{-8}$,

$$\begin{aligned} \left[\left(Q^{(w,G)} - Q^{(w)} \right) \left(p^{(w)} - \boldsymbol{\rho} \right) \right]_w &= (1 - \alpha) \sum_{v=1}^N \left(P_{vw}^{(w,G)} - P_{vw}^{(w)} \right) \left(p_v^{(w)} - \boldsymbol{\rho}_v \right) \\ &= (1 - \alpha) \sum_{v=1}^N \frac{1}{\mathcal{d}_v} \left(p_v^{(w)} - \boldsymbol{\rho}_v \right) \mathbf{1}_{(w,v) \notin E} \\ &\stackrel{\text{w.h.p.}}{\leq} (1 - \alpha) \left(4\rho \sqrt{\frac{\rho \log N}{\delta}} + \frac{16 \log N}{3 \delta} \right) \left\| p^{(w)} - \boldsymbol{\rho} \right\|_\infty. \end{aligned}$$

For any $u \neq w$, the u -th term inside vector norm is

$$\begin{aligned} \left[\left(Q^{(w,G)} - Q^{(w)} \right) \left(p^{(w)} - \boldsymbol{\rho} \right) \right]_u &= (1 - \alpha) \sum_{v=1}^N \left(P_{vu}^{(w,G)} - P_{vu}^{(w)} \right) \left(p_v^{(w)} - \boldsymbol{\rho}_v \right) \\ &= (1 - \alpha) \left(P_{vv}^{(w,G)} - P_{uu}^{(w)} \right) \left(p_u^{(w)} - \boldsymbol{\rho}_u \right) \\ &\quad + (1 - \alpha) \left(P_{vw}^{(w,G)} - P_{uw}^{(w)} \right) \left(p_w^{(w)} - \boldsymbol{\rho}_w \right) \\ &= -(1 - \alpha) \left(P_{vw}^{(w,G)} - P_{uw}^{(w)} \right) \left(p_u^{(w)} - \boldsymbol{\rho}_u \right) \\ &\quad + (1 - \alpha) \left(P_{vw}^{(w,G)} - P_{uw}^{(w)} \right) \left(p_w^{(w)} - \boldsymbol{\rho}_w \right). \end{aligned}$$

Recognizing that

$$P_{uw}^{(w)} - P_{uw}^{(w,G)} = \mathcal{A}_{uw} \mathcal{d}_u^{-1} \mathbf{1}_{(u,w) \notin E},$$

we have from (13) that

$$\left| \left[\left(Q^{(w,G)} - Q^{(w)} \right)^\top \left(p^{(w)} - \boldsymbol{\rho} \right) \right]_u \right| \leq 2\mathcal{A}_{uw} \mathcal{d}_u^{-1} \mathbf{1}_{(u,w) \notin E} (1 - \alpha) \left\| p^{(w)} - \boldsymbol{\rho} \right\|_\infty.$$

Hence, we have with probability at least $1 - \mathcal{O}(N^{-8})$,

$$\begin{aligned} I_{212}^w &\leq (1 - \alpha) \left(4\rho \sqrt{\rho} \sqrt{\frac{\log N}{\delta}} + \frac{16 \log N}{3 \delta} + 2 \sqrt{\sum_{u:u \neq w} \frac{\mathbf{1}_{(u,w) \notin E}}{\mathcal{D}_{uu}^2}} \right) \left\| p^{(w)} - \boldsymbol{\rho} \right\|_\infty \\ &\stackrel{(i)}{\leq} (1 - \alpha) \left(4\rho \sqrt{\rho} \sqrt{\frac{\log N}{\delta}} + \frac{16 \log N}{3 \delta} + 2\rho \sqrt{\frac{\rho}{\delta}} \right) \left\| p^{(w)} - \boldsymbol{\rho} \right\|_\infty, \end{aligned}$$

where (i) follows from the high probability event that $d_{\max} \leq 3\rho\delta/2$. Combining the above two bounds,

we have with probability at least $1 - \mathcal{O}(N^{-8})$ that

$$\begin{aligned}
I_{21}^w &\leq \sqrt{\alpha + \frac{2\rho}{\delta} \frac{\sqrt{\kappa}}{\gamma}} (I_{211}^w + I_{212}^w) \\
&\leq c(1 - \alpha) \left(8\rho^2 \sqrt{\frac{\rho \log N}{\delta}} \|p^{(w)}\|_\infty + \left(2\rho \sqrt{\frac{\rho}{\delta}} + 4\rho \sqrt{\frac{\rho \log N}{\delta}} + \frac{16 \log N}{3} \frac{\rho}{\delta} \right) \|p^{(w)} - \mathcal{P}\|_\infty \right) \\
&\stackrel{(i)}{\leq} 8c\rho^2(1 - \alpha) \sqrt{\frac{\rho \log N}{\delta}} \|\mathcal{P}\|_\infty \\
&\quad + c(1 - \alpha) \left(8\rho^2 \sqrt{\frac{\rho \log N}{\delta}} + 2\rho \sqrt{\frac{\rho}{\delta}} + 4\rho \sqrt{\frac{\rho \log N}{\delta}} + \frac{16 \log N}{3} \frac{\rho}{\delta} \right) \|p^{(w)} - \mathcal{P}\|_\infty \\
&\stackrel{(ii)}{\leq} 8c\rho^2(1 - \alpha) \sqrt{\frac{\rho \log N}{\delta}} \|\mathcal{P}\|_\infty + \frac{c}{2} \|p^{(w)} - \mathcal{P}\|_\infty \\
&\stackrel{(iii)}{\leq} 16c\rho^2(1 - \alpha) \sqrt{\frac{\rho \log N}{\delta}} \|\mathcal{P}\|_\infty + c\|p - \mathcal{P}\|_\infty.
\end{aligned}$$

where $c = \sqrt{\alpha + \frac{2\rho}{\delta} \frac{\sqrt{\kappa}}{\gamma}}$, and (i) follows from the triangle inequality $\|p^{(w)}\|_\infty \leq \|p^{(w)} - \mathcal{P}\|_\infty + \|\mathcal{P}\|_\infty$, and (ii) holds as long as $\delta > c_0(1 - \alpha)^2 \log N$ for some $c_0 > 0$ sufficiently large, and (iii) comes from the triangle inequality $\|p^{(w)} - \mathcal{P}\|_\infty \leq \|p^{(w)} - p\|_2 + \|p - \mathcal{P}\|_\infty$.

(d) Now it is left to estimate the last item I_{22}^w . Note that

$$\begin{aligned}
I_{22}^w &= \sum_{v=1}^N \mathbf{1}_{(v,w) \in E} Q_{vw} (p_v^{(w)} - \mathcal{P}_v) \\
&= \sum_{v=1}^N \left[\alpha \mathbf{1}_{\{w=1\}} + (1 - \alpha) \frac{1}{d_v} \mathbf{1}_{(v,w) \in E} \right] (p_v^{(w)} - \mathcal{P}_v) \\
&= \underbrace{\alpha \sum_{v=1}^N \mathbf{1}_{\{w=1\}} (p_v^{(w)} - \mathcal{P}_v)}_{:= I_{221}^w} + \underbrace{(1 - \alpha) \sum_{v=1}^N \frac{\mathbf{1}_{(v,w) \in E}}{d_v} (p_v^{(w)} - \mathcal{P}_v)}_{:= I_{222}^w} \\
&\quad + \underbrace{(1 - \alpha) \sum_{v=1}^N \left(\frac{1}{d_v} - \frac{1}{\mathcal{d}_v} \right) \mathbf{1}_{(v,w) \in E} (p_v^{(w)} - \mathcal{P}_v)}_{:= I_{223}^w}.
\end{aligned}$$

Since both $p^{(w)}$ and \mathcal{P} are distribution vector, $I_{221}^w = 0$. Then, due to Hoeffding's inequality (Lemma S4),

$$\begin{aligned}
|I_{222}^w| &\leq 4\rho(1 - \alpha) \sqrt{\frac{\rho \log N}{\delta}} \|p^{(w)} - \mathcal{P}\|_\infty, \\
|I_{223}^w| &\leq 2\rho(1 - \alpha) \sqrt{\frac{\rho \log N}{\delta}} \|p^{(w)} - \mathcal{P}\|_\infty,
\end{aligned}$$

with probability at least $1 - \mathcal{O}(N^{-8})$. Thus, we reach the high probability event

$$|I_{22}^w| \leq 6\rho(1-\alpha)\sqrt{\frac{\rho \log N}{\delta}} \|p^{(w)} - \mathcal{P}\|_\infty.$$

In sums, we reach with probability at least $1 - \mathcal{O}(N^{-8})$,

$$\begin{aligned} |I_2^w| &\leq 16\rho^2(1-\alpha)\frac{\sqrt{\kappa\rho}}{\gamma}\sqrt{\alpha + \frac{2\rho}{\delta}}\sqrt{\frac{\log N}{\delta}}\|\mathcal{P}\|_\infty \\ &\quad + \left(\frac{\sqrt{\kappa}}{\gamma}\sqrt{\alpha + \frac{2\rho}{\delta}} + 6\rho(1-\alpha)\sqrt{\frac{\rho \log N}{\delta}}\right)\|p - \mathcal{P}\|_\infty. \end{aligned} \quad (17)$$

(e) Collecting the preceding bounds (14) and (17) together, we conclude that with high probability

$$\begin{aligned} \|p - \mathcal{P}\|_\infty &= \max_w |p_w - \mathcal{P}_w| \\ &\leq c_2(1-\alpha)\sqrt{\frac{\log N}{\delta}}\|\mathcal{P}\|_\infty + c_3\|p - \mathcal{P}\|_\infty, \end{aligned}$$

as long as $\delta/[(1-\alpha)\log N]$ is sufficiently large, which controls the entrywise error of p ,

$$\frac{\|p - \mathcal{P}\|_\infty}{\|\mathcal{P}\|_\infty} \leq c_1(1-\alpha)\sqrt{\frac{\log N}{\delta}}, \quad (18)$$

for some sufficiently large constant $c_1, c_2, c_3 > 0$.

REMARK. c_2 and c_3 are controlled by constants ρ, κ, γ , which are thereby driven from the model parameters \mathbf{B}, Θ, K , and Z .

(f) Finally, we accomplish the proof by observing that

$$\begin{aligned} \frac{\|p^* - \mathcal{P}^*\|_\infty}{\|\mathcal{P}^*\|_\infty} &\leq \frac{2 \max(d_{\min}^{-1}, \mathcal{d}_{\min}^{-1})}{\mathcal{d}_{\min}^{-1}} \frac{\|p - \mathcal{P}\|_\infty}{\|\mathcal{P}\|_\infty} \\ &\leq \frac{4\|p - \mathcal{P}\|_\infty}{\|\mathcal{P}\|_\infty}. \end{aligned}$$

Above observation together with the inequality (18) allow us to control the entrywise error of p^* as claimed, with probability at least $1 - \mathcal{O}(N^{-5})$,

$$\frac{\|p^* - \mathcal{P}^*\|_\infty}{\|\mathcal{P}^*\|_\infty} \leq c_2(1-\alpha)\sqrt{\frac{\log N}{\delta}},$$

for some sufficiently large constant $c_2 > 0$. □

S1.3 Concentration inequalities

The following is a standard concentration inequality used throughout the paper.

Lemma S4 (Hoeffding's inequality). *Let $\{X_i\}_{1 \leq i \leq n}$ be a sequence of independent random variables where*

$X_i \in [a_i, b_i]$ for each $1 \leq i \leq n$, and $S_n = \sum_{i=1}^n X_i$. Then,

$$\mathbb{P}(|S_n - \mathbb{E}S_n| \geq t) \leq 2 \exp \left\{ -\frac{t^2}{\sum_{i=1}^n (b_i - a_i)^2} \right\}.$$

The next lemma is a special case of Chernoff's bound.

Lemma S5 (Chernoff's bounds). *Let $\{X_i\}_{1 \leq i \leq n}$ be a sequence of independent random variables, whose sum is S_n , each having probability p_i of being equal to a_i , otherwise 0. Define $\mu = \sum_i p_i a_i$. Then, for any $\epsilon > 0$,*

$$\mathbb{P}(X_i \geq (1 + \epsilon)\mu) \leq (1 + \epsilon)^{-\epsilon\mu},$$

$$\mathbb{P}(X_i \leq (1 - \epsilon)\mu) \leq (1 - \epsilon)^{\epsilon\mu}.$$

For the use of this paper, we only invoke a simpler version of Bernstein inequality.

Lemma S6 (Bernstein's inequality). *Let $\{X_i\}_{1 \leq i \leq n}$ be a sequence of independent random variables with $|X_i| \leq B$ for each $1 \leq i \leq n$, and $S_n = \sum_{i=1}^n X_i$ and $T_n = \sum_{i=1}^n X_i^2$. Then, with probability at least $1 - 2n^{-a}$,*

$$|S_n - \mathbb{E}[S_n]| \leq \sqrt{2a \log n \mathbb{E}[T_n]} + \frac{2a}{3} B \log n$$

for any $a \geq 2$.

The proofs of Lemma S4, S5, and S6 can be found in Boucheron et al. [2013], hence are omitted.

S2 Additional information on model parameters

S2.1 Block connectivity matrix \mathbf{B}

In the paper, we assume that the block connectivity matrix \mathbf{B} corresponds to a strongly connected graph at block level and is positive definite. These assumptions asserts the efficacy of PPR clustering and is primarily a technical assumption sufficient for our theoretical results. In fact, we require \mathbf{B} to represent to a strongly connected graph because this enables the block-wise PPR vector to have the largest value corresponding to the block of seed(s) (Lemma 1 in the paper). On the other hand, we impose the positive definiteness on \mathbf{B} because this allows us to intuitively define the notion of local cluster, yet our statistical theory (i.e., the entrywise control of sample PPR vector) does not explicitly rely on such positive-definiteness per se. It is not clear yet whether these constraints are *necessary* in order for PPR clustering to function; possible generalizations of them are of research interest.

We list a few concrete examples showing that (i) if we break the strongly-connectivity assumption, the PPR clustering can fail, despite a reasonable teleportation constant, $\alpha = 0.15$, but (ii) PPR clustering often works as hoped even when \mathbf{B} is not positive-definite. Throughout, we assume that the first block is targeted and consider directed graphs with three underlying blocks ($K = 3$). The first two instances of \mathbf{B} demonstrates the necessity of the strongly-connectivity constraint, which ensures the block-wise aPPR vector to possess the largest first element. The third and fourth instances, on the other hand, indicate that \mathbf{B} need not to be positive definite.

S2.1.1 Violating the strongly-connective assumption

Hierarchy case. Let the block connectivity matrix

$$\mathbf{B} = \begin{bmatrix} p & p & p \\ 0 & p & p \\ 0 & 0 & p \end{bmatrix}$$

for some constant $p > 0$. \mathbf{B}_{ij} is the number (or the probability) of edges from the i -th block to the j -th block in population. Then, the directed graph represented by \mathbf{B} is not strongly connected, as block 3 has no path to the first block. In fact, this graph (specified by upper triangular \mathbf{B}) has a hierarchical structure, where the third block is in the center (or the highest hierarchy) of the graph, and the member of first block are essentially satellite from outside. Particularly, edges only come from outsiders to insiders.

We now perform the PPR clustering on the first cluster. The block-wise transition matrix is

$$\mathbf{P} = \begin{bmatrix} 1/3 & 1/3 & 1/3 \\ 0 & 1/2 & 1/2 \\ 0 & 0 & 1 \end{bmatrix}.$$

Then, both \mathbf{B} and \mathbf{P} are positive definite, with eigenvalues of (p, p, p) and $(1, 1/2, 1/3)$ respectively. To ease the calculation, we set $p = 3$. Then the block-wise PPR vector is approximately

$$\mathbf{p} = (0.209, 0.103, 0.688),$$

and the block-wise aPPR vector is approximately (after adjusting by column sums of \mathbf{B})

$$\mathbf{p}^* = (0.0698, 0.0172, 0.0764).$$

As shown, neither block-wise PPR vector nor aPPR vector properly recognize the local cluster 1.

Adding a small amount of circulation. If we add a small quantity to the left bottom element of above \mathbf{B} matrix, then the block connectivity matrix corresponds to a connected graph. To illustrate, we assign a small value to it, $\mathbf{B}_{31} = 0.1$, then the new block connectivity matrix becomes

$$\mathbf{B}' = \begin{bmatrix} p & p & p \\ 0 & p & p \\ 0.1 & 0 & p \end{bmatrix}.$$

To explore the PPR vector, we set $p = 3$ once again. In this case, \mathbf{B}' has one real eigenvalue (≈ 4.069) and two imaginary eigenvalues. The block-wise PPR vector is approximately

$$\mathbf{p} = (0.235, 0.115, 0.650),$$

and the block-wise aPPR vector is approximately (after adjusting by column sums of \mathbf{B}')

$$\mathbf{p}^* = (0.0755, 0.0192, 0.0723).$$

In this case, the PPR clustering works like a charm.

S2.1.2 Violating the positive-definite assumption

Consider again the $K = 3$ design with equally distributed block size. We present two examples breaking the positive-definite assumption on \mathbf{B} , where the PPR cluster still operates properly.

Indefinite case. Given some constants $r > p > 0$, define

$$\mathbf{B} = \begin{bmatrix} p & r & r \\ r & p & r \\ r & r & p \end{bmatrix}.$$

In this case, the random graphs generated from such configuration of \mathbf{B} have a unique characteristic: two vertices with different block memberships are more likely to connect than those pairs belonging to the same block. Note that the three eigenvalues of \mathbf{B} are $p + 2r$, $p - r$, and $p - r$. Hence, B is an indefinite matrix (so does the block-wise transition matrix \mathbf{P}).

Interestingly, the PPR clustering continues working under this circumstance. For simplicity, setting $p = 3$ and $r = 9$, and we articulate the block-wise PPR vector and aPPR vector. In fact, the block-wise PPR vector is approximately

$$\mathbf{p} = (0.386, 0.306, 0.306).$$

Since \mathbf{B} has homogeneous column sums, it follows that the first element in the block-wise aPPR vector is also the largest, suggesting the effectiveness of PPR clustering. The same conclusion hold when we set $p = 3$ and $r = 99$ (or 999).

Singular case. Suppose $p > 0$ and let

$$\mathbf{B} = \begin{bmatrix} 0 & p & 0 \\ p & 0 & p \\ 0 & p & 0 \end{bmatrix}.$$

In this case, nodes in block 1 only connect with those nodes in block 2, and the nodes in block 3 only have edges with block 2's members. Note that \mathbf{B} is singular because three of its eigenvalues are 1, -1, and 0. So does the block-wise transition matrix. However, the PPR clustering remain effective. In fact, the block-wise PPR vector and aPPR vector are

$$\mathbf{p} = (0.345, 0.459, 0.195) \quad \text{and} \quad \mathbf{p}^* = \frac{1}{p}(0.345, 0.230, 0.195).$$

In both cases (when \mathbf{B} is not positive-definite), the block-wise aPPR vector correctly assigns the largest value to the first element and thus is still effective for targeted sampling. These examples suggest a potentially greater applicability of the PPR clustering under the block model graph.

S2.1.3 Comments

Putting together above demonstrations, we briefly comment on \mathbf{B} and the PPR clustering. (i) The strongly-connectivity assumption is essential for the PPR clustering to be consistent. (ii) The efficacy of PPR clustering is conditioning on the fact that teleportation constant is sufficiently large. If we assign an

extremely small to it, e.g. $\alpha = 0.001$, the PPR clustering collapses. (iii) Beyond community-like graphs (where \mathbf{B} is positive-definite), the PPR clustering has potential for working on a more general block model graphs.

S2.2 Spectral analysis on graph transition \mathcal{P}

In this section, we present a spectral analysis of graph transition matrix, which demonstrates that (1) under the population DC-SBM, a graph transition matrix \mathcal{P} has exactly K positive eigenvalues, and $N - K$ zero eigenvalues, and (2) in a random graph generated from the DC-SBM, the graph transition matrix P is close to its population, with respect to spectral norm.

Lemma S7 (Eigen-decomposition for \mathcal{P} and \mathbf{P}). *Under the population DC-SBM with K blocks and parameters $\{\mathbf{B}, Z, \Theta\}$, let $\mathcal{P} \in \mathbb{R}^{N \times N}$ be the population graph transition matrix and $\mathbf{P} \in \mathbb{R}^{K \times K}$ be the block-wise transition matrix. Then, \mathcal{P} and \mathbf{P} have the same K positive eigenvalues. The remaining $N - K$ eigenvalues of \mathcal{P} are all zeros. Denote the K positive eigenvalues of both matrices as $\lambda_1 \geq \lambda_2 \geq \dots \geq \lambda_K \geq 0$, and let $\mathcal{X} \in \mathbb{R}^{N \times K}$ and $\mathcal{Y} \in \mathbb{R}^{K \times K}$ contain the left eigenvector of \mathcal{P} and \mathbf{P} respectively, corresponding to λ_i in their i -th column. Then, there exists a orthogonal matrix $U \in \mathbb{R}^{K \times K}$, such that*

- (a) $\mathcal{X}^\top = \mathcal{D}^{-1/2} \Theta^{1/2} Z U$; and
- (b) $\mathcal{Y}^\top = \mathbf{D}^{-1/2} U$.

Proof. We follow the proof of Lemma 3.3 in Qin and Rohe [2013]. Define $\mathbf{L} = \mathbf{D}^{-1/2} \mathbf{B} \mathbf{D}^{-1/2}$, then $\mathbf{P} = \mathbf{D}^{-1/2} \mathbf{L} \mathbf{D}^{1/2}$. By model assumption, $\mathbf{P} \succ 0$.

Define the graph Laplacian $\mathcal{L} = \mathcal{D}^{-1/2} \mathcal{A} \mathcal{D}^{-1/2}$, then by Lemma 2(b),

$$\mathcal{L}_{uv} = \frac{\mathcal{A}_{uv}}{\sqrt{d_u d_v}} = \frac{\theta_u \theta_v \mathbf{B}_{z(u)z(v)}}{\sqrt{d_u d_v}} = \frac{\mathbf{B}_{z(u)z(v)} \sqrt{\theta_u \theta_v}}{\sqrt{\mathbf{d}_{z(u)} \mathbf{d}_{z(v)}}} = [\mathbf{L}]_{z(u)z(v)} \sqrt{\theta_u \theta_v},$$

or equivalently,

$$\mathcal{L} = \Theta^{1/2} Z \mathbf{L} Z^\top \Theta^{1/2}.$$

Then

$$\mathcal{X}^\top \Lambda \mathcal{X}' = \mathcal{D}^{-1/2} \Theta^{1/2} Z U \Lambda U^\top Z^\top \Theta^{1/2} \mathcal{D}^{1/2} = \mathcal{D}^{-1/2} \mathcal{L} \mathcal{D}^{1/2} = \mathcal{D}^{-1} \mathcal{A} = \mathcal{P},$$

and

$$\mathcal{Y}^\top \Lambda \mathcal{Y}' = \mathbf{D}^{-1/2} U \Lambda U^\top \mathbf{D}^{1/2} = \mathbf{D}^{-1/2} \mathbf{L} \mathbf{D}^{1/2} = \mathbf{P},$$

where $\mathcal{X}' = U^\top Z^\top \Theta^{1/2} \mathcal{D}^{1/2}$ and $\mathcal{Y}' = U^\top \mathbf{D}^{1/2}$ are right eigenvectors of \mathcal{P} and \mathbf{P} respectively. Recognizing that $\mathcal{X}^\top \mathcal{X}' = \mathcal{Y}^\top \mathcal{Y}' = I_K$ completes the proof. \square

Lemma S8. *Let L be a symmetric matrix, let D be a diagonal matrix, and let $P = D^{-1/2} L D^{1/2}$. If x is an eigenvector of L corresponding to eigenvalue λ , then*

- (a) $D^{-1/2} x$ is a right eigenvector of P with eigenvalue λ ,
- (b) $\|P^\top P\| = \|L\|^2$.

Proof. Let $y = D^{-1/2} x$, then

$$P y = D^{-1/2} L D^{1/2} y = D^{-1/2} L x = \lambda D^{-1/2} x = \lambda y.$$

Supplementary Table S1: Number of nodes examined/reached by Algorithm 3 with seed node @NBCPolitics and different teleportation constants, and a fixed tolerance parameter $\epsilon = 10^{-7}$, as in August 2019.

α	Examined	Reached
0.1	7,445	342,454
0.15	5,919	272,985
0.25	4,860	228,561
1/3	3,984	193,848

Part (a) of the lemma follows. To see (b), observe that y is also an eigenvector of $P^\top P$ with eigenvalue λ^2 . \square

Lemma S8 implies that P has the same spectral norm of graph Laplacian L . Since L concentrates to \mathcal{L} (see for example Qin and Rohe [2013] for a proof), we have under a random graph generated from the DC-SBM, the graph transition matrix P concentrates to its population \mathcal{P} with respect to spectral norm.

S2.3 Teleportation constant α

In the paper, we state that a sufficiently large teleportation constant α enables the entrywise control of sample PPR vector, thus facilitating the PPR clustering in a random graph. Here, from a practical perspective, we further illustrate the sensitivity of PPR clustering to α , with the Twitter friendship network. To this end, we investigate the targeted sampling returned by four configurations of the teleportation constant, $\alpha \in \{0.1, 0.15, 0.25, 1/3\}$, where NBC Politics (@NBCPolitics) is the seed. The tolerance parameter is fixed, $\epsilon = 10^{-7}$, in four targeted sampling.

Table S1 lists the number of Twitter users we examined and the total number of users we “reached” (as of August 2019) in four attempts. Here, we examine a user by retrieving its friend list (after which it gets a positive p_u value in Algorithm 3), and reach a user once it appears in a user’s friend list (at which point, it possesses a positive r_v value in Algorithm 3). Given the same tolerance parameter, varying the teleportation constant largely affects the number of nodes examined/reached. This demonstrates the role of teleportation constant in leveraging between the seed preference and the standard random walk.

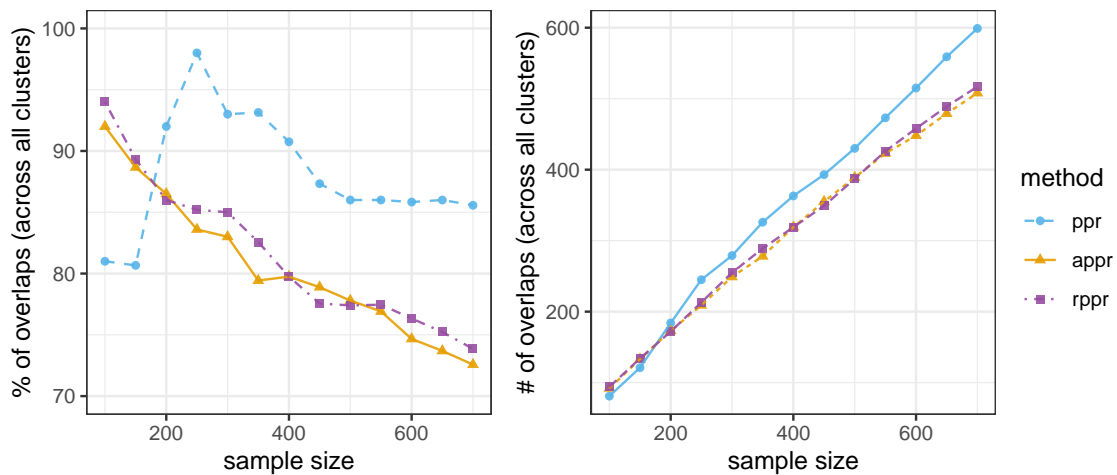
Despite the fact that different α ’s result in substantial difference in network coverage, when the algorithm stops, the estimated local clusters appear to share a vast majority in common. To demonstrate this immediately, we inspect the local clusters of size $n = 300$ returned by Algorithm 4 with four α ’s and quantify to what degree do they overlap each other. Table S2 shows the percentage of common members between each pair of four returned local clusters. As shown, most pairs have about 90% overlapping members, indicating that PPR clustering is fairly robust against the teleportation constant.

The stability of PPR clustering continues to show when we vary the cluster size, $n = 100, 150, \dots, 700$. Figure S1 shows the proportion of common members across *all* four local clusters, returned by PPR, aPPR, and rPPR (with the regularizer $\tau = 10$). Overall, the PPR clustering produces a fairly consistent local cluster, with around 80% of members overlapping across four different strengths of teleportation (see Supplementary Materials).

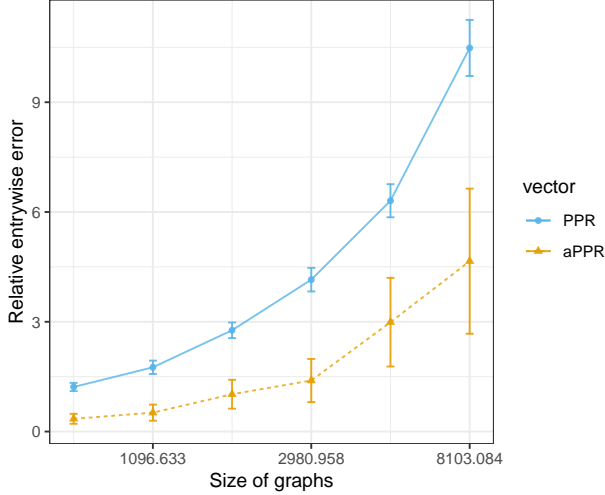
We conclude that in practice, PPR clustering (i) is mainly influential to the number of nodes examined in the targeted sampling and (ii) has fairly robust performance with respect to the choice of teleportation constant.

Supplementary Table S2: Percentage of pairwise overlapping among three local clusters around @NBCPolitics with different teleportation constants, $\alpha \in \{0.1, 0.15, 0.25, 1/3\}$, as in August 2019.

α	0.1	0.15	0.25	1/3
0.1	100%	92.7%	89.3%	87.7%
0.15		100%	93.3%	90%
0.25			100%	92%
1/3				100%



Supplementary Figure S1: Sensitivity to the teleportation constant, $\alpha = \{0.1, 0.15, 0.25, 1/3\}$. Shown are the percentage (left) and number (right) of common members across all four local clusters returned by three PPR clustering methods. The targeted sample size increases from 100 to 700 with the increment of 50.



Supplementary Figure S2: Entrywise error rate versus the graph sizes. Shown are relative entrywise error (REE) corresponding to different underlying graph sizes, averaged over 30 replicates. For each dot, an error bar indicates the standard error. The RER for aPPR vector is scaled down by a factor of 240 to improve visualization. The ticks in x-axis are transformed through logarithm with the natural base.

S2.4 The graph size N

In the paper, we provide an entrywise error control for the PPR vector and the aPPR vector (Theorem 2), assuming the edge density is sufficiently large (i.e., inequality (7) in the main paper). Simulation 3 in Section 5 demonstrates the relationship between the expected degree (δ) and the error rate of PPR clustering, as promised by the theorem. Here, we provide another simulation to illustrate Theorem 2. Specifically, we further investigate the affect of graph size (N) on the relative entrywise error (REE) of the PPR vector ($\frac{\|p-p\|_\infty}{\|p\|_\infty}$), given some edge density (δ).

We generate 30 replicates of networks of size $N = e^x$, where $x \in \{6.5, 7, 7.5, 8, 8.5, 9\}$, from the four-parameter stochastic block model, $\text{SBM}(K = 3, N, b_1 = 9, b_2 = 3)$. The average expect degree is set to $\delta = 125$. Both PPR vectors and aPPR vectors are calculated for every network, with teleportation constant $\alpha = 0.15$ and 10 seeds randomly selected from the first block. Figure S2 depict the REE with respect to different graph sizes (scaled by a logarithm transformation with the natural base). As shown, with δ fixed (not growing at the rate of $\log N$), the REE increases as the graph expands, so does the variance of REE for both PPR and aPPR vectors, matching the results in Theorem 2.

S3 Connection to linear discriminant analysis

In this section, we give another representation of PPR vectors in the landing probability space, which builds upon Kloumann et al. [2017]. This asserts PPR to a greater functional regime. Then, we extend the previous result that links the PPR vectors with linear discriminant functions under the DC-SBM. In particular, when every block has the same degree (volume), where \mathbf{D} becomes a scalar matrix, the PPR vector is asymptotically equivalent to the optimal linear discriminant function.

First, we briefly introduce linear discriminant analysis in landing probability space, which the PPR vector also lives in. Consider a random walk on the graph starting from a seed node. Define the *landing probability* r_s^v to be the probability that the random walk ends up at $v \in V$ after exactly s steps. The *landing probability*

space is the space of landing probability of any nodes.

A *linear discriminant* (LD) analysis keeps the first S landing probability on each node, $r^v = (r_0^v, r_1^v, \dots, r_S^v) \in \mathbb{R}^S$, and divides vertices into two sets by thresholding on the linear discriminant score vector $l \in \mathbb{R}^N$, whose v -th entry is defined to be inner product

$$l_v = \langle \omega, r^v \rangle$$

with some weights $\omega \in \mathbb{R}^S$. For example, let $\omega = r^{v_1} - r^{v_2}$, where v_1, v_2 are empirical centroids of two node sets. Then l_v increases as v slides from v_1 to v_2 , and thresholding $(\|v_1\|^2 - \|v_2\|^2)/2$ allocates vertices to nearest centroid.

REMARK. The landing probability of the s -th step, $r_s = (r_s^1, r_s^2, \dots, r_s^N) \in \mathbb{R}^N$, is defined as $(P^s)^\top \pi$. It follows from proposition 1 that PPR vector $p = \sum_{s=0}^{\infty} \phi_s r_s$ with $\phi_s = \alpha(1 - \alpha)^s$. Keeping the first S terms yields an LD score vector with the weights $\omega_{PPR} = (\phi_0, \phi_1, \dots, \phi_{S-1})$.

We then perform population (expectation) analysis for PPR in the landing probability space. Define the population *block landing probability* \mathbf{W}_s^k to be the probability that a random walk from v_0 ends up in block k after exactly s steps, where $k = 1, 2, \dots, K$ and $s = 0, 1, \dots, S - 1$. Given that v_0 is in block 1, $\mathbf{W}_0 = (1, 0, \dots, 0)^\top$. Using the first S steps block landing probabilities, the next lemma gives an explicit form of LD vectors.

Lemma S9 (Explicit form of LD vectors). *Under the population DC-SBM with K blocks and parameters $\{\mathbf{B}, \mathbf{Z}, \Theta\}$, assume all blocks have the same degrees. Let $\ell(k)$ be the linear discriminant score vector between block 1 and block k . Then,*

- (a) $\mathbf{W}_s = \mathbf{P}^\top \mathbf{W}_{s-1}$, $s = 1, 2, \dots, S - 1$; and
- (b) $\ell(k) = \Theta \mathbf{Z} \mathbf{U}(k)$, $k = 2, \dots, K$, where $\mathbf{U}(k) = \mathbf{W} \mathbf{W}^\top (e_1 - e_k)$.

Here, e_k is the elementary unit vector on the direction of k -th block.

Proof. We prove (a) using following quantities. Let E_s^k be the number of paths from v_0 to block k with exact length s , and let \mathcal{E}_s^k be the expected number of paths from v_0 to block k with exact length s . Recall from 3 that \mathbf{B}_{ij} represents the expected number of edges between block i and j if $i \neq j$, or twice of that if $i = j$. Then,

$$\mathcal{E}_s^k = \sum_{j=1}^K \mathbf{B}_{kj} \mathcal{E}_{s-1}^j.$$

To see $\mathbf{W}_s = \mathbf{P}^\top \mathbf{W}_{s-1}$, observe that

$$\mathbf{W}_s^k = \frac{\mathcal{E}_s^k}{\sum_{i=1}^K \mathcal{E}_s^i} = \frac{\sum_{j=1}^K \mathbf{B}_{kj} \mathcal{E}_{s-1}^j}{\sum_{i=1}^K \sum_{j=1}^K \mathbf{B}_{ij} \mathcal{E}_{s-1}^j} = \frac{\sum_{j=1}^K \mathbf{B}_{kj} \mathcal{E}_{s-1}^j}{\sum_{j=1}^K \mathbf{d}_j \mathcal{E}_{s-1}^j} = \sum_{j=1}^K \mathbf{P}_{kj} \mathbf{W}_{s-1}^j.$$

The last equality comes from the assumption that all blocks have the same degrees, which means \mathbf{d}_i is constant.

Now, we prove part (b) of the lemma. Let $R \in \mathbb{R}^{N \times S}$ collect all landing probabilities r_s^v of the first S steps, where $v = 1, 2, \dots, N$ and $s = 0, 1, \dots, S - 1$. Without loss of generality, assume the seed node corresponds to the first row. Define $\mathcal{R} = \mathbb{E}(R) \in [0, 1]^{N \times S}$ to be the population version of R . Then the population landing probability is explicitly

$$\mathcal{R}_s^v = \frac{d_v}{\mathbf{d}_{z(v)}} \mathbf{W}_s^{z(v)} = \theta_v \mathbf{W}_s^{z(v)},$$

or compactly,

$$\mathcal{R} = \Theta Z \mathbf{W}.$$

In linear discriminant, the weights vector ω is the geometric difference between centroid of block 1 and k , which can be written as

$$\left(\sum_{v:z(v)=1} \mathcal{R}_1^v - \sum_{v:z(v)=k} \mathcal{R}_1^v, \sum_{v:z(v)=1} \mathcal{R}_2^v - \sum_{v:z(v)=k} \mathcal{R}_2^v, \dots, \sum_{v:z(v)=1} \mathcal{R}_S^v - \sum_{v:z(v)=k} \mathcal{R}_S^v \right),$$

or compactly

$$\omega = \mathcal{R}^\top Z(e_1 - e_k).$$

By Lemma 2, the linear discriminant score vector reads

$$\begin{aligned} \langle \mathcal{R} \cdot \omega \rangle &= \mathcal{R} \mathcal{R}^\top Z(e_1 - e_k) \\ &= \Theta Z \mathbf{W} \mathbf{W}^\top (e_1 - e_k), \end{aligned}$$

for $k = 2, \dots, K$. Setting $\mathbf{l}(k) = \mathbf{W} \mathbf{W}^\top (e_1 - e_k)$ completes the proof. \square

Recall from Theorem 1 that $\boldsymbol{\rho} = \Theta Z \mathbf{p}$. The LD score vector ℓ has a similarly simple form that separates the block-related information (\mathbf{W}) and the node specific information (Θ and Z). Lemma S9 provides a population (expectation) representation of PPR in the landing probability space. To facilitate its application in random graphs, the next lemma provides a control of the landing probabilities on a random block model graph.

Lemma S10 (Concentration of landing probabilities). *Let $G = (V, E)$ be a graph of N vertices generated from the DC-SBM with K blocks and parameters $\{B, Z, \Theta\}$. Let $R_s^u \in [0, 1]^N$ be the landing probabilities of the k -th step, and $\mathcal{R}_s^u = \mathbb{E}(R_s^u)$ be its expectation. Then, for any $\epsilon > 0$ and any vertex $u = 1, 2, \dots, N$,*

$$\begin{aligned} \mathbb{P}(R_s^u \geq (1 + \epsilon)\mathcal{R}_s^u) &\leq (1 + \epsilon)^{-\epsilon N r}, \\ \mathbb{P}(R_s^u \leq (1 - \epsilon)\mathcal{R}_s^u) &\leq (1 - \epsilon)^{\epsilon N r}, \end{aligned}$$

where $r = \min_{v \in V} \theta_u \theta_v \mathbf{P}_{z(u)z(v)} \mathbf{W}_{s-1}^{z(v)}$.

Proof. Note that $R_s^u = \sum_{v \in V} X_{uv}$, where

$$X_{uv} = \frac{\mathbf{W}_{s-1}^{z(v)}}{\mathbf{d}_{z(v)}} \mathbf{1}_{\{A_{uv}=1\}}$$

are independent random variables having probability $\theta_u \theta_v \mathbf{B}_{z(u)z(v)}$ of being equal to $\mathbf{W}_{s-1}^{z(v)} / \mathbf{D}_{z(v)z(v)}$. Then,

$$\mathbb{E}[R_s^u] = \sum_{v \in V} \frac{\mathbf{W}_{s-1}^{z(v)}}{\mathbf{d}_{z(v)}} \theta_u \theta_v \mathbf{B}_{z(u)z(v)} = \theta_u \sum_{k=1}^K \mathbf{P}_{z(u)k} \mathbf{W}_{s-1}^k = \mathcal{R}_s^u.$$

We can apply Chernoff's bounds (Lemma S5) on R_s^u and obtain bounds for any fixed u ,

$$\mathbb{P}(R_s^u \geq (1 + \epsilon)\mathcal{R}_s^u) \leq (1 + \epsilon)^{-\epsilon \mathcal{R}_s^u},$$

and

$$\mathbb{P}(R_s^u \leq (1 - \epsilon)\mathcal{R}_s^u) \leq (1 - \epsilon)^{\epsilon\mathcal{R}_s^u}.$$

Recognizing that $\mathcal{R}_s^u \geq Nr$ completes the proof. \square

Lemma S10 provides an entrywise concentration bound for landing probabilities. The next theorem equates PPR and LD vectors when blocks are equally distributed. Together, they asserts the asymptotically equivalence between PPR and LD vectors, in symmetric block model graphs.

Theorem S1 (Equivalence between PPR and LD vectors). *Under the population DC-SBM with K blocks and parameters $\{\mathbf{B}, Z, \Theta\}$, assume $B_{ii} = b_1$ for all i , and $B_{ij} = b_2$ for $i \neq j$ ($b_1 > b_2 > 0$). Let λ_2 the second largest eigenvalue of \mathcal{P} . Let $\boldsymbol{\rho}$ be the personalized PageRank vector, and let $\ell(k)$ be the linear discriminant score vector between block 1 and block k , $k = 2, \dots, K$. If the teleportation constant $\alpha = 1 - \lambda_2$, then*

$$\boldsymbol{\rho} \propto \ell(k).$$

Proof. From Section S2.2 and Lemma S9(a), the block landing probability is precisely

$$\mathbf{W}_s^k = \sum_{j=1}^K \lambda_j^s U_{kj} U_{1j},$$

where λ_k is the k -th eigenvalues of \mathcal{P} and U is the orthogonal matrix used in Lemma S2.2.

Note that \mathbf{B} has eigenvalues $\lambda_1 = 1$ and $\lambda_2 = \frac{b_1 - b_2}{b_1 + b_2}$, with complexity indices 1 and $k - 1$ respectively. In addition, we know the orthogonal matrix above precisely as well,

$$U = \begin{bmatrix} \frac{1}{\sqrt{N}} & \frac{1}{\sqrt{2}} & \frac{1}{\sqrt{2}} & \cdots & \frac{1}{\sqrt{2}} \\ \frac{1}{\sqrt{N}} & -\frac{1}{\sqrt{2}} & 0 & \cdots & 0 \\ \frac{1}{\sqrt{N}} & 0 & -\frac{1}{\sqrt{2}} & \cdots & 0 \\ \vdots & \vdots & \vdots & & \vdots \\ \frac{1}{\sqrt{N}} & 0 & 0 & \cdots & -\frac{1}{\sqrt{2}} \end{bmatrix}.$$

Then it follows from Lemma S9(b) that the LD weight vector is

$$\begin{aligned} \omega_{LD} &= \mathcal{R}^\top Z(e_1 - e_k) \\ &= \mathbf{W}^\top(e_1 - e_k) \\ &= \mathbf{W}^1 - \mathbf{W}^k \\ &= \sum_{j=1}^K \lambda_j^s (U_{1j} - U_{kj}) U_{1j} \\ &= \frac{K}{2} \begin{bmatrix} 1 \\ \lambda_2 \\ \lambda_2^2 \\ \vdots \\ \lambda_2^{S-1} \end{bmatrix}. \end{aligned}$$

On the other hand, the weight vector of PPR on landing probability space is $\omega_{PPR} = (\phi_0, \phi_1, \dots)$, where

$\phi_s = \alpha(1 - \alpha)^s$. Hence, setting the teleportation constant $\alpha = 1 - \lambda_2$ asymptotically equates approximate PPR and LD vectors, up to a scalar factor. \square

REMARK. First, a positive factor that differentiates PPR and LD vectors does not change the relative ranking of the nodes, because the ranking via ρ or $c\rho$ is equivalent. Hence, Theorem S1 shows that the PPR vector is equivalent to an optimal LD score vector under described population DC-SBM. Second, Theorem S1 is an extension of Kloumann et al. [2017]. Combining Theorem S1 and Lemma S10 gives the asymptotic equivalence between PPR and LD vectors under the particular DC-SBM stated.

S4 Lists of top 200 handles

In this section, we supply three lists of handles resulting from sampling using PPR, aPPR, and rPPR vectors with @NBCPolitics as the seed, as of December 2018. We conceal handles with followers count fewer than 200 for privacy considerations. The biographical descriptions are trimmed for unifying displays. In addition, we annotate handles with whether or not they are followed (“Followed”) by the seed node.

S4.1 A PPR’s sample of 200

Supplementary Table S3: Top (selected) handles returned by PPR.

	Name	Followed	Followers	Description
1	Melania Trump	Yes	11242283	This account is run by the Office of First Lady Melania Trum...
2	The White House	Yes	17625630	Welcome to @WhiteHouse! Follow for the latest from President...
3	Chuck Todd	Yes	2032038	Moderator of @meetthepress and @nbcnews political director; ...
4	NBC News	Yes	6280551	The leading source of global news and info for more than 75 ...
5	NBC Nightly News	Yes	962290	Breaking news, in-depth reporting, context on news from arou...
6	Andrea Mitchell	Yes	1737764	NBC News Chief Foreign Affairs Correspondent/anchor, Andrea ...
7	Savannah Guthrie	Yes	881669	Mom to Vale & Charley, TODAY Co-Anchor, Georgetown Law...
8	Joe Scarborough	Yes	2521215	With Malice Toward None
9	MSNBC	Yes	2261911	The place for in-depth analysis, political commentary and in...
10	Rachel Maddow MSNBC	Yes	9498076	I see political people... (Retweets do not imply endorsement...
11	Breaking News	Yes	9223158	
12	NBC News First Read	Yes	53847	The first place for news and analysis from the @NBCNews Poli...
13	TODAY	Yes	4276453	America’s favorite morning show Snapchat: todayshow
14	Meet the Press	Yes	566713	Meet the Press is the longest-running television show in his...
15	The Wall Street Journal	Yes	16188842	Breaking news and features from the WSJ.
16	Pete Williams	Yes	70062	NBC News Justice Correspondent. Covers US Supreme Court, ...
17	Mark Murray	Yes	97571	Mark Murray is the senior political editor for NBC News, as ...
18	POLITICO	Yes	3695835	Nobody knows politics like POLITICO. Got a news tip for us? ...
19	Katy Tur	Yes	587474	MSNBC anchor @2pm, NBC News correspondent, author of NYT ...
20	Bill Clinton	Yes	10697521	Founder, Clinton Foundation and 42nd President of the United ...
21	Kasie Hunt	Yes	381704	@NBCNews Capitol Hill Correspondent. Host, @KasieDC, Sundays...
22	TIME	Yes	15584815	Breaking news and current events from around the globe. Host...
23	Kelly O’Donnell	Yes	195765	White House Correspondent @NBCNews Veteran of Cap Hill ...
24	John McCain	Yes	3181773	Memorial account for U.S. Senator John McCain, 1936-2018. To...
25	Peter Alexander	Yes	283522	@NBCNews White House Correspondent / Weekend @TODAYshow ...
26	Hallie Jackson	Yes	359099	Chief White House Correspondent / @NBCNews / @MSNBC ...
27	Kristen Welker	Yes	182244	@NBCNews White House Correspondent. Links and retweets ...
28	Carrie Dann	Yes	37119	.@NBCNews / @NBCPolitics. RTs not endorsements.
29	Willie Geist	Yes	807536	Host @NBC #SundayTODAY, Co-Host @Morning_Joe, Sunday ...
30	Morning Joe	Yes	563650	Live tweet during the show! Links to must-read op-eds and ...
31	Frank Thorp V	Yes	58152	Producer & Off-Air Reporter covering Congress at @NBCNews ...
32	Mark Knoller	Yes	318923	CBS News White House Correspondent
33	Tom Brokaw	Yes	308276	Special correspondent, @NBCNews
34	Mika Brzezinski	Yes	868124	”Bipartisanship helps to avoid extremes and imbalances. It ...
35	Chris Jansing	Yes	72375	@msnbc Senior National Correspondent, intrepid traveler and ...
36	John Harwood	Yes	251246	a Dad who covers Washington, the economy and national politi...
37	Nicolle Wallace	Yes	413153	Author of 18 Acres series, mom, dog walker, wife, gardener. ...
38	NBC News Signal	Yes	83715	A new streaming news channel from @NBCNews. Catch us Thursda...
39	Sam Stein	Yes	392003	Daily Beast/MSNBC newsletter: https://t.co/DVURxntWdL Emai...
40	Chris Matthews	Yes	882434	Host of @hardball M-F at 7PM ET on @MSNBC and author of ”Bob...
41	Carol Lee	Yes	51240	Reporter for NBC News, former WSJ & POLITICO, Hudson’s mom, ...
42	Ali Vitali	Yes	78839	@NBCnews Political Reporter. Covered Trump campaign, WH + ...
43	Ken Dilanian	Yes	124635	Intelligence and national security reporter for the NBC News...
44	Jim Miklaszewski	Yes	14196	Jim Miklaszewski is Chief Pentagon Correspondent for NBC New...
45	John Heilemann	Yes	247616	@SHO_TheCircus host/ep; NBCNews/@MSNBC natl affairs analyst;...
46	Stephanie Ruhle	Yes	352895	Mom, MSNBC LIVE Anchor 9AM M-F, VELSHI & RUHLE 1 PM ...
47	Nick Confessore	Yes	172359	Reporter for @NYTimes, writer-at-large for @NYTmag, MSNBC ...
48	Talking Points Memo	Yes	275692	Breaking news and analysis from the TPM team. Ill leave ...
49	Tom Costello	Yes	17268	NBC News Correspondent covering Aviation, Transportation, Ec...
50	Post Politics	Yes	384611	The latest political news and analysis from The Washington P...
51	Alex Moe	Yes	28245	@NBCNews Capitol Hill Producer + Off-Air Reporter; ’12 & ’16...
52	Benjy Sarlin	Yes	100896	Political reporter for @NBCNews. I cover elections and their...
53	Preet Bharara	Yes	945030	Patriotic American & proud immigrant. Movie buff. @Springste...
54	Matthew Miller	Yes	229867	Partner at Vianovo. MSNBC Justice & Security Analyst. Recove...
55	Leigh Ann Caldwell	Yes	20714	NBC Capitol Hill reporter. Formerly at CNN and public radio....
56	Ken Strickland	Yes	2693	NBC News Washington Bureau Chief
57	Ron Fournier	Yes	64356	President: Truscott Rossman. Best-seller https://t.co/09CdTN...
58	Mike Memoli	Yes	39693	National Political Reporter @nbcnews; @latimes alum mike dot...
59	Miguel Almaguer	Yes	14082	Prolific coffee drinker. Chronic under sleeper. Raging road ...

... continued

	Name	Followed	Followers	Description
60	Courtney Kube	Yes	9494	NBC News National Security & Military Reporter. Links and ...
61	NBC News World	Yes	279165	A dynamic look at world events from @NBCNews.
62	Jonathan Martin	Yes	241690	Nat'l Political Correspondent, NY Times. Husband of the ...
63	Steve Schmidt	Yes	498812	"Patriotism means to stand by the country. It does not mean ...
64	Jenna Bush Hager	Yes	207106	Mama to M and P, NBC News correspondent, Editor-at-Large ...
65	Sean Spicer	Yes	406957	President of RigWil, Sr Advisor @AmericaFirstPAC check out ...
66	Roll Call	Yes	356374	Breaking news, reporter tweets and analysis from the Source ...
67	POLITICO 45	Yes	88470	A daily diary of the 45th president of the United States.
68	Scott Foster	Yes	3464	Senior Producer, Washington @NBCNEWS @TODAYshow
69	Domenico Montanaro	Yes	83999	"Congress shall make no law respecting an est. of religion, ...
70	Tom Winter	Yes	40777	NBC News Investigations reporter based in New York focusing ...
71	Kailani Koenig	Yes	11416	Producer with @MSNBC & @NBCNews. Team @MeetThePress ...
72	Capital Journal	Yes	131212	WSJs home for politics, policy and national security news. ...
73	NBC News Videos	Yes	7838	The latest video from http://t.co/xPyvMOTEF6
74	Diane Sawyer	Yes	876906	I like my news 24/7, my food spicy, my drinks caffeinated, ...
75	Jane C. Timm	Yes	6478	@nbcnews political reporter and fact checker. More fun than ...
76	Elyse PG	Yes	2697	White House producer @nbcnews @USCAnnenberg alum LA kid ...
77	Libby Leist	Yes	7946	Executive Producer @todayshow
78	Mike Barnicle	Yes	116588	Mike Barnicle is an award-winning print and broadcast journa...
79	Reuters Politics	Yes	259106	U.S. political coverage, breaking news and special investiga...
80	Beth Fouhy	Yes	13684	Senior editor, politics, NBC News and MSNBC
81	HuffPost	Yes	11401771	Know what's real.
82	Joey Scarborough	Yes	6277	NBC News Social Media Editor. New York Daily News Alum. RTs ...
83	Marianna Sotomayor	Yes	11965	Running around Capitol Hill for @NBCNews. Covers politics ...
84	Shaquille Brewster	Yes	5362	@NBCNews Producer/Politics @HowardU Alum Journalist ...
85	Joyce Alene	Yes	185116	U of Alabama Law Professor @MSNBC Contributor Obama US ...
86	Garrett Haake	Yes	40714	Correspondent @msnbc Taller than I look on TV Long-suffe...
87	Andrew Rafferty	Yes	16567	Senior political editor for @newsy Before that @NBCNews ...
88	Jacob Soboroff	Yes	144153	@MSNBC correspondent. Instagram & Snapchat: jacobsoboroff
89	Perry Bacon Jr.	Yes	26853	I write about government (mostly federal, often state, ...
90	Alex Witt	Yes	28126	Weekend host on @MSNBC (9am, noon & 1pm). Tiggers mom ...
91	Mark Halperin	Yes	332564	New York, New York
92	Heidi Przybyla	Yes	66489	NBC News, n'tl political reporter "Prezbella" Heidi.Przyb...
93	Morgan Radford	Yes	20967	@NBCNews Correspondent: @TODAYShow/@NBCNightlyNews .
94	Savannah Sellers	Yes	4637	News junkie. Host of NBC's "Stay Tuned" on Snapchat. Storyte...
95	Marist Poll	Yes	16030	Founded in 1978, MIPO is home to the Marist Poll and regular...
96	Jill Wine-Banks	Yes	158753	@NBCNews & @MSNBC Contributor. Speaker. Watergate prosecutor...
97	NBC Field Notes	Yes	1390	NBC News correspondents and http://t.co/1eSopOQt8s reporters...
98	Olivia Nuzzi	Yes	190919	Washington Correspondent, New York Magazine
99	NBC News THINK	Yes	12017	THINK is NBC News' home for fresh opinion, sharp analysis ...
100	Making a Difference	Yes	670	@NBCNightlyNews' popular feature profiles ordinary people do...
101	adam nagourney	Yes	25307	LA Bureau Chief for The New York Times. Story ideas welcome ...
102	Phil McCausland	Yes	2519	@NBCNews Digital reporter focused on the rural-urban divide...
103	Katie Couric	Yes	1746116	Journalist, podcaster, @SU2C founder, doc filmmaker of @FedU...
104	Monica Alba	Yes	30034	@NBCNews White House team. Covered Hillary Clinton on the ...
105	Vicente Fox Quesada	Yes	1244017	Presidente de Mxico de 2000 a 2006 y ahora trabajando po...
106	Alex Johnson	Yes	4371	News, data and analysis for @NBCNews; data geek; non-celebri...
108	Alex Seitz-Wald	Yes	50168	Political reporter for @NBCNews covering Democrats Tips, ...
109	Anthony Terrell	Yes	6827	Emmy Award winning journalist. Political observer. Covered ...
110	Sam Petulla	Yes	2588	Editor @cnnpolitics Usually looking for datasets. You can ...
111	Debra Messing	Yes	532941	Actor. Mama. Global Ambassador for HIV/AIDS for PSI. Activis...
112	Corky Siemaszko	Yes	2538	Senior Writer at NBC News Digital (former NY Daily News rewr...
114	Zach Haberman	Yes	3693	Lead Breaking News Editor, @NBCNews. Previously had other jobs ...
115	NBC Latino	Yes	67920	Elevating the conversation around Latino news in the United ...
116	Vivian Salama	Yes	16020	White House reporter for @WSJ. Formerly AP Baghdad bureau ...
117	Zeke Miller	Yes	215054	White House Reporter @AP. Email: zekejmiller@gmail.com Links...
118	Vaughn Hillyard	Yes	31464	On the Road, Meeting Good Folk NBC News Arizonan IG: @...
119	Jonathan Allen	Yes	44477	political reporter, @NBCNews Digital co-author, NYT bestse...
121	HuffPost Politics	Yes	1428870	The latest political news from HuffPost's politics team.
122	Nick Akerman	Yes	14949	Partner in the AmLaw 100 law firm of Dorsey & Whitney, Water...
123	CSPAN	Yes	1915821	Capitol Hill. The White House. National Politics.
124	John McCormack	Yes	30688	Senior writer at The Weekly Standard.

...continued

	Name	Followed	Followers	Description
125	Jo Ling Kent	Yes	32957	NBC News Correspondent @NBCNightlyNews, @TODAYshow ...
126	PolitiFact	Yes	628659	Home of the Truth-O-Meter and independent fact-checking ...
127	Bob Corker	Yes	10042	Serving Tennesseans in the U.S. Senate
128	Elise Jordan	Yes	58884	Co-host of @WMM_podcast podcast. @MSNBC/@NBCNews political...
129	Greg Martin	Yes	1161	Political Booking Producer at @nbcnews @todayshow
130	Education Nation	Yes	276468	Hosted by @NBCNews. Creator of Parent Toolkit & moderator of...
131	Micah Grimes	Yes	25948	Head of Social, @NBCNews & @MSNBC – Foreign and domestic ...
132	Jill Lawrence	Yes	17282	Commentary editor and columnist @USATODAY. Author of The Art...
133	McKay Coppins	Yes	131623	Staff writer at @TheAtlantic. Author of THE WILDERNESS. 'Sor...
134	Emmanuelle Saliba	Yes	4004	Head of Social Media Strategy @Euronews Launched #THECUBE ...
135	Hasani Gittens	Yes	3002	Level 29 Mage. Senior News Ed. @NBCNews. Sheriff of Nattahna...
136	Rebecca Sinderbrand	Yes	18691	Now: @NBCNews Senior Washington Editor, visiting lecturer @Y...
137	BuzzFeed Politics	Yes	121646	News and updates from the politics team @BuzzFeedNews.
138	Adam Edelman	Yes	2341	Political reporter @nbcnews. Wisconsin native, Bestchester r...
139	Ethan Klapper	Yes	18292	Journalist (@YahooNews) and #avgeek.
140	President Trump	No	24593638	45th President of the United States of America, @realDonaldTrump...
141	Vice President Mike ...	No	6795022	Vice President Mike Pence. Husband, father, & honored to ...
142	Donald J. Trump	No	56050499	45th President of the United States of America
143	Karen Pence	No	403315	Educator, mom, wife of @VP Pence. Passionate about art thera...
144	Sarah Sanders	No	3522219	@WhiteHouse Press Secretary. Proudly representing @POTUS ...
145	Kellyanne Conway	No	2506546	Mom. Patriot. Catholic. Counselor.
146	DRUDGE REPORT	No	1408129	The DRUDGE REPORT is a U.S. based news aggregation website ...
147	White House History	No	104010	The White House Historical Association is a non-profit organ...
148	The New York Times	No	42412491	Where the conversation begins. Follow for breaking news, ...
149	White House Archived	No	13379715	This is an archive of an Obama Administration account mainta...
150	Dan Scavino Jr.	No	324561	Assistant to President @realDonaldTrump, Director of Social ...
151	Drudge Buzz	No	104111	Tracking the buzz made by Americas #1 newsmaker Matt Drudge...
152	David Gregory	No	1749373	CNN, Georgetown U
153	Hillary Clinton	No	23643522	2016 Democratic Nominee, SecState, Senator, hair icon. Mom, ...
154	CNN Breaking News	No	54476034	Breaking news from CNN Digital. Now 54M strong. Check @cnn ...
155	The Cabinet	No	123597	The @WhiteHouse Office of Cabinet Affairs. Tweets may be arc...
156	Lester Holt	No	501427	Anchor @NBCNightlyNews and @datelinebc, reporting on the to...
157	John Dickerson	No	48122	Co-host CBS This Morning. This account @johndickerson is mos...
158	CNN	No	40854429	Its our job to #GoThere & tell the most difficult stories. ...
159	J Earnest (Archived)	No	1182091	WH Press Secretary. This is an archive of an Obama Administr...
160	The Washington Post	No	13117609	Breaking news, analysis, and opinion. Founded in 1877. Our ...
161	Adam Liptak	No	61589	Supreme Court reporter for The New York Times
162	NSC	No	35905	National Security Council Tweets may be archived ...
163	MSNBC video	No	40669	Favorite video highlights from @msnbc.
164	Gorsuch Facts	No	39143	Judge Gorsuch will be fair to all regardless of their backgr...
165	Greg Stohr	No	11651	Supreme Court reporter for Bloomberg News. Baseball dad ...
166	OMB Press	No	11182	Office of Management and Budget Tweets may be archived: ...
167	Richard Engel	No	288066	@NBCNews Chief Foreign Correspondent
168	Norah O'Donnell	No	195549	Wife, mother of 3, Co-Host @cbsthismorning, #1 fan of @chefg...
169	Robert Barnes	No	37361	Robert Barnes covers the Supreme Court for The Washington Po...
170	Luke Russert	No	253495	Sometimes nothing can be a real cool hand. STA'04/BC'08
171	Stephen Colbert	No	18269222	the guy on CBS
172	Mark Sherman	No	6336	
173	U.S. Attorney EDVA	No	5709	Led by U.S. Attorney G. Zachary Terwilliger. 130+ attorneys ...
174	The Associated Press	No	13051963	News from The Associated Press, and a taste of the great jou...
175	Joe Palazzolo	No	10938	WSJ reporter covering legal issues. joe.palazzolo@wsj.com. ...
176	Natalie Morales	No	443991	@TODAYshow Anchor and @AccessOnline Anchor, Author, mom ...
177	Brent Kendall	No	5451	WSJ legal affairs reporter in Washington. Native Tar Heel, ...
178	Joan Biskupic	No	11021	CNN legal analyst & Supreme Court biographer; Chicago native...
179	Keith Olbermann	No	1097676	Dogs. And sports. And whales (Tom Jumbo-Grumbo on BoJack ...
180	Brian Williams	No	230947	
181	Pope Francis	No	17791867	Welcome to the official Twitter page of His Holiness Pope Fr...
182	Ezra Klein	No	2500383	Founder and editor-at-large, https://t.co/5gESirESRH. Why ...
183	Anderson Cooper	No	9967099	tweets by Anderson Cooper. Anchor @AC360 and correspondent...
184	BBC News (World)	No	24153838	News, features and analysis from the World's newsroom. Break...
185	Reince Priebus	No	935431	President @MichaelBestLaw; Exclusive Speaker @WashSpeakers; ...
186	Joe Biden	No	3111675	Represented Delaware in the Senate for 36 years, 47th Vice P...

...continued

	Name	Followed	Followers	Description
187	Department of State	No	5149607	Welcome to the official U.S. Department of State Twitter acc...
188	Jim Miklaszewski	No	1956	Chief Pentagon Correspondent for NBC News
189	Tony Mauro	No	20310	Supreme Court correspondent, https://t.co/571ZdQnzo2 and The...
190	David Axelrod	No	1113850	Director, UChicago Institute of Politics. Senior Political ...
191	Nate Silver	No	3176243	Editor-in-Chief, @FiveThirtyEight. Author, The Signal and ...
192	George Bush	No	356042	A tribute site to the 41st President of the United States of...
193	CBS News	No	6537991	Your source for original reporting and trusted news.
194	Jonathan Karl	No	206986	ABC News Chief White House Correspondent. insta @jonkarl ...
195	BBC Breaking News	No	38539186	Breaking news alerts and updates from the BBC. For news, ...
196	Mitt Romney	No	1977201	Senator-elect from Utah.
197	ABC News	No	13985606	All the news and information you need to see, curated by the...
198	Deborah Turness	No	10389	President of NBC News International
199	The Hill	No	3162118	The Hill is the premier source for policy and political news...
200	Ann Curry	No	1536122	Journalism is an act of faith in the future.

S4.2 An aPPR's sample of 200

Supplementary Table S4: Top (selected) handles returned by aPPR. The handles with fewer than 200 followers are hidden for privacy considerations.

	Name	Followed	Followers	Description
1		Yes	198	Enroll America National Regional Director http://t.co/X6jJIE...
2	Jennifer Sizemore	Yes	386	
3	Alissa Swango	Yes	441	Director of Digital Programming at @natgeo. All things food....
4	Making a Difference	Yes	670	@NBCNightlyNews' popular feature profiles ordinary people do...
5		No	1	
6		No	3	
7	Greg Martin	Yes	1161	Political Booking Producer at @nbcnews @todayshow
8		No	1	I am Area Man. I pwn your news feed.
9		No	2	
10	NBC Field Notes	Yes	1390	NBC News correspondents and http://t.co/1eSopOQt8s reporters...
11		No	2	
12		No	2	
13		No	1	
14		No	1	
15		No	1	
16		No	1	
17		No	3	yet another activist twitter, fighting all those fun -isms ...
18		No	4	
19		No	7	Dianne Kube is an Author with a passion, for family, holiday...
20		No	7	
21	Adam Edelman	Yes	2341	Political reporter @nbcnews. Wisconsin native, Bestchester ...
22	Phil McCausland	Yes	2519	@NBCNews Digital reporter focused on the rural-urban divide....
23	Corky Siemaszko	Yes	2538	Senior Writer at NBC News Digital (former NY Daily News rewr...
24	Sam Petulla	Yes	2588	Editor @cnnpolitics Usually looking for datasets. You can ...
25	Ken Strickland	Yes	2693	NBC News Washington Bureau Chief
26		No	7	
27	Elyse PG	Yes	2697	White House producer @nbcnews @USCAnnenberg alum LA kid ...
28		No	2	Change your thoughts & you change your world. -Norman Vincen...
29		No	4	
30		No	13	
31		No	6	
32		No	154	We distribute new, never-worn clothing and merchandise to ...
33		No	10	
34	Hasani Gittens	Yes	3002	Level 29 Mage. Senior News Ed. @NBCNews. Sheriff of Nattahna...
35		No	1	
36	Scott Foster	Yes	3464	Senior Producer, Washington @NBCNEWS @TODAYshow
37		No	2	
38		No	13	
39		No	5	
40	Zach Haberman	Yes	3693	Lead Breaking News Editor, @NBCNews. Previously had other jobs...
41		No	3	just like to stay in the know :) just like to stay in the ...
42		No	2	
43		No	5	
44		No	7	
45		No	1	
46	Emmanuelle Saliba	Yes	4004	Head of Social Media Strategy @Euronews Launched #THECUBE ...
47		No	2	
48	Alex Johnson	Yes	4371	News, data and analysis for @NBCNews; data geek; non-celebri...
49		No	8	
50	Savannah Sellers	Yes	4637	News junkie. Host of NBC's "Stay Tuned" on Snapchat. Storyte...
51		No	21	
52		No	6	Anti-money laundering professional with federal law enforcem...
53		No	15	
54	Shaquille Brewster	Yes	5362	@NBCNews Producer/Politics @HowardU Alum Journalist Pol...
55		No	2	Just another DIY, punk kid from the black land dirt of NEPA?...
56		No	18	Cdr Bob Mehal, Public Affairs Office, Office of the Secretar...
57		No	5	

...continued

	Name	Followed	Followers	Description
58		No	4	
59		No	8	
60		No	10	
61		No	2	
62	Joey Scarborough	Yes	6277	NBC News Social Media Editor. New York Daily News Alum. RTs ...
63		No	5	
64		No	1	
65	Voices United	No	310	Voices United is a non profit educational organization for ...
66	Jane C. Timm	Yes	6478	@nbcnews political reporter and fact checker. More fun than ...
67	Social Headlines	No	344	Daily roundup of top social media and networking stories.
68	James Miklaszewski	No	337	Writer, Photographer, Editor, Director, Producer, Newshound ...
69		No	12	
70	Anthony Terrell	Yes	6827	Emmy Award winning journalist. Political observer. Covered ...
71		No	10	
72		No	8	
73		No	8	I'm the real Charlie Sheen. If you are a Winner, stick aroun...
74		No	9	Quotes from a nice jewish mom who's just tryna get some nice...
75		No	2	
76		No	4	
77		No	6	"Rawr!"
78	NBC News Videos	Yes	7838	The latest video from http://t.co/xPyvMOTEF6
79		No	9	
80		No	4	
81	Libby Leist	Yes	7946	Executive Producer @todayshow
82		No	8	
83		No	2	I'm running for President of the United States of America.
84		No	35	
85		No	8	
86		No	2	
87		No	2	
88		No	16	
89		No	4	
90		No	5	Happy princess
91		No	1	
92		No	4	
93	Courtney Kube	Yes	9494	NBC News National Security & Military Reporter. Links and ...
94		No	5	
95		No	5	
96		No	169	
97		No	5	
98		No	2	
99	Vets Helping Heroes	No	449	Raising funds to sponsor the training of assistance dogs for...
100		No	12	
101		No	4	
102		No	8	
103	Bob Corker	Yes	10042	Serving Tennesseans in the U.S. Senate
104		No	4	
105		No	2	
106		No	11	Spécialiste développement produit et marketing des produits ...
107		No	4	
108		No	8	Not your average Grandma
109		No	29	
110		No	2	
111		No	6	
112	Kailani Koenig	Yes	11416	Producer with @MSNBC & @NBCNews. Team @MeetThePress alum. 20...
113		No	13	
114		No	14	
115	Gloria Turkin	No	204	I am honest and straight to the point. Retired Civilian Fed...
116		No	7	
117		No	28	An unconventional appreciation account for @DeadlineWH host,...
118		No	6	
119		No	10	Live like Bones

...continued

	Name	Followed	Followers	Description
120		No	2	
121	Marianna Sotomayor	Yes	11965	Running around Capitol Hill for @NBCNews. Covers politics ...
122	NBC News THINK	Yes	12017	THINK is NBC News' home for fresh opinion, sharp analysis ...
123		No	1	
124		No	15	
125		No	2	
126		No	3	Photographer, artist, newsletter editor, designer, writer...
127		No	18	
128		No	5	
129		No	5	The Quest for the Denim Jacket
130		No	9	
131		No	15	
132		No	16	Author of A Traumatic History: A Unique Look at PTSD and ...
133		No	5	
134		No	7	
135		No	5	
136		No	7	
137		No	7	
138	Beth Fouhy	Yes	13684	Senior editor, politics, NBC News and MSNBC
139	Jim Miklaszewski	Yes	14196	Jim Miklaszewski is Chief Pentagon Correspondent for NBC New...
140	Miguel Almaguer	Yes	14082	Prolific coffee drinker. Chronic under sleeper. Raging road ...
141		No	16	
142		No	4	
143		No	3	
144		No	19	The Northeast Tennessee Victory program will create a grassr...
145		No	17	
146		No	14	Just a dude with a crappy job.
147		No	5	
148	Nick Akerman	Yes	14949	Partner in the AmLaw 100 law firm of Dorsey & Whitney, Water...
149		No	5	
150		No	59	
151		No	8	
152		No	8	
153		No	4	Grad student at JHU
154		No	6	
155	Marist Poll	Yes	16030	Founded in 1978, MIPO is home to the Marist Poll and regular...
156		No	10	Sharing the best news from the e-Discovery world. Tweets by ...
157		No	7	
158		No	4	
159		No	11	Workforce and Economic Development Consultant; Employment ...
160		No	7	We're the workers of the @villagevoice, trying to get a fair...
161	Vivian Salama	Yes	16020	White House reporter for @WSJ. Formerly AP Baghdad bureau ...
162		No	8	
163		No	24	
164		No	19	I should be the real trix rabbit
165		No	4	
166		No	24	Curious food lover always looking for the best food everywhe...
167	Andrew Rafferty	Yes	16567	Senior political editor for @newsy Before that @NBCNews. And...
168		No	5	
169		No	36	
170	Tom Costello	Yes	17268	NBC News Correspondent covering Aviation, Transportation, ...
171		No	68	Wanderlust journalist ... A man is but the product of ...
172		No	6	Bibliophile, Animal lover, Realtor, Volunteer,
173		No	25	
174		No	70	Director or Product Marketing @ Microsoft. My tweets. My li...
175		No	3	Experienced (and successful) grantwriter, author, wife, moth...
176		No	5	
177	Jill Lawrence	Yes	17282	Commentary editor and columnist @USATODAY. Author of The Art...
178		No	8	Howard McKinnon is Town Manager of Havana, Florida.
179		No	136	
180		No	59	
181		No	8	

...continued

	Name	Followed	Followers	Description
182		No	12	
183		No	7	
184		No	8	
185		No	8	
186		No	15	Old and getting older.
187		No	15	
188		No	15	Married
189		No	4	
190		No	2	Director of the Essex, Connecticut Public Library aka "Your ...
191	Ethan Klapper	Yes	18292	Journalist (@YahooNews) and #avgeek.
192		No	38	
193		No	5	
194	Rebecca Sinderbrand	Yes	18691	Now: @NBCNews Senior Washington Editor, visiting lecturer ...
195		No	3	
196		No	11	Tireless trend researcher.
197		No	5	
198		No	5	
199		No	11	
200		No	3	

S4.3 An rPPR's sample of 200

Supplementary Table S5: Top (selected) handles returned by rPPR. The handles with fewer than 200 followers are hidden for privacy considerations.

	Name	Followed	Followers	Description
1		Yes	198	Enroll America National Regional Director http://t.co/X6jJIE...
2	Jennifer Sizemore	Yes	386	
3	Alissa Swango	Yes	441	Director of Digital Programming at @natgeo. All things food....
4	Making a Difference	Yes	670	@NBCNightlyNews' popular feature profiles ordinary people do...
5	Greg Martin	Yes	1161	Political Booking Producer at @nbcnews @todayshow
6	NBC Field Notes	Yes	1390	NBC News correspondents and http://t.co/1eSopOQt8s reporters...
7	Adam Edelman	Yes	2341	Political reporter @nbcnews. Wisconsin native, Bestchester ...
8	Phil McCausland	Yes	2519	@NBCNews Digital reporter focused on the rural-urban divide....
9	Corky Siemaszko	Yes	2538	Senior Writer at NBC News Digital (former NY Daily News ...
10	Sam Petulla	Yes	2588	Editor @cnnpolitics Usually looking for datasets. You can ...
11	Ken Strickland	Yes	2693	NBC News Washington Bureau Chief
12	Elyse PG	Yes	2697	White House producer @nbcnews @USCAnnenberg alum LA kid ...
13	Hasani Gittens	Yes	3002	Level 29 Mage. Senior News Ed. @NBCNews. Sheriff of Nattahna...
14	Scott Foster	Yes	3464	Senior Producer, Washington @NBCNEWS @TODAYshow
15	Zach Haberman	Yes	3693	Lead Breaking News Editor, @NBCNews. Previously had other jobs ...
16	Emmanuelle Saliba	Yes	4004	Head of Social Media Strategy @Euronews Launched #THECUBE ...
17	Alex Johnson	Yes	4371	News, data and analysis for @NBCNews; data geek; non-celebri...
18	Savannah Sellers	Yes	4637	News junkie. Host of NBC's "Stay Tuned" on Snapchat. Storyte...
19		No	154	We distribute new, never-worn clothing and merchandise to ...
20	Shaquille Brewster	Yes	5362	@NBCNews Producer/Politics @HowardU Alum Journalist Pol...
21	Joey Scarborough	Yes	6277	NBC News Social Media Editor. New York Daily News Alum. RTs ...
22	Jane C. Timm	Yes	6478	@nbcnews political reporter and fact checker. More fun than ...
23	Anthony Terrell	Yes	6827	Emmy Award winning journalist. Political observer. Covered ...
24	NBC News Videos	Yes	7838	The latest video from http://t.co/xPyvMOTEF6
25	Libby Leist	Yes	7946	Executive Producer @todayshow
26	Voices United	No	310	Voices United is a non profit educational organization for ...
27	Social Headlines	No	344	Daily roundup of top social media and networking stories.
28	James Miklaszewski	No	337	Writer, Photographer, Editor, Director, Producer, Newshound ...
29	Courtney Kube	Yes	9494	NBC News National Security & Military Reporter. Links and ...
30	Bob Corker	Yes	10042	Serving Tennesseans in the U.S. Senate
31	Kailani Koenig	Yes	11416	Producer with @MSNBC & @NBCNews. Team @MeetThePress alum...
32	Vets Helping Heroes	No	449	Raising funds to sponsor the training of assistance dogs for...
33	Marianna Sotomayor	Yes	11965	Running around Capitol Hill for @NBCNews. Covers politics ...
34	NBC News THINK	Yes	12017	THINK is NBC News' home for fresh opinion, sharp analysis ...
35	Beth Fouhy	Yes	13684	Senior editor, politics, NBC News and MSNBC
36	Jim Miklaszewski	Yes	14196	Jim Miklaszewski is Chief Pentagon Correspondent for NBC New...
37	Miguel Almaguer	Yes	14082	Prolific coffee drinker. Chronic under sleeper. Raging road ...
38		No	169	
39	Nick Akerman	Yes	14949	Partner in the AmLaw 100 law firm of Dorsey & Whitney, Water...
40	Marist Poll	Yes	16030	Founded in 1978, MIPO is home to the Marist Poll and regular...
41	Vivian Salama	Yes	16020	White House reporter for @WSJ. Formerly AP Baghdad bureau ...
42	Andrew Rafferty	Yes	16567	Senior political editor for @newsy Before that @NBCNews. And...
43	Tom Costello	Yes	17268	NBC News Correspondent covering Aviation, Transportation, ...
44	Gloria Turkin	No	204	I am honest and straight to the point. Retired Civilian Fed...
45	Jill Lawrence	Yes	17282	Commentary editor and columnist @USATODAY. Author of The Art...
46	Ethan Klapper	Yes	18292	Journalist (@YahooNews) and #avgeek.
47	Rebecca Sinderbrand	Yes	18691	Now: @NBCNews Senior Washington Editor, visiting lecturer ...
48	Leigh Ann Caldwell	Yes	20714	NBC Capitol Hill reporter. Formerly at CNN and public radio....
49	Morgan Radford	Yes	20967	@NBCNews Correspondent: @TODAYShow/@NBCNightlyNews/...
50	GuardAnglSolPet	No	927	Supporting the Military, our Veterans and their Beloved Pets...
51	adam nagourney	Yes	25307	LA Bureau Chief for The New York Times. Story ideas welcome ...
52		No	13	
53	Micah Grimes	Yes	25948	Head of Social, @NBCNews & @MSNBC – Foreign and domestic ...
54	Perry Bacon Jr.	Yes	26853	I write about government (mostly federal, often state, occas...
55		No	21	
56	Alex Moe	Yes	28245	@NBCNews Capitol Hill Producer + Off-Air Reporter; '12 & '16...
57	Ray Farmer	No	603	NBC News staff photographer. Colorado based

...continued

	Name	Followed	Followers	Description
58	Alex Witt	Yes	28126	Weekend host on @MSNBC (9am, noon & 1pm). Tiggers mom + ...
59	Monica Alba	Yes	30034	@NBCNews White House team. Covered Hillary Clinton on the ...
60	Jim Miklaszewski	No	1956	Chief Pentagon Correspondent for NBC News
61		No	13	
62	John McCormack	Yes	30688	Senior writer at The Weekly Standard.
63		No	136	
64	Vaughn Hillyard	Yes	31464	On the Road, Meeting Good Folk NBC News Arizonan IG...
65		No	35	
66	Madelyn Monteath	No	257	NFL Network, wife, mother.. not necessarily in that order.
67	Thomas DeFrank	No	593	Veteran White House correspondent (every prez since LBJ) and...
68	Jo Ling Kent	Yes	32957	NBC News Correspondent @NBCNightlyNews, @TODAYshow...
69		No	10	
70	Carrie Dann	Yes	37119	.@NBCNews / @NBCPolitics. RTs not endorsements.
71		No	3	
72		No	7	Dianne Kube is an Author with a passion, for family, holiday...
73		No	18	Cdr Bob Mehal, Public Affairs Office, Office of the Secretar...
74		No	7	
75	Mike Memoli	Yes	39693	National Political Reporter @nbcnews; @latimes alum mike dot...
76	John Boxley	No	1201	NBC News Producer...Living life one day at a time.
77		No	15	
78	Tom Winter	Yes	40777	NBC News Investigations reporter based in New York focusing ...
79		No	7	
80	Garrett Haake	Yes	40714	Correspondent @msnbc Taller than I look on TV Long-suffe...
81		No	59	
82		No	70	Director or Product Marketing @ Microsoft. My tweets. My li...
83		No	68	Wanderlust journalist ... A man is but the product of ...
84		No	158	Marketing nerd at Cornerstone OnDemand.
85	Jonathan Allen	Yes	44477	political reporter, @NBCNews Digital co-author, NYT bestse...
86	NBC News First Read	Yes	53847	The first place for news and analysis from the @NBCNews Poli...
87		No	92	Smokin Meat & Raising Kids That Raise Hell. Live Every Day ...
88	Sam Singal	No	1016	Executive Producer, @nbcnightlynews
89		No	29	
90		No	59	
91	Carol Lee	Yes	51240	Reporter for NBC News, former WSJ & POLITICO, Hudson's mom, ...
92	Alex Seitz-Wald	Yes	50168	Political reporter for @NBCNews covering Democrats Tips, ...
93		No	28	An unconventional appreciation account for @DeadlineWH host,...
94		No	188	I am a Senior Video Producer at NBCNews.com, as well a few ...
95	HailYeah63	No	483	#RedskinsTweetTeam #HTTR
96	Eva's Heroes	No	2067	To enrich the lives of individuals with intellectual special...
97		No	6	
98	Chi Omega	No	278	Chi Omega Chapter at CU Boulder
99	Aarne Heikkila	No	1210	Coordinating Producer for @JacobSoboroff @MSNBC & @NBCNews, ...
100	Dani	No	447	only here to talk shit & complain
101	Frank Thorp V	Yes	58152	Producer & Off-Air Reporter covering Congress at @NBCNews. ...
102	Youcef	No	228	
103		No	76	Pentagon correspondent http://t.co/Qo0w3AnYob
104	project c.u.r.e.	No	2260	delivering donated medical supplies and equipment to develop...
105		No	117	
106		No	4	
107	Elise Jordan	Yes	58884	Co-host of @WMM_podcast podcast. @MSNBC/@NBCNews political ...
108	Patrick Burkey	No	2313	Executive Producer, @NBCNews, @MSNBC. Former EP, @NBCNightly...
109	bill hartnett	No	2500	Stripmining the internets for remarkable ephemera Social Mus...
110		No	7	
111		No	8	
112		No	16	
113		No	36	
114	Ron Fournier	Yes	64356	President: Truscott Rossman. Best-seller https://t.co/09CdTN...
115		No	12	
116	Pete Williams	Yes	70062	NBC News Justice Correspondent. Covers US Supreme Court, ...
117		No	65	Wife, Mother. Litigation Specialist. Designer. Activist for ...
118		No	10	
119	Heidi Przybyla	Yes	66489	NBC News, n'tl political reporter "Prezbella" Heidi.Przyb...

...continued

	Name	Followed	Followers	Description
120	NBC Latino	Yes	67920	Elevating the conversation around Latino news in the United ...
121		No	189	
122		No	38	
123	Chris Jansing	Yes	72375	@msnbc Senior National Correspondent, intrepid traveler and ...
124		No	1	
125	Brent Kendall	No	5451	WSJ legal affairs reporter in Washington. Native Tar Heel, ...
126		No	2	
127	U.S. Attorney EDVA	No	5709	Led by U.S. Attorney G. Zachary Terwilliger. 130+ attorneys ...
128		No	74	Life long learner Paralegal Arts & Culture Black Community ...
129		No	2	
130		No	2	
131	Tammy Fine	No	1584	Corporate Communications by day. Teen Negotiator by night...
132	Bonnie Optekman	No	2242	Digital media strategist. Voice over artist. News junkie, ...
133		No	3	yet another activist twitter, fighting all those fun -isms ...
134		No	109	Communicator through an eclectic lens of #healthcare #hospit...
135		No	88	Earth and Physical Science Teacher, Mom of 2, Self-declared ...
136	Amy Lynn-Cramer	No	1590	Mommy to 2 amazing kiddos, Wife to @tecramer AND Corporate ...
137		No	5	
138	prodjay	No	304	NBC News producer
139		No	109	
140		No	10	
141	Meghann Ludemann	No	216	Stay Tuned Associate Producer @NBCNews on @Snapchat
142		No	4	
143	Ali Vitali	Yes	78839	@NBCnews Political Reporter. Covered Trump campaign, WH + ...
144	Doug Adams	No	1902	NBC Sr. Political desk editor; Father; Baseball fan; Lover ...
145		No	99	
146	Mark Sherman	No	6336	
147	Robin Gradison	No	272	NBC News DC Deputy Bureau Chief, politics junkie, road run...
148	NBC News Signal	Yes	83715	A new streaming news channel from @NBCNews. Catch us Thursda...
149		No	45	Professor at Columbia Journaism School.
150		No	8	
151		No	18	
152	Stacey Klein	No	914	@NBCNews White House Producer, Born and raised in BalDimore ...
153		No	97	
154	Rich Latour	No	1883	From Broadcast News to Digital Storytelling. Dad of 3 Boys ...
155	Domenico Montanaro	Yes	83999	"Congress shall make no law respecting an est. of religion, ...
156		No	5	
157		No	6	Anti-money laundering professional with federal law enforcem...
158		No	24	
159		No	24	Curious food lover always looking for the best food everywhe...
160		No	25	
161		No	161	1 of 12 U.S.-led PRTs. Improving Panjshir's stability, incre...
162	Anna Matthews	No	230	
163		No	46	
164	POLITICO 45	Yes	88470	A daily diary of the 45th president of the United States.
165		No	9	Quotes from a nice jewish mom who's just tryna get some nice...
166		No	19	The Northeast Tennessee Victory program will create a grassr...
167		No	130	@NBCNews Producer in London, Links & retweets aren't endorse...
168	samgo	No	1161	Executive Producer, @MSNBC Digital
169	Megan Stark	No	263	over served Coloradan
170		No	70	
171	Katie Yu	No	484	NBC News Senior Producer / formerly @Nightline, @NBCNightlyN...
172	Mark Murray	Yes	97571	Mark Murray is the senior political editor for NBC News, as ...
173	Kevin Thurm	No	1946	Chief Executive Officer @ClintonFdn. Dad, sports fan & trivi...
174		No	122	Mom, wife, grandma, Airedale Terrier lover
175		No	173	Providing conservatives with breaking news, opinion, blogs ...
176		No	14	
177		No	12	
178		No	137	Celebrate the simple loveliness of every day things, scarves...
179		No	15	
180		No	8	
181		No	16	Author of A Traumatic History: A Unique Look at PTSD and ...

...continued

	Name	Followed	Followers	Description
182		No	9	
183		No	8	I'm the real Charlie Sheen. If you are a Winner, stick aroun...
184	David Espo	No	1308	Dad, AP Special Correspondent, Dad, Red Sox fan, Dad.
185		No	40	
186	matt toder	No	253	supervising producer, documentaries/verticals at NBC News ...
187		No	13	
188	Benjy Sarlin	Yes	100896	Political reporter for @NBCNews. I cover elections and their...
189		No	15	
190		No	29	
191		No	17	
192		No	28	Director of the Marist Poll, poll obsessed, epistemophilic,...
193		No	16	
194		No	144	Vice President, Standards @NBCNews
195		No	108	trey.daly@gmail.com
196	Daniella Mayer	No	314	DON'T forget the A. I think everything about North Korea is ...
197	Bill Hatfield	No	635	Washington news producer for NBC News TODAY; politics/histor...
198		No	19	I should be the real trix rabbit
199		No	50	
200	Phil Griffin	No	231	

References

- Edoardo M Airoldi, David M Blei, Stephen E Fienberg, and Eric P Xing. Mixed membership stochastic blockmodels. *Journal of Machine Learning Research*, 9(Sep):1981–2014, 2008.
- M. Alamgir and U. von Luxburg. Multi-agent random walks for local clustering. pages 18–27, Piscataway, NJ, USA, December 2010. Max-Planck-Gesellschaft, IEEE.
- Reid Andersen and Kevin J. Lang. Communities from seed sets. In *Proceedings of the 15th International Conference on World Wide Web*, WWW '06, pages 223–232, New York, NY, USA, 2006. ACM. ISBN 1-59593-323-9. doi: 10.1145/1135777.1135814. URL <http://doi.acm.org/10.1145/1135777.1135814>.
- Reid Andersen and Yuval Peres. Finding sparse cuts locally using evolving sets. In *Proceedings of the Forty-first Annual ACM Symposium on Theory of Computing*, STOC '09, pages 235–244, New York, NY, USA, 2009. ACM. ISBN 978-1-60558-506-2. doi: 10.1145/1536414.1536449. URL <http://doi.acm.org/10.1145/1536414.1536449>.
- Reid Andersen, Fan Chung, and Kevin Lang. Local graph partitioning using pagerank vectors. In *Proceedings of the 47th Annual IEEE Symposium on Foundations of Computer Science*, FOCS '06, pages 475–486, Washington, DC, USA, 2006. IEEE Computer Society. ISBN 0-7695-2720-5. doi: 10.1109/FOCS.2006.44. URL <http://dx.doi.org/10.1109/FOCS.2006.44>.
- Albert-László Barabási and Réka Albert. Emergence of scaling in random networks. *science*, 286(5439):509–512, 1999.
- Pavel Berkhin. Bookmark-coloring algorithm for personalized pagerank computing. *Internet Mathematics*, 3(1):41–62, 2006.
- Stéphane Boucheron, Gábor Lugosi, and Pascal Massart. *Concentration inequalities: A nonasymptotic theory of independence*. Oxford university press, 2013.
- Pierre Brémaud. *Markov chains: Gibbs fields, Monte Carlo simulation, and queues*, volume 31. Springer Science & Business Media, 2013.
- Sergey Brin and Lawrence Page. The anatomy of a large-scale hypertextual web search engine. *Comput. Netw. ISDN Syst.*, 30(1-7):107–117, April 1998. ISSN 0169-7552. doi: 10.1016/S0169-7552(98)00110-X. URL [http://dx.doi.org/10.1016/S0169-7552\(98\)00110-X](http://dx.doi.org/10.1016/S0169-7552(98)00110-X).
- Yuxin Chen, Jianqing Fan, Cong Ma, and Kaizheng Wang. Spectral method and regularized mle are both optimal for top- k ranking. *Ann. Statist.*, 47(4):2204–2235, 08 2019. doi: 10.1214/18-AOS1745. URL <https://doi.org/10.1214/18-AOS1745>.
- Chandler Davis and William Morton Kahan. The rotation of eigenvectors by a perturbation. iii. *SIAM Journal on Numerical Analysis*, 7(1):1–46, 1970.
- Georg Ferdinand Frobenius, Ferdinand Georg Frobenius, Ferdinand Georg Frobenius, Ferdinand Georg Frobenius, and Germany Mathematician. *Über Matrizen aus nicht negativen Elementen*. Königliche Akademie der Wissenschaften, 1912.

- Shayan Oveis Gharan and Luca Trevisan. Approximating the expansion profile and almost optimal local graph clustering. In *Proceedings of the 2012 IEEE 53rd Annual Symposium on Foundations of Computer Science*, FOCS '12, pages 187–196, Washington, DC, USA, 2012. IEEE Computer Society. ISBN 978-0-7695-4874-6. doi: 10.1109/FOCS.2012.85. URL <https://doi.org/10.1109/FOCS.2012.85>.
- Gourab Ghoshal and Albert-László Barabási. Ranking stability and super-stable nodes in complex networks. *Nature communications*, 2:394, 2011.
- David F Gleich. Pagerank beyond the web. *SIAM Review*, 57(3):321–363, 2015.
- Pankaj Gupta, Ashish Goel, Jimmy Lin, Aneesh Sharma, Dong Wang, and Reza Zadeh. Wtf: The who to follow service at twitter. In *Proceedings of the 22nd international conference on World Wide Web*, pages 505–514. ACM, 2013.
- Taher H Haveliwala. Topic-sensitive pagerank: A context-sensitive ranking algorithm for web search. *IEEE transactions on knowledge and data engineering*, 15(4):784–796, 2003.
- Paul W Holland, Kathryn Blackmond Laskey, and Samuel Leinhardt. Stochastic blockmodels: First steps. *Social networks*, 5(2):109–137, 1983.
- Glen Jeh and Jennifer Widom. Scaling personalized web search. In *Proceedings of the 12th International Conference on World Wide Web*, WWW '03, pages 271–279, New York, NY, USA, 2003. ACM. ISBN 1-58113-680-3. doi: 10.1145/775152.775191. URL <http://doi.acm.org/10.1145/775152.775191>.
- Brian Karrer and Mark EJ Newman. Stochastic blockmodels and community structure in networks. *Physical Review E*, 83(1):016107, 2011.
- George Karypis and Vipin Kumar. Multilevelk-way partitioning scheme for irregular graphs. *Journal of Parallel and Distributed computing*, 48(1):96–129, 1998.
- Rajiv Khanna, Ethan Elenberg, Alexandros G Dimakis, and Sahand Negahban. On approximation guarantees for greedy low rank optimization. *arXiv preprint arXiv:1703.02721*, 2017.
- Isabel M. Kloumann, Johan Ugander, and Jon Kleinberg. Block models and personalized pagerank. *Proceedings of the National Academy of Sciences*, 114(1):33–38, 2017. ISSN 0027-8424. doi: 10.1073/pnas.1611275114. URL <https://www.pnas.org/content/114/1/33>.
- Can M Le, Elizaveta Levina, Roman Vershynin, et al. Optimization via low-rank approximation for community detection in networks. *The Annals of Statistics*, 44(1):373–400, 2016.
- Chung-Shou Liao, Kanghao Lu, Michael Baym, Rohit Singh, and Bonnie Berger. IsoRankN: spectral methods for global alignment of multiple protein networks. *Bioinformatics*, 25(12):i253–i258, 05 2009. ISSN 1367-4803. doi: 10.1093/bioinformatics/btp203. URL <https://doi.org/10.1093/bioinformatics/btp203>.
- László Lovász. Random walks on graphs: A survey. In D. Miklós, V. T. Sós, and T. Szőnyi, editors, *Combinatorics, Paul Erdős is Eighty*, volume 2, pages 353–398. János Bolyai Mathematical Society, Budapest, 1996.
- Xin Lu, Jens Malmros, Fredrik Liljeros, Tom Britton, et al. Respondent-driven sampling on directed networks. *Electronic Journal of Statistics*, 7:292–322, 2013.

- Kathy Macropol, Tolga Can, and Ambuj K. Singh. Rrw: repeated random walks on genome-scale protein networks for local cluster discovery. *BMC Bioinformatics*, 10(1):283, Sep 2009. ISSN 1471-2105. doi: 10.1186/1471-2105-10-283. URL <https://doi.org/10.1186/1471-2105-10-283>.
- Mark Newman, Albert-Laszlo Barabasi, and Duncan J. Watts, editors. *The Structure and Dynamics of Networks*. Princeton University Press, Princeton, NJ, USA, 2006.
- L. Page, S. Brin, R. Motwani, and T. Winograd. The pagerank citation ranking: Bringing order to the web. In *Proceedings of the 7th International World Wide Web Conference*, pages 161–172, Brisbane, Australia, 1998. URL citeseer.nj.nec.com/page98pagerank.html.
- Oskar Perron. Zur theorie der matrices. *Mathematische Annalen*, 64(2):248–263, 1907.
- Tai Qin and Karl Rohe. Regularized spectral clustering under the degree-corrected stochastic blockmodel. In *Proceedings of the 26th International Conference on Neural Information Processing Systems - Volume 2, NIPS'13*, pages 3120–3128, USA, 2013. Curran Associates Inc. URL <http://dl.acm.org/citation.cfm?id=2999792.2999960>.
- Karl Rohe, Sourav Chatterjee, and Bin Yu. Spectral clustering and the high-dimensional stochastic block-model. *The Annals of Statistics*, 39(4):1878–1915, 2011.
- Srijan Sengupta and Yuguo Chen. A block model for node popularity in networks with community structure. *Journal of the Royal Statistical Society: Series B (Statistical Methodology)*, 80(2):365–386, 2018.
- Daniel A Spielman and Shang-Hua Teng. Spectral partitioning works: Planar graphs and finite element meshes. In *Foundations of Computer Science, 1996. Proceedings., 37th Annual Symposium on*, pages 96–105. IEEE, 1996.
- Daniel A Spielman and Shang Hua Teng. Nearly-linear time algorithms for graph partitioning, graph sparsification, and solving linear systems. In *Proceedings of the thirty-sixth annual ACM symposium on Theory of computing*, pages 81–90. ACM, 2004.
- Duncan J Watts and Steven H Strogatz. Collective dynamics of small-worldnetworks. *nature*, 393(6684):440, 1998.
- Yaojia Zhu, Xiaoran Yan, and Cristopher Moore. Oriented and degree-generated block models: generating and inferring communities with inhomogeneous degree distributions. *Journal of Complex Networks*, 2(1):1–18, 2013.